TECHNISCHE UNIVERSITÄT WIEN
Vienna University of Technology

Aalto University

Master Thesis

Recycling of Euro Banknotes

by means of the Ioncell® Process

carried out for the purpose of obtaining the degree of Dipl. Ing. submitted at TU Wien, Faculty of Mechanical and Industrial Engineering, by

Matthias Selinger

[redacted]

Supervisor: Senior Scientist Dipl.-Ing. Dr.techn. Andreas Bartl

Co-Supervisor: Professor Dr. Herbert Sixta

Advisors: Dr. Inge Schlapp-Hackl & Dr. Marja Rissanen

Vienna, June 2022

Die approbierte gedruckte Originalversion dieser Diplomarbeit ist an der TU Wien Bibliothek verfügbar
The approved original version of this thesis is available in print at TU Wien Bibliothek.
TU Bibliothek Your knowledge hub

This work was supported by FINIX (www.finix.aalto.fi)

I confirm, that going to press of this thesis needs the confirmation of the examination committee.

Affidavit

I declare in lieu of oath, that I wrote this thesis and performed the associated research myself, using only literature cited in this volume. If text passages from sources are used literally, they are marked as such.

I confirm that this work is original and has not been submitted elsewhere for any examination, nor is it currently under consideration for a thesis elsewhere.

I acknowledge that the submitted work will be checked electronically-technically using suitable and state-of-the-art means (plagiarism detection software). On the one hand, this ensures that the submitted work was prepared according to the high-quality standards within the applicable rules to ensure good scientific practice "Code of Conduct" at the TU Wien. On the other hand, a comparison with other student theses avoids violations of my personal copyright.

City and Date	*Signature*

Die approbierte gedruckte Originalversion dieser Diplomarbeit ist an der TU Wien Bibliothek verfügbar
The approved original version of this thesis is available in print at TU Wien Bibliothek.

Acknowledgements

This thesis was conducted at the Department of Biosystems and Bioproducts at Aalto University within the FINIX project (project title: Sustainable textile systems: Co-creating resource-wise business for Finland in global textile networks). I would like to express my sincerest gratitude to the whole Spinning Group for kindly including me in the group, for their selfless support in difficult and challenging moments as well as for their friendship.

Foremost I would like to specially thank Professor Dr. Herbert Sixta for giving me this eminently wonderful opportunity to work within his research group and for all his scientific support. A special thanks and a large portion of credit goes to my thesis advisor Inge Schlapp-Hackl for her daily guidance, help and constant support during the whole research project. I highly appreciate her way of teaching, her never ending stream of ideas and her interest in science. I also want to thank my second thesis advisor Marja Rissanen for all the fiber related support and help as well as for all her wise inputs. A big thanks goes to Professor Dr. Andreas Bartl for his assistance from the distance and all his scientific as well as fast and uncomplicated handling of various requests. Appreciation is also extended to the members of the research team, in particular Eva Gonzalez as well as to Yibo Ma, Lê Huy Quang, Daisuke Sawada, and Helena Sederholm for their assistance in showing me various techniques.

The biggest thanks goes to my parents as well as to my brothers and sister for their constant support over all these years who always remind me what is really important in life. Without them I would never have achieved what I have.

I also want to express my appreciation to David Inflünzer, for being a mayor inspiration during this work. Finally, I want to thank all my friends I made during the time I was in Finland as well as all my friends from Austria, which made this time abroad a truly wonderful experience.

"Not everything that counts can be counted and not everything that can be counted counts" – Albert Einstein

Die approbierte gedruckte Originalversion dieser Diplomarbeit ist an der TU Wien Bibliothek verfügbar
The approved original version of this thesis is available in print at TU Wien Bibliothek.
TU Bibliothek Your knowledge hub WIEN

Table of Contents

Page

Table of Contents I
Abstract (German) II
Abstract (English) III
List of Abbreviations and Symbols IV

1. Introduction and Motivation 1
2. Background 3
2.1 Ioncell® Process 3
2.2 Banknotes 5
2.3 Cellulose 7
2.4 Cellulose Solvents 9
2.5 Dry-jet wet Spinning 12
3. Material and Methods 14
3.1 Banknotes 14
3.2 Pre-Treatment of Banknotes 15
3.3 Particle Size Distribution 23
3.4 Ash Content 23
3.5 Viscosity Measurement 24
3.6 Ionic Liquid 25
3.7 Dissolution Studies 26
3.8 Dope Preparation 26
3.9 Rheology 27
3.10 Fiber Spinning 27
3.11 Characterization of Fibers 29
3.11.1. Mechanical Properties 29
3.11.2. Birefringence 29
3.11.3. Scanning Electron Microscopy 30
3.11.4. Gel Permeation Chromatography 30
3.11.5. X-Ray Diffraction Measurements 31
3.12 Inductively Coupled Plasma - Optical Emission Spectroscopy 32
3.13 Fourier-Transform Infrared Spectroscopy 33

Die approbierte gedruckte Originalversion dieser Diplomarbeit ist an der TU Wien Bibliothek verfügbar
The approved original version of this thesis is available in print at TU Wien Bibliothek.

3.14 Differential Scanning Calorimetry & Thermogravimetric Analysis 34
3.15 Elemental Analysis 35
3.16 Carbohydrate Analysis 35
4. Results and Discussion 37
4.1 Impact of the Pre-treatment Process 37
4.2 Dissolution Results 46
4.3 Dope Rheology 47
4.4 Fibers – Spinning & Properties 49
4.4.1. Fiber Spinning 49
4.4.2. Mechanical Properties 51
4.4.3. Birefringence 53
4.4.4. Scanning Electron Microscopy 55
4.4.5. Molecular Mass Distribution 57
4.4.6. X-Ray Diffraction Measurements 58
4.5 Elemental Analysis 59
4.6 FTIR – Analysis 61
4.7 Simultaneous Thermal Analysis (STA) 63
4.8 Green Pigments 67
5. Conclusion 69
6. References 71
7. Appendix 77

Die approbierte gedruckte Originalversion dieser Diplomarbeit ist an der TU Wien Bibliothek verfügbar
The approved original version of this thesis is available in print at TU Wien Bibliothek.

Abstract

Diese Masterarbeit zeigt eine Möglichkeit auf, zellulosebasierte, ausrangierte Euro-Banknoten mit Hilfe des innovativen und umweltschonenden Ioncell® Prozesses (Sixta et al., 2015) zu rezyklieren. Im Zuge dieser Arbeit wurde eine Sequenz von mechanischen und chemischen Behandlungsschritten entwickelt, um die nicht Zellulosen- Bestandteile auf ein Minimum zu reduzieren und im Weiteren die aufgereinigte Baumwolle wiederzugewinnen. Bei den Verunreinigungen handelt es sich vorrangig um Polymere, Metalle und metallische Komplexe. Der erschlossene Baumwollkern wurde mittels des Ioncell® Prozesses chemisch recycelt. Dabei wurde das auf Zellulose basierende Material in einer Ionischen Flüssigkeit, 1,5-diazabicyclo(4.3.0)non-5-enium acetate [DBNH][OAc], gelöst. Eine hoch viskose Spinnlösung wurde erhalten, welche mittels einer Spinndüse zu Zellulose Fasern verarbeitet wurde. Die Zellulose wurde in einem Spinnbad ausgefällt, im Anschluss gewaschen, getrocknet und zu einem Stück Stoff weiterverarbeitet. Die physikalischen und chemischen Eigenschaften (Aschegehalt, elementare Zusammensetzung, intrinsische Viskosität, etc.) der Banknoten wurden im jeweiligen Behandlungsschritt ausführlich durch geeignete analytische Messmethoden bestimmt. Eine deutliche Reduktion der Verunreinigungen und damit eine einhergehende Erhöhung des Zellulosegehalts von 86,1% des Ausgangsmaterials auf 95,1% der vollständig aufgereinigten Banknoten war zu beobachten. Durch die Behandlung wurde die intrinsische Viskosität von etwa 600 ml/g auf knapp unter 400 ml/g reduziert. Zudem wurden die mechanischen und optischen Eigenschaften der regenerierten Fasern anhand von analytischen Messmethoden (Zugfestigkeitsmessung, Birefringenz, SEM, XRD, FTIR, STA, Elementaranalyse, GPC) ermittelt. Im Laufe der Arbeit wurden zwei unterschiedliche Fasern produziert, grüne Ioncell® Fasern nach 5, und weiße Ioncell® Fasern nach 7 aufeinander folgenden Behandlungsschritten. Die produzierten grünen Fasern wiesen eine Reißfestigkeit von rund 36 cN/tex bei einer Reißdehnung von etwa 8 % auf. Die weißen Fasern erzielten mit einer Reißfestigkeit von rund 32 cN/tex bei einer Reißdehnung von etwa 6 % etwas geringere Werte auf. Die Eigenschaften sämtlicher Fasern lagen zwar unter den Werten der Referenz - Ioncell® Fasern, welche aus Holzzellstoff (Enocell – 4) hergestellt wurden, allerdings liegen die Werte im Bereich von kommerziell verwendeten Fasern wie etwa Viskose und Lyocell Fasern. Die weißen Fasern zeichnen sich durch eine höhere Orientierung und einen größeren kristallinen Anteil im Vergleich zu den grünen Fasern aus. Die chemische Struktur der weißen und grünen Fasern erwies sich als ident.

Die approbierte gedruckte Originalversion dieser Diplomarbeit ist an der TU Wien Bibliothek verfügbar
The approved original version of this thesis is available in print at TU Wien Bibliothek.
TU Bibliothek Your knowledge hub WIEN

Abstract

This master thesis portrays a possibility to recycle cotton-based euro banknotes using the innovative and environmentally friendly Ioncell® process. By developing a sequence of mechanical and chemical treatment steps the amount of additives (polymers, metals, metallic complexes, and others) could be reduced to a minimum. Physical and chemical properties (particle size distribution, ash content, elemental composition, intrinsic viscosity, etc) of the banknotes after the respective treatment steps were determined in detail by suitable analytical methods. A significant reduction of impurities could be achieved resulting in an increased cellulose content from 86.1% of the milled starting material to 95.1% of the completely purified banknotes. Certain chemical treatment steps resulted in the reduction of the intrinsic viscosity from around 600 ml/g to just below 400 ml/g, which is close to the standard wood pulp material for the Ioncell® spinning process. The purified starting material was dissolved in the ionic liquid 1,5-diazabicyclo(4.3.0)non-5-enium acetate [DBNH][OAc]. A cellulose-IL solution was received. By the use of the Lyocell type dry- jet - wet spinning process Ioncell®, green and white cellulose fibers were produced, washed, and further processed to a piece of fabric. Mechanical and optical properties of the regenerated fibers were determined by analytical methods (tensile strength measurement, birefringence, SEM, XRD, FTIR, STA, elemental analysis, GPC). The green Ioncell® fibers exhibited a tensile strength of about 36 cN/tex with an elongation at break of about 8%. The white fibers showed lower values with a tensile strength of about 32 cN/tex at an elongation at break of about 6 %. Although all fibers were below the values of the reference - Ioncell® fibers made from wood pulp (Enocell – 4) - the values are in the range of commercially used fibers such as Viscose and Lyocell fibers. The white fibers showed a higher orientation and an increased crystallinity compared to the green fibers. No significant difference in chemical structure could be observed.

Die approbierte gedruckte Originalversion dieser Diplomarbeit ist an der TU Wien Bibliothek verfügbar
The approved original version of this thesis is available in print at TU Wien Bibliothek.

List of Abbreviations and Symbols

CED	Cupriethylenediamine
CoP	Cross-over Point
[DBNH][OAc]	1,5-diazabicyclo[4,3,0] non-5-enium acetate
DJW	Dry- Jet Wet
DMAc	Dimethylacetamide
DMC	Dry Matter Content
DMSO	Dimethyl sulfoxide
DP	Degree of Polymerization
DR	Draw Ratio
DSC	Differential Scanning Calorimetry
FTIR	Fourier-Transform Infrared Spectroscopy
GPC	Gel Permeation Chromatography
ICP	Inductively Coupled Plasma
IL	Ionic Liquid
NMMO	N-Methylmorpholin-N-oxide
OES	Optical Emission Spectroscopy
PSD	Particle Size Distribution
SEC	Size Exclusion Chromatography
SEM	Scanning Electron Microscope
SRS	Sugar Recovery Standard
STA	Simultaneous Thermal Analysis
TGA	Thermogravimetric Analysis
XRD	X-Ray Diffraction Analysis

Die approbierte gedruckte Originalversion dieser Diplomarbeit ist an der TU Wien Bibliothek verfügbar
The approved original version of this thesis is available in print at TU Wien Bibliothek.

1. Introduction and Motivation

"The euro is an everyday reminder of the benefits of European integration" – (ecb.europa.at, 2022). Almost 20 years ago, on 01.01.2002, the euro was introduced for the first time in 12 EU member states. Today, the euro is the official currency for a total of 19 countries, the so-called euro zone and its more than 340 million inhabitants. On the one hand, the euro is a sign of European integration and enables the uncomplicated trade of goods and services as well as a free market economy within the euro zone. On the other hand, the euro is also a symbol of stability and is the second most important reserve currency in the world after the dollar (Aristovnik & Čeč, 2009).

As a means of payment, there are 8 different coins and a total of 13 different banknotes (bills) in circulation in the euro area. Although there has been a significant decline in cash payments over the past few decades, due to the pleasant cashless payment possibilities, cash payment is still one of the most common payment methods in many European countries. For example, 54.3% of all transactions in Austria were made in cash, 72.1% in Slovakia, and more than three-quarters of all payments, 75.2% were conducted in cash in Greece, according to statista.com in the year 2019 (statista.com, 2021). Euro bills are produced to endure enhanced wear and tear. Depending on environmental factors such as humidity, light, temperature, abrasion, and contaminations, the average lifespan of a euro banknote can vary greatly, smaller denominations usually exhibit shorter lifespans. A 20€ bill for instance, endures 2.6 years in average (Schautzer & Stix, 2019). Unfit and worn banknotes are removed from circulation and are disposed. As a result, up to 5.000 tons of euro banknote waste is generated each year in all 19 eurozone countries according to the Bank of Finland. The predominant part of this waste is incinerated in order to use the thermal energy. Significant amounts of CO_2 are produced. The carbon dioxide emissions [Gg/yr] due to waste incineration can be calculated as follows according to the Intergovernmental Panel on Climate Change (IPCC, 2006).

$$CO_2 \text{ emissions} = \sum (SW_i * dm_i * CF_i * FCF_i * OF_i) * \frac{44}{12} \qquad (1)$$

Die approbierte gedruckte Originalversion dieser Diplomarbeit ist an der TU Wien Bibliothek verfügbar
The approved original version of this thesis is available in print at TU Wien Bibliothek.

with SW_i as the total amount of solid waste of type i (wet weight) incinerated or open-burned [Gg/yr] and dm_i as the dry matter content of each waste constituent [-]. CF_i is the total carbon content in dry matter [-], FCF_i the fraction of fossil carbon in the total carbon [-], OF_i is the oxidation factor [-], and 44/12 is the conversion factor from carbon to CO_2. This would amount to more than 7700 tons of CO_2 emission, assuming complete combustion and totally dry banknotes ($dm_i = FCF_i = OF_i = 1$, $SW_i = 5000$ tons, $CF_i = 0.422$ see Table 13) Furthermore, other greenhouse gases are produced during incineration, as well as contaminated ash is generated which consequently leads to further disposal issues. Apart from this direct environmental impact, valuable resources that could be reused by appropriate recycling methods are destroyed. Especially the substrate of the banknotes, pure cotton linters, is of great interest for recycling purpose. It is the declared goal of the European Central Bank to rethink the entire cycle of euro banknotes in respect to its environmental impact. Not only the production steps and the materials used are being reconsidered, but also options for the end-of-life management of the banknotes are being reassessed. Here, the approach taken within this master thesis comes into place. A possible process to recycle old Euro banknotes by means of the innovative and environmentally friendly Ioncell® process.

The Ioncell® process, a Lyocell type spinning process, is dedicated to contributing its part in improving the carbon footprint of one of the world's most polluting industries. The clothing and textile industry is responsible for roughly 1.2 billion tons of greenhouse gas emissions every year (Change, 2018). The global clothing consumption quadrupled since the beginning of this century (Jia et al., 2020) and global fiber production is at an all-time high with more than 108 million metric tons of textile fibers and more than 80 million metric tons of synthetic fibers produced in 2020 (statista.com, 2022). The fast fashion trend and the increase of the populations purchasing power is responsible for the steady growth. Global players in this sector such as Nike, Adidas, H&M, Shein and Zara create fake demands for the newest and trendiest cheaply produced products. Together they are responsible for generating enormous amounts of textile waste where up to today only 25% are recycled, the rest is either incinerated or ends up on a landfill (Rapsikevičienė et al., 2019). In addition to the enormous emissions and waste production, the production of textiles requires a considerable amount of water and chemicals and is also responsible for water pollution around the world. (Berger et al., 2021).

The circular economy and sustainable fiber production approach underlying the Ioncell® process makes this process a valuable addition to existing processes.

Die approbierte gedruckte Originalversion dieser Diplomarbeit ist an der TU Wien Bibliothek verfügbar
The approved original version of this thesis is available in print at TU Wien Bibliothek.
TU Bibliothek Your knowledge hub WIEN

2. Background

2.1 Ioncell® Process

The Ioncell® (Sixta et al., 2015) process is a lyocell-type dry- jet wet spinning process which uses a so-called direct solvent, an Ionic liquid to dissolve cellulose-based materials and turn them into fibers. These fibers can further be spun into yarn which is knitted or woven into fabrics using standard textile instruments. The produced fabrics can be further used for various applications. The process is constantly improved and extended. Research currently done at the Aalto University in Finland is working on the recycling of various natural-based polymers and also on the recycling of diverse Ionic liquids, used for the dissolution (Elsayed et al., 2020, 2021). Thereby, a closed loop process thriving for the creation of a more economically friendly textile industry is developed. Figure 1 illustrates the Ioncell® process and its individual sequential steps (ioncell.fi/research, 2022).

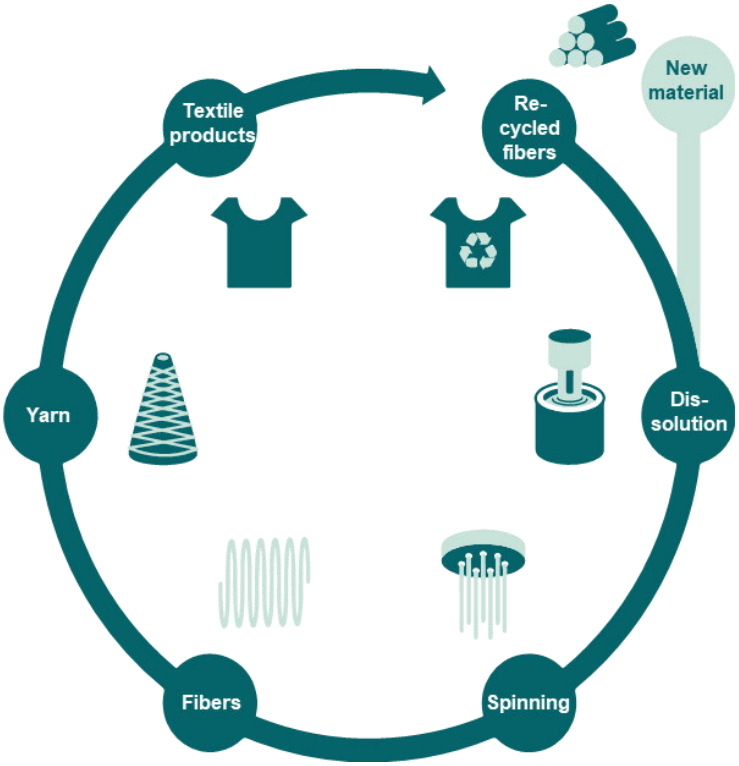

Figure 1. The path of Ioncell® production (ioncell.fi/research, 2022).

Die approbierte gedruckte Originalversion dieser Diplomarbeit ist an der TU Wien Bibliothek verfügbar
The approved original version of this thesis is available in print at TU Wien Bibliothek.

The main advantage of this process is the production of fibers at moderate temperatures. While other comparable processes (e.g.: Lyocell process, Viscose process) use temperatures significantly above 100°C (Woodings, 2001), the Ioncell® process operates below 100°C, thereby consuming significantly less energy. Furthermore, ILs are frequently considered to be greener alternatives to commonly used chemicals such as NMMO. ILs are environmentally friendly solvents not flammable, easy to handle and on top of that, recyclable (Elsayed et al., 2020, 2021). The Ioncell® process has successfully proven its ability to produce durable fibers and furthermore to be used for the recycling of natural polymer-based waste. As shown by recent studies, cotton waste (Asaadi et al., 2016), waste papers and cardboards (Ma et al., 2016), newsprints (Ma et al., 2018), cotton polyester blends (Haslinger et al., 2019) and reactive and vat dyed cotton fabrics (Haslinger et al., 2019) were successfully recycled by the Ioncell® process. Fibers obtained by the Ioncell® process show properties which are in the range or sometimes even exceed the values of other commercially used fibers.

All in all, it can be said, that the Ioncell® process has the outstanding potential to surpass other well-established processes as a more environmentally friendly alternative while equal or even better fiber properties are obtained.

Die approbierte gedruckte Originalversion dieser Diplomarbeit ist an der TU Wien Bibliothek verfügbar
The approved original version of this thesis is available in print at TU Wien Bibliothek.

2.2 Banknotes

Banknotes have been in use for several hundred years, as a more forgery-proof and handy alternative to coins. There is evidence of the first paper banknotes in China as early as the beginning of the 5th century. In Europe, on the other hand, this alternative to coins was not used until more than a millennium later (Beattie, 2015). Nowadays, the use of banknotes is still indispensable in many parts of the world and guarantees the independent and secure circulation of goods and services. Although, cashless payment methods have been increasing over the last decades, and cryptocurrencies are on the rise, cash payments are still among the favorite payment methods in many European countries (statista.com, 2021). As an alternative to conventional paper banknotes, more and more countries, such as Canada, Australia, and New Zealand, are using polymer-based banknotes. These polymer banknotes are famous due to their longer shelf life, and their special resistance to moisture, which makes them very attractive for the use in tropical countries. Moreover, it is claimed that they are more secure against counterfeiting than their paper counterparts (Singh, 2008). Although, the production is more expensive, it was shown by (Wakefield et al., 2019) on the example of Australia, that the use of polymer banknotes can be cost-effective over time. The less durable yet widely established paper-based banknotes are still used in most countries around the world. The substrate of the euro banknotes, for instance, is pure cotton (Yousef et al., 2021). While the end-of-life polymer banknotes usually serve as secondary materials for various recycled plastic products, options for end-of-life paper banknotes are scarce (Worrell, 2014). Due to this lack of alternatives, the life cycle of a euro bill usually ends after approximately 3 years in incineration (Luján-Ornelas et al., 2018). Although at least the thermal energy is used, a valuable resource is destroyed, and a significant amount of greenhouse gases is produced. The results of this master thesis could offer a possible alternative to recycle this extremely valuable resource of cotton fibers and give used euro banknotes a new life.

A single banknote consists of many components and can be considered as a highly heterogeneous substrate. However, the core (cotton) is the same and similar characteristic features can be found in all natural – polymer - based euro banknotes (Yousef et al., 2021). Figure 2 depicts typical features found on euro banknotes (ecb.europa.eu, 2022). A magnetic strip is incorporated into each banknote, which helps ATMs to read the bill. In addition, there are various security features that are intended to guarantee that the banknotes are forgery-prove. Polymers are used in some cases for this purpose.

Die approbierte gedruckte Originalversion dieser Diplomarbeit ist an der TU Wien Bibliothek verfügbar
The approved original version of this thesis is available in print at TU Wien Bibliothek.
TU Bibliothek Your knowledge hub WIEN

A special process known as intaglio printing is used to color the banknotes. The colors used are organic compounds which often contain metals or metallic complexes. Moreover, small denominations (5€, 10€ and 20€) have a polymer protective coating to increase their lifespan, due to the increased use of these bills (ecb.europa.eu, 2022).

Figure 2. Illustration of a 5€ Banknote-Specimen and its features (ecb.europa.eu, 2022).

To summarize, euro banknotes primarily consist of pure cotton, which is the substrate and accounts for about 90% of the BNs. The rest are additives like polymers, other organic compounds as well as metals and metallic complexes. These additives are responsible for the coloring, increased lifetime, or security of the banknotes. The object of interest of this master thesis was the cotton substrate. Consequently, all additives are considered as, and will henceforth called contaminations. One main objective was to figure out a process to separate the non-cellulosic fraction from the cotton.

Die approbierte gedruckte Originalversion dieser Diplomarbeit ist an der TU Wien Bibliothek verfügbar
The approved original version of this thesis is available in print at TU Wien Bibliothek.

2.3 Cellulose

Cellulose is the most abundant organic compound and polysaccharide as well as the most common and inexhaustible biomolecule on earth. Cellulose is the main component of secondary cell walls in plants (e.g., wood, hemp etc.) and most forms of algae. It is also produced by tunicates and some form of bacteria. (S. Kalia et al., 2011).

Its D – glucose monomers are covalently bond through an oxygen element by C1 of one glucose ring and C4 of the following glucose ring forming the so-called β (1-4) glycosidic bond (Bajpai, 2017). Resulting in a linear polymer with both reducing properties on the one side of the cellulose chain and non-reducing properties (C4 – OH bond) on the other end of the polymer chain. In Figure 3 the molecular structure of cellulose is illustrated (Klemm et al., 2005).

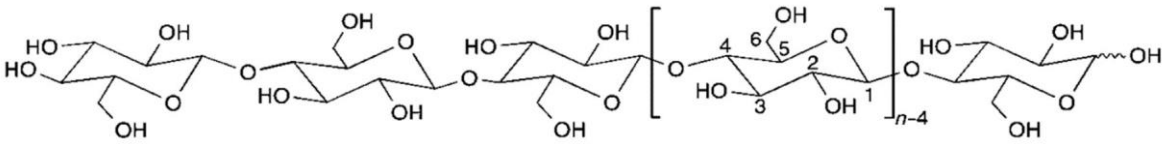

Figure 3. Molecular structure of cellulose. D - glucose monomer units linked by β (1-4) D - glycosidic bonds with n as the degree of polymerization (Klemm et al, 2005).

The degree of polymerization (DP), the number of repetitions of glucose units in the cellulose chain, can differ greatly from one substrate to another. Usually, the DP is around 15.000 for native cellulose (O'sullivan, 1996).

The three different hydroxy groups present in the cellulose chain at C6, C2 and C3 are responsible for the formation of hydrogen bonds both within the molecule itself (intramolecular bonds) and with adjacent molecules (intermolecular bonds). These intra- and intermolecular bonds do not only stabilize the structure and are responsible for a high axial stiffness (Bajpai, 2017) but are also responsible for the cellulose tendency to form parallel arrangements of crystallites and crystalline strands. Moreover, intermolecular bonds are the reason for the formation of cellulose sheets (Nishiyama et al., 2002). Ultimately, the cellulose structure comprises highly ordered (crystalline) and less ordered (amorphous) regions. The ratios of crystalline and amorphous regions can differ severely, depending on the origin of the cellulose (O'sullivan, 1996). Undoubtably, structural as well as mechanical and chemical properties (e.g., stiffness, solubility, etc.) highly depend on the composition of the cellulose (Gardivert, 1975).

Die approbierte gedruckte Originalversion dieser Diplomarbeit ist an der TU Wien Bibliothek verfügbar
The approved original version of this thesis is available in print at TU Wien Bibliothek.

Different crystalline modifications within the cellulose exist. These polymorphs can be distinguished and are usually categorized in four major groups: cellulose I, II, III & IV. Cellulose I, also referred to as natural or native cellulose is characterized mainly by its exclusively parallel oriented chains which are oriented in the same direction (Gross & Chu, 2010). Cellulose I can be subdivided in Cellulose I_α & I_β and is found in plants, algae, and bacterial cellulose in different concentrations while one of them is usually more dominant. While the I_α crystal structure comprises of a triclinic unit cell with one chain, the I_β crystal structure displays a monolithic unit cell with two chains (Maurer et al., 2013).

Cellulose II can be directly obtained from cellulose I (see Figure 4 (O'sullivan, 1996)). It is either obtained by regeneration or by mercerization. For the regeneration process, the cellulose is dissolved in a suitable solvent and subsequently recrystallized in water. Mercerization is done by treating cellulose I in alkaline conditions. Cellulose II shows a more stable structure and is more thermodynamically stable compared to cellulose I (Maurer et al., 2013). Moreover, it is the most common polymorph found in most commercially produced man-made cellulose fibres.

Cellulose III_I and III_{II} is synthesized directly from cellulose I and II by liquid ammonia treatment at -80°C, respectively. Finally, cellulose IV_I and IV_{II} can be obtained by thermal treatment of cellulose III_I and III_{II} in glycerol, respectively (Wada et al., 2004)

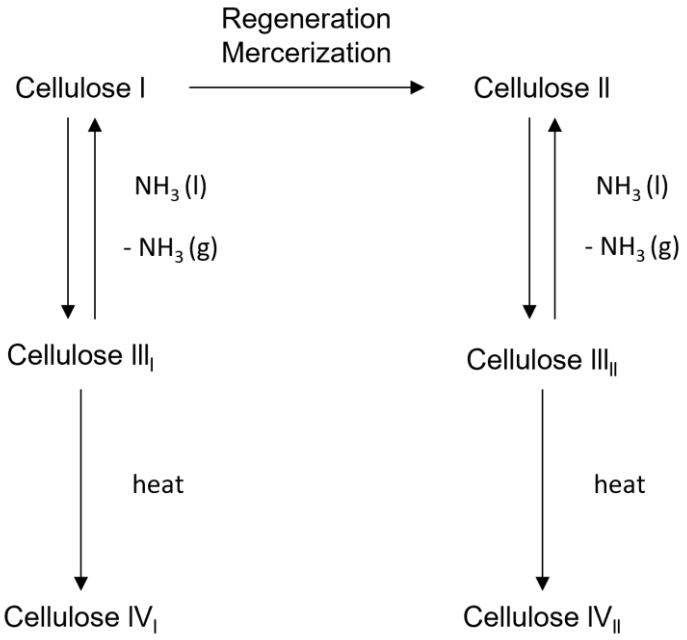

Figure 4. Interconversions of the polymorphs of cellulose (O´Sullivan, 1996)

Die approbierte gedruckte Originalversion dieser Diplomarbeit ist an der TU Wien Bibliothek verfügbar
The approved original version of this thesis is available in print at TU Wien Bibliothek.

2.4 Cellulose Solvents

Cellulose is not soluble in water and many other polar and non-polar solvents, mainly due to its strong intra- and intermolecular hydrogen bonds and crystalline domains (Klemm et al., 2005). Dissolution of cellulose was researched early on, and research is still ongoing to improve methods or find new ways to dissolve cellulose. Many methods already exist, especially in the field of cellulose-based material production.

A very common cellulose solvent used in the lyocell fiber process is N-methylmorpholine-N-oxide (NMMO) (Eichinger & Eibl M., 1996). The disadvantages of this process include the poor thermal stability of NMMO, as well as problems with the recyclability. Also, side reactions followed by solvent and cellulose degradation cannot be ruled out because of its strong oxidizing behavior (Wang et al., 2012) (Rosenau et al., 2001).

Other cellulose solvents are LiOH/urea and NaOH/urea aqueous solutions, which dissolve cellulose easily and quickly at low temperatures below -10° (Cai & Zhang, 2005). However, these methods are not yet sufficiently explored. In addition, the low temperatures pose problems, since it is very energy intensive and such processes do not seem efficient on a larger scale.

Another method for cellulose dissolution is the use of LiCl salt dissolved in Dimethylacetamide (DMAc). Since this method was used in this work, it will now be explained in more detail. To dissolve the cellulose in a supersaturated LiCl /DMAc solution, the cellulose must first be activated, e.g., with water and acetone. If water is used it must be replaced by solvent exchange, since the presence of water has a significant influence on the solubility (Chrapava et al., 2003). The exact dissolution process is still widely debated but can best be described as follows (Striegel, 2002). The Cl^- anion is separated from the Li^+ cation due to the cations interaction with the oxygen of the amide group of the DMAc, forming a $[DMAc_n + Li]^+$ macro-cation. These macro-cations form weak interactions with the cellulose oxygens while the Cl^- anions disrupt the hydrogen bonds within the cellulose (see Figure 5 (Zhang et al., 2014)), thereby breaking up the strong intra- and intermolecular bonds and ultimately dissolving cellulose strains. The dissolution can take place at room temperature as well at elevated temperatures. However, it should be mentioned that degradation of cellulose can be expected at elevated temperatures (Potthast et al., 2002).

Die approbierte gedruckte Originalversion dieser Diplomarbeit ist an der TU Wien Bibliothek verfügbar
The approved original version of this thesis is available in print at TU Wien Bibliothek.
TU Bibliothek Your knowledge hub WIEN

The main advantage of this method is the cellulose solubility at room temperatures. The weak points are the poor recyclability of the solvent and the price of the chemicals used.

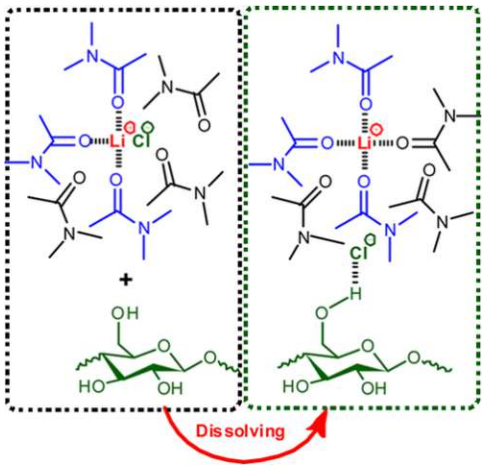

Figure 5. Dissolution process of cellulose in LiCl / DMAc solution (Zhang et al., 2014).

A more recent method in the field of cellulose-based material production is the use of so-called ionic liquids (ILs) as a cellulose solvent. ILs have been known since the mid-19th century and are sometimes described as liquid salts or liquids composed entirely of ions. Today, they are often referred to as high potential green solvents. As diverse as the set of different ionic liquids is, so are the application areas today. ILs are used in the pharmaceutical industry, biochemical processes, rare earth recycling, and many other areas (MacFarlane et al., 2017). The discovery of cellulose dissolution in an ionic liquid was made by Graenacher as early as 1934, although widespread attention came decades later when direct dissolution and regeneration of cellulose became of interest (Swatloski et al., 2002).

Said knowledge is also applied in the Ioncell® process. ILs are used as a solvent to dissolve the cellulose based starting material. This IL- cellulose solution is subsequently extruded through a spinneret into a water bath where the cellulose is regenerated, and fibers are formed. The main ionic liquids currently used in the Ioncell® process are [DBUH][OAc], [mTBDH][OAc] and [DBNH][OAc] which are depicted in Figure 6.

Die approbierte gedruckte Originalversion dieser Diplomarbeit ist an der TU Wien Bibliothek verfügbar
The approved original version of this thesis is available in print at TU Wien Bibliothek.

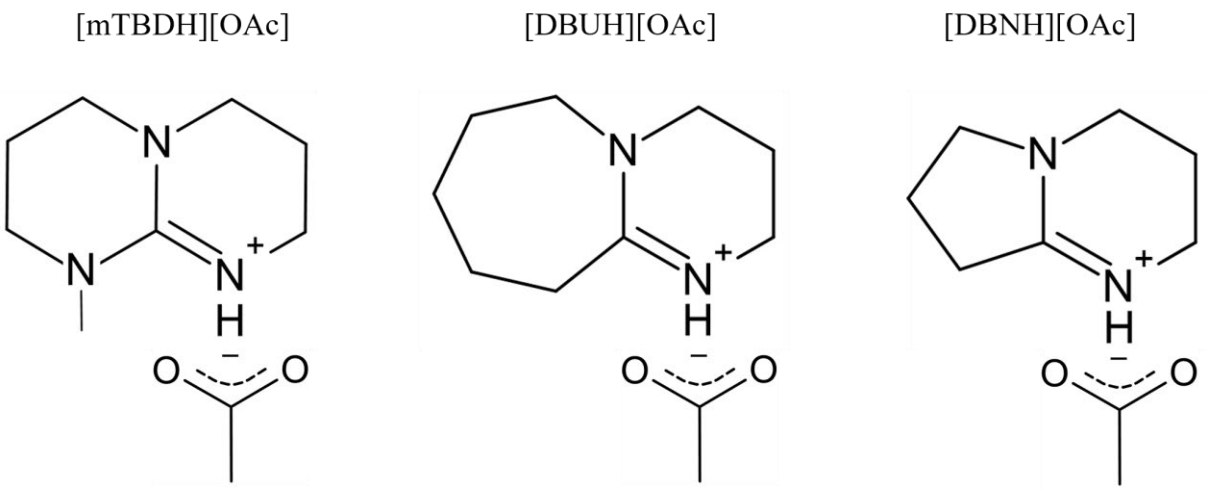

Figure 6. Three different ionic liquids currently used in the Ioncell® process.

The exact mechanism behind the dissolution of cellulose in the IL is not trivial and has not yet been fully researched. However, it has been proven that both the cation and the anion contribute to the dissolution (Parviainen et al., 2013), see Figure 7. The anions are presumably responsible for the actual dissolution process through interaction with the hydrogen bonds present in the cellulose (Pinkert et al., 2009) (Sun et al., 2009) (Wang et al., 2012). These interactions cause the intermolecular bonds to break, leading to an opening of the molecular structure and ultimately to a dissolution of the cellulose in the IL.

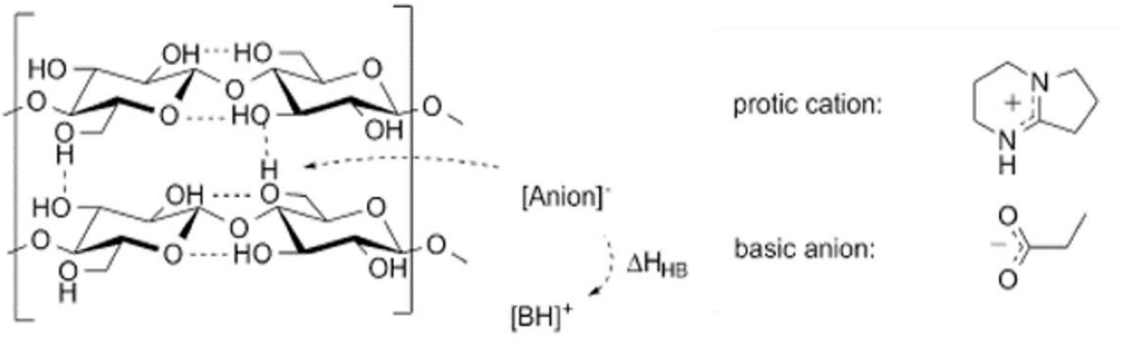

Figure 7. Cellulose-dissolution model in protic ILs with competitive hydrogen-bond donation from cellulose and the protic cation with the basic anion. (Parviainen et al., 2013).

Die approbierte gedruckte Originalversion dieser Diplomarbeit ist an der TU Wien Bibliothek verfügbar
The approved original version of this thesis is available in print at TU Wien Bibliothek.

2.5 Dry-jet wet Spinning

The dry- jet wet spinning process is the second most used process for producing cellulose-based regenerated fibers, after wet spinning, which is used in the viscose process (Ma, 2018). In either of these processes, the cellulose is first dissolved using a suitable solvent. Next the cellulose solution is extruded through a spinneret and immersed into a bath filled with an anti-solvent. In the wet spinning process, the spinneret is placed in the coagulation bath and the dissolved cellulose solution is directly extruded into the bath, where the cellulose immediately regenerates. The formed filaments are guided through the bath and stretched. In the dry- jet wet spinning process, the spinneret is located outside the bath. The polymer solution is extruded and stretched into an air gap. The cellulose is regenerated in a water bath and fibers are guided to godets. Figure 8 illustrates a simplified dry- jet wet spinning system (Michud, 2016).

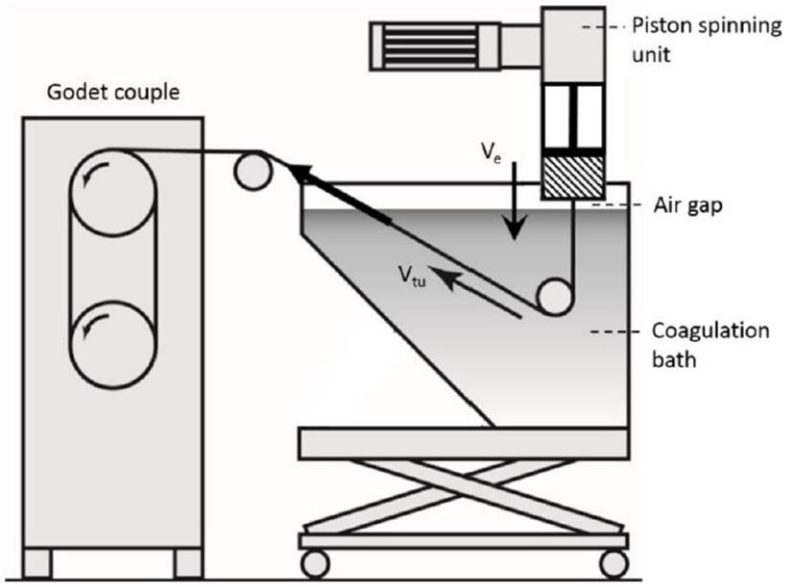

Figure 8. Simplified illustration of a Dry- Jet Wet Spinning Unit (Michud., 2016).

In the course of the dry-jet wet spinning process, the cellulose solvent solution, the so-called dope, is placed in the piston, where a heating jacket ensures that the dope is heated up and kept at a constant temperature suitable for the spinning process. By properly adjusting the temperature, the viscoelastic properties of the dope solution can be set. This has a major influence on the spinnability of a dope and furthermore affects the properties of the produced fibers (Sixta et al., 2015). Subsequently the solution is extruded through the spinneret at a certain extrusion velocity (V_e).

Die approbierte gedruckte Originalversion dieser Diplomarbeit ist an der TU Wien Bibliothek verfügbar
The approved original version of this thesis is available in print at TU Wien Bibliothek.

By adjusting the speed of the collecting rolls (godets) (V_{tu}) the filaments are stretched, and the desired DR can be achieved. The DR is the ratio of the take up velocity and the extrusion velocity (Hauru et al., 2014).

The final structure of the polymer chains is influenced by the spinning process. Depending on the processing stage the polymer experiences various structural changes. The steps leading to the final structure formation are illustrated in Figure 9 (Hauru, 2017). First the cellulose (a) is dissolved in the ionic liquid at elevated temperatures, filtered and transferred into the piston where the polymer chains are present in a very disordered manner (b and c). The heated dope is extruded under pressure through the spinneret inlet cone (d) and the capillary (e). Die swell occurs at the beginning of the air gap (f). The filament is stretched and cooled in the air gap, where the polymer chains begin slightly to orient (g), while the relaxation of the fiber orientation finally happens in the coagulation bath. The polymer is desolvated with the antisolvent (h). Crystalline parts are finally formed by washing and drying of the fibers (i and j) (Sixta et al., 2015).

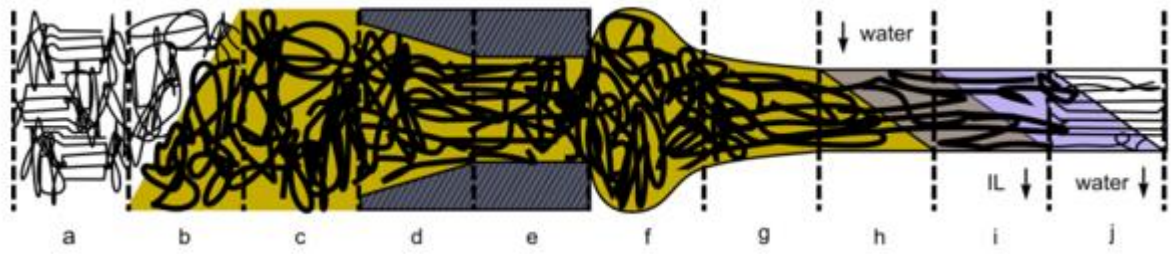

Figure 9. Structure formation steps: a) cellulose, b) dissolution, c) solution, d) inlet cone, e) capillary, f) die swell, g) draw, h) desolvation, i) washing, j) drying (Hauru, 2017).

Die approbierte gedruckte Originalversion dieser Diplomarbeit ist an der TU Wien Bibliothek verfügbar
The approved original version of this thesis is available in print at TU Wien Bibliothek.

3. Material and Methods

In the following section the details are explained, and the used materials are described.

3.1 Banknotes

The Banknotes, which were used for the investigations in this thesis were provided by two different cooperation partners:

1. Federico Frascà (Ferrara University, Italy)

2. Bank of Finland

(a) (b)

Figure 10. Banknotes provided by Federico Frascà (a) and by the Bank of Finland (b).

Banknotes from Frederico Frascà were received on 06.03.2020. The initial raw material consisted of small, shredded banknotes with a size of approximately 2x6 mm, pressed into two bales with a mass of 736 g in total. By taking a closer look at the individual stripes, most of them can be allocated as 5€ banknotes. Above all, the color and pattern largely agree with the 5€, see Figure 10 (a). The emerald, green security pattern and the shiny security stripe are also clearly visible. Assuming that all the banknotes are 5€ banknotes, the value of these 2 bales is approximately 5250€ (5€ banknote ~ 0.7 g). No precise statements about the contamination due to daily use can be made.

Die approbierte gedruckte Originalversion dieser Diplomarbeit ist an der TU Wien Bibliothek verfügbar
The approved original version of this thesis is available in print at TU Wien Bibliothek.

The banknotes provided by the Bank of Finland were received on 11.05.2021. The original raw material consisted of small, shredded banknotes measuring approximately 2x11 mm and was delivered in large plastic bags. According to the Bank of Finland and visual observation, the mix consisted of all 13 different Euro banknote bills in circulation in Europe (see Figure 10 (b)). The total quantity of banknotes was 4.9 kg. According to Yousef et al. (2021) and under the assumption that 10 euro is the main series this amount equals roughly 4.6 million euros. However according to the Bank of Finland it is equivalent to approximately €100.000. As the banknotes were withdrawn from circulation, additional contamination from daily use cannot be ruled out. Traces of hazardous microorganisms (Mändar et al., 2016), widely spread drugs such as cocaine (Troiano et al., 2017), or other organic contaminations might be present.

The banknotes obtained from Frederico Frascà served as the object of study initially. However, due to the limited quantity, the banknote mixture provided by the Bank of Finland was used for further investigations as well as for the main part of the research, including fiber production. Consequently, all results presented in this thesis are achieved by using this batch. These banknotes will henceforth be referred to as BN for banknote or BNs for banknotes.

3.2 Pre-Treatment of Banknotes

To ensure a stable spinning process and to produce durable fibers, it is important to purify the cellulose as much as possible. In the course of this work, numerous trials were carried out to remove the non-cellulosic compounds. Through trial and error, the following sequence of pre-treatment steps, shown in Figure 11, has proven successful to gradually reduce the contamination of the specimen in question and to access the cotton core.

Figure 11. Developed pre-treatment sequence to remove non-cellulosic compounds from euro banknotes.

The pre-treatment process developed during this thesis in order to remove non-cellulosic compounds from the banknotes is summarized and depicted in Figure 11. Initially the BNs were milled using a Wiley mill 475 – A (Thomas Scientific, USA) followed by the sieving procedure using a Retsch woven wire mesh sieve with a mesh size of 200µm.

Die approbierte gedruckte Originalversion dieser Diplomarbeit ist an der TU Wien Bibliothek verfügbar
The approved original version of this thesis is available in print at TU Wien Bibliothek.

Particles bigger than 200µm were subsequently subjected to a magnetic treatment in aqueous conditions using a big permanent magnet. The ensuing treatment with an excess amount of acetone was followed by a bleaching treatment with a specific amount of sodium hypochlorite. This bleached material was the starting product to produce green fibers. By implementing further treatment steps, it was possible to reduce the non-cellulosic compounds to a minimum, to produce almost pure white cotton and to spin white fibers. For this purpose, the bleached BNs were dissolved in a supersaturated 90 g/l LiCl / DMAc solution at room temperature. A highly viscose blue greenish solution was received, which was further centrifuged at 4000 rpm at 4°C. Green pigments were separated and the white cellulose was regenerated. This white cellulose was used to produce white fibers.

The influence of the pre-treatment on the chemical composition and physical properties was investigated in detail. The results can be found under section 4.1.

Die approbierte gedruckte Originalversion dieser Diplomarbeit ist an der TU Wien Bibliothek verfügbar
The approved original version of this thesis is available in print at TU Wien Bibliothek.

In the following subsections, each treatment step is explained in detail. Additionally, all failed tests during the investigation are listed and explained shortly under 3.2.8.

3.2.1 Milling

To ensure homogeneity of the samples and to make the cellulose more accessible, the banknotes were milled. The initial raw material was ground using a Wiley mill 475 – A (Thomas Scientific, USA) with a screen size 30 mesh. The material is introduced into the milling chamber, where it is shredded by stationary and rotating knives. Particles fine enough, pass through the screen and are collected. The grinding of the BNs resulted in a rather dry, powdery consistency with small flat sheets and fluffy webs in between. The exact size and size distribution of the particles can be found under section 4.1.1.

3.2.2 Sieving

By means of particle size distribution analysis (PSD-analysis) the presence of 2 types of particles, flat sheets and small, dark, fluffy webs was confirmed. For separation a sieving step was implemented. Therefore a "Retsch woven wire mesh sieve" with a mesh size of 200 µm was used. The milled and dried BNs were added to the sieve and shaken manually, until the two fractions were separated completely (controlled by PSD-analysis). Particles smaller than 200 µm (BN $p < 200\mu m$) showed a higher contamination, thus these particles were excluded from further treatment and discarded. However, a significant amount of cellulose was lost in this step. The particles bigger than 200 µm (BN $p > 200$ µm), were kept for further treatment.

3.2.3 Magnetic Separation

Paramagnetic compounds of the magnetic security thread were removed by a simple mechanical separation via a magnet. Carrying out the separation in water, using a strong permanent magnet has proven as quite effective. The principle used here, can be compared to a magneto gravimetric separation process (Zimmels et al., 1977). The water-BN suspension was stirred, while the magnet was submerged in the container. Particles with paramagnetic compounds stuck to the magnet. By pulling out the magnet, these could be separated from the non-magnetic fraction. This procedure was repeated until no particles stuck to the magnet anymore.

Die approbierte gedruckte Originalversion dieser Diplomarbeit ist an der TU Wien Bibliothek verfügbar
The approved original version of this thesis is available in print at TU Wien Bibliothek.
TU Bibliothek Your knowledge hub WIEN

The water was removed from the banknotes and a drying step was conducted. The paramagnetic fraction was excluded from further treatment and discarded. The loss of cellulose during this treatment step was rather small and was neglected. The banknotes free from paramagnetic materials were treated further.

3.2.4 Acetone Treatment

Acetone (C_3H_6O) is a very powerful and widely used solvent. By using acetone, it was possible to dissolve and remove colors (mainly red and orange) from the BNs. The pre-treated banknotes were added to an excess of acetone and stirred at room temperature for several minutes. The mixture was subsequently filtered, and the acetone was recovered using a Rotavapor Büchi R210 (Büchi AG, Switzerland) at 40°C and below 250 mbar. The recovered acetone was again added to the BNs and stirred at room temperature for several minutes. This process was repeated until no visible dissolution of colors was observed anymore. The treated material was brighter and greenish. The BNs were air-dried and treated further.

3.2.5 Bleaching

Furthermore, the BNs were bleached to further reduce the impurities. Therefore, treatment with sodium hypochlorite (NaClO) was performed. Sodium hypochlorite is a well-known bleaching agent commonly used in the pulp and paper industry. For the treatment the pH value must be adjusted to approximately pH = 7.5 – 10.0. If the pH drops to pH = 2 or below, chlorine gas is formed (Farr et al., 2003). To avoid intoxication by chlorine gas formation, the experiments were carried out in an airtight, customized apparatus in which the effluent gas was directed through a KI solution to bind the Cl_2 gas. First, a water bath was heated to 40°C. Deionized water (400 ml) and a 12% sodium hypochlorite solution (8 ml) were added to a 3 necked round bottom flask and positioned in the water bath. A magnetic stirrer was added, and the temperature was measured via an analogue thermometer. The flask was connected to a washing bottle, filled with 20% KI aqueous solution by a gas line. Additionally, the flask was equipped with a dropping funnel filled with sufficient HCl (1 molar). The pH was adjusted to pH = 8-9 by adding HCl (approximately 1.5 ml), which was checked using pH- indicator strips (pH 0-14). The solution was brought to process temperature and the sample was added (30 g) under constant magnetic stirring. After the reaction time was elapsed (60 min), more HCl was added until a pH of 1 was reached. Due to the low pH, the remaining hypochlorite reacted.

Die approbierte gedruckte Originalversion dieser Diplomarbeit ist an der TU Wien Bibliothek verfügbar
The approved original version of this thesis is available in print at TU Wien Bibliothek.
TU Bibliothek Your knowledge hub WIEN

Next, NaOH (1 molar) was added until a final pH of 7 was reached. The chamber was purged with air and finally the samples were washed with deionized water, filtered and air dried.

Bleaching resulted in a significant improvement in brightness. However, the green pigments remained in the banknotes. Many other tests have also shown that the green color in particular was extremely stable. For this reason, two different methods were chosen from here on. On the one hand, green fibers were produced from the bleached banknotes. On the other hand, banknotes were first completely freed of color in order to obtain white cellulose. However, since the resistant green pigments were difficult or almost impossible to dissolve, the goal was to dissolve the cellulose rather than the pigments and gain the pure cellulose from precipitation.

3.2.6 LiCl/DMAc Dissolution

The banknotes were dissolved in a super saturated 90 g/l LiCl / DMAc solution. Therefore, the LiCl/DMAc solution was prepared according to (Dupont, 2003). Water can hinder a proper solution of cellulose (Chrapava et al., 2003) (Dupont, 2003). To guarantee a proper solution cellulose has to be activated. There are several options to do so. Here, the activation was carried out according to (Chrapava et al., 2003). The BNs were activated by solvent exchange from water to acetone to DMAc by covering the samples in solution overnight, respectively. Subsequently, the excess DMAc used for activation was filtered off. The activated banknotes were then swiftly transferred into the LiCl/DMAc solution under constant stirring resulting in a concentration of 10 g/l BNs to LiCl/DMAc. The solution was stirred at room temperature until all the banknotes were dissolved, resulting in a highly viscose blue-greenish solution.

3.2.7 Sedimentation & Precipitation

The blue greenish LiCl/DMAc – BN solution was treated using a Thermo Scientific SL40FR Centrifuge. By centrifuging the solution at 4000 rpm, 4°C for 1h it was possible to separate the dissolved cellulose from the undissolved colored pigments. The purified solution was simply decanted into a separate container. The cellulose was subsequently precipitated using an excess of deionized water. The cellulose was separated by filtration, dried at 105°C for several hours, grinded and afterwards used for the spinning of white fibers.

Die approbierte gedruckte Originalversion dieser Diplomarbeit ist an der TU Wien Bibliothek verfügbar
The approved original version of this thesis is available in print at TU Wien Bibliothek.

3.2.8 Unsuccessful Tests

Many attempts have been made to reduce the share of contaminations of the banknotes, not always with success. The following are those attempts that did not lead to a noticeable improvement or which were too aggressive towards the cellulose.

Acetic Treatment

In analogy to Yousef et al. (2021) the effect of nitric acid on the BN was investigated as an attempt to destroy non-cellulosic compounds. 100 g/l ground BNs were treated at 70°C for 10, 20 and 30 minutes, respectively under constant stirring with HNO_3. In the first trial a HNO_3 concentration of 2 mol/liter was chosen. This treatment showed no effect. Next, the HNO_3 concentration was increased to 3 mol/liter. Opposed to Yousef et al., (2021) a reduction of the impurities was not achieved. Into the bargain, a significant decrease in particle size and a severe reduction of the intrinsic viscosity (by up to 70%) was observed. Due to the low effectiveness and harshness of this method, it was not further investigated.

Dimethyl sulfoxide Treatment

3 g banknotes were treated with 10 ml dimethyl sulfoxide (DMSO) at 50 °C for 2h. This was an attempt to dissolve and separate organic compounds from the banknotes as proposed by Yousef et al. (2021). The treatment showed little to no effect and therefore this path was not further examined.

Alkaline Treatment

A 9% sodium hydroxide solution was used to investigate its effect on the milled BNs. Treatment of 100 g/l ground banknotes in NaOH under constant stirring for 60 minutes at 100°C showed little to almost no effect. Due to these circumstances, no further action was taken in this direction.

Die approbierte gedruckte Originalversion dieser Diplomarbeit ist an der TU Wien Bibliothek verfügbar
The approved original version of this thesis is available in print at TU Wien Bibliothek.

Ozone Bleaching

Ozone bleaching is in general a very effective method to increase the brightness of various materials (e.g., pulps, fibers, fabric, etc.). Here, it was attempted to bleach the acetone treated and sodium-hypochlorite bleached banknotes as well as the green fibers with ozone, respectively. First, the pH value was set close to 2 in order to increase selectivity and effectiveness (Tripathi et al., 2019). Ozone was produced by an Wedeco GSO 30 ozone generator (Wedeco ITT industries, United States) and the sample, which was attached to the system via a round bottom flask, was exposed to the ozone stream for a defined period. To ensure safety and avoid intoxication due to ozone inhalation, additional safety measures were taken (gas mask, neutralization of the excess of ozone by KI- solution). Despite partly extended treatment times, no major differences in brightness were observed. Especially the green pigment remained unaffected.

Flotation

The flotation process is a common technique in many recycling processes, e.g., the deinking of paper. Thereby, the separation of particles is conducted based on the hydrophilicity and hydrophobicity of molecules. A detergent (in this case, sodium stearate) is added to the flotation cell. Air is dispersed, resulting in the formation of bubbles. Hydrophobic particles adhere to the bubbles and float to the top. By a turning rake these particles are removed. Milled as well as acetone treated BNs were treated in a self-made laboratory scale flotation cell. The samples were treated according to Ma et al. (2018). Unfortunately, no purification was achieved.

Dissolution in NaOH/Urea aqueous solution

Inspired by the paper of (Cai et al.2004) the dissolution behavior of cellulose in an NaOH Urea-aqueous solution was investigated. It is stated that cellulose shows an almost instant dissolution in a NaOH - Urea aqueous solution (7:12:81 by weight ratio) at temperatures below -5°C. In this trial approximately 14 g of banknotes were pretreated (shredded, sieved, magnetic treatment and acetone treatment, respectively) and finally, added to the above-mentioned solution. The solution was precooled to -10°C using ethanol and liquid nitrogen. After several minutes of stirring only a marginal dissolution of cellulose was noticed. Therefore, this path was not further investigated.

Die approbierte gedruckte Originalversion dieser Diplomarbeit ist an der TU Wien Bibliothek verfügbar
The approved original version of this thesis is available in print at TU Wien Bibliothek.
TU Bibliothek Your knowledge hub WIEN

Cellulose Separation in LiCl/DMAc Solution

Several trials were conducted to separate the green color from a cellulose - LiCl/DMAc solution. The solution was filtered through several layers of filters (mesh size 9µm) at elevated temperatures using a heated hydraulic manual filtration unit. The filtration caused only a slight decolorization. A very effective filtration method was using a syringe with a 0.45 µm syringe filter. The filtrate became colorless and clear, the regenerated cellulose was bright and white. Though, this could not be scaled up due to lack of larger filters with a similar mesh size.

Furthermore, an attempt was made to purify the solution by phase separation using various solvents (Dichloromethane (DCM)/ Hexane / water). For this purpose, the solution and the solvent were placed in a separation funnel and then shaken properly. Only in DCM a slight dissolution of the green color was recognized. However, not all the colors could be removed from the LiCl/DMAc solution. It is possible that a greater effect could have been achieved by using more DCM, but this was not pursued further.

Die approbierte gedruckte Originalversion dieser Diplomarbeit ist an der TU Wien Bibliothek verfügbar
The approved original version of this thesis is available in print at TU Wien Bibliothek.

3.3 Particle Size Distribution

To obtain information on the particle sizes and particle size distribution (PSD) of the ground materials, samples were measured using a Malvern Mastersizer 2000 (UK) (Leykin & Ioelovich, 2004). Thereby, the samples are dispersed in deionized water using a Hydro 2000 MU wet dispersion unit and then measured by laser diffraction using a helium-neon laser and a solid-state light source (with particle refractive index = 1.59, particle absorption index = 0.1 and a dispersant refractive index = 1.33). The particle size range was between 2 µm and 2000 µm. The particle size distribution was measured for each of the previously mentioned pre-treatment steps, respectively. The effect of the pre-treatment steps on the particle size and particle size distribution can be found in section 4.1.1.

3.4 Ash Content

The ash content was determined according to ISO 1762:2019 for paper, board, pulp, and cellulose nanomaterials. By treating the dried and ground samples at a constant temperature of 575°C for 5 hours in a suitable muffle furnace (SELECTA-HORN), the organic compounds are oxidized. The residues are inorganic compounds, and the amount helps to define the purity of the samples. The amount of ash is expressed in weight percent related to the dried initial sample.

Table 1. Mean values [%] and standard deviations σ [%] of ash-content measurements.

SAMPLE	Ø Ash-content [%]	σ [%]
Milled Banknotes	7.49	0.44
Sieved Banknotes (p>200µm)	6.77	0.14
Sieved Banknotes (p<200µm)	7.39	0.28
Magnetic treated Banknotes	5.69	0.50
Paramagnetic Fraction	14.69	0.49
Acetone treated Banknotes	5.97	0.40
Bleached Banknotes	5.46	0.23
Green BN1 Fibers	4.80	0.12
LiCl cleaned Banknotes	1.45	0.43
Green Pigments (from LiCl solution)	50.71	1.01

Die approbierte gedruckte Originalversion dieser Diplomarbeit ist an der TU Wien Bibliothek verfügbar
The approved original version of this thesis is available in print at TU Wien Bibliothek.

The ash content was determined after each pre-treatment step, of each separated fraction and further of the produced green fibers, respectively. Each sample was measured three times. The mean value and the associated standard deviations are given in Table 1.

3.5 Viscosity Measurement

Intrinsic viscosity was measured according to the standard method Scan-CM 15:88. A certain amount of the sample (120, 150, 200 or 250 mg) was placed in small vessels. 25 ml of deionized water and 5 pieces of copper wire (approximately 2 cm long, with a diameter of 2 mm) were added to each of the vessels and then shaken in a customized shaker for up to 30 minutes. Then, 25 ml of pure cupriethylenediamine (CED) was added to the dissolution vials and shaken again for 30 minutes. This procedure should ensure complete dissolution of the cellulose-based samples. Due to the high dependence of temperature and viscosity, via a water bath the samples were kept at 25°C for several minutes to guarantee standardized conditions. For the measurement a capillary viscosimeter, with a water heating jacket (25 °C) was used. The solution was filled to the viscosimeter and drained without force. Thereby the viscosity is measured by the determination of the speed of the solution in comparison to a standard solution between two calibration points. Each sample was analyzed three times. The measured efflux time in seconds is multiplied with the determined constant of the viscometer (h) resulting in the viscosity ratio η_{rel}. Next, [ŋ]c can be obtained from a table in the standard in relation to η_{rel}. From this value the average viscosity η_{avg} is calculated. In addition, the average viscosity is used to calculate the degree of polymerization (DP). If samples are contaminated with inorganic substances (in this case, metal complexes and other impurities), the sample may not dissolve completely in the CED-water mixture, which can lead to inconclusive results. It should be noted that due to the high percentage of impurities, a complete dissolution of the entire sample was not always achieved. Therefore, these results should serve mainly as an indication for the intrinsic viscosity changes between steps and not as absolute values.

The intrinsic viscosity was determined after each pre-treatment step. The results of the measurements can be found in Table 2 as well as under section 4.1.3.

Die approbierte gedruckte Originalversion dieser Diplomarbeit ist an der TU Wien Bibliothek verfügbar
The approved original version of this thesis is available in print at TU Wien Bibliothek.

Table 2. Results of the intrinsic viscosity measurement of each pre-treatment step

SAMPLE	Ø Intrinsic Viscosity [ml/g]	σ [ml/g]
Milled Banknotes	576.5	6.8
Sieved Banknotes	554.3	6.0
Magnetic treated Banknotes	613.2	14.0
Acetone treated Banknotes	637.1	6.7
Bleached Banknotes	394.4	5.3
LiCl cleaned Banknotes	376.2	14.7

Furthermore, the effect of treatment with sulfuric acid on the intrinsic viscosity of the milled banknotes was investigated (Asaadi et al., 2016). The Banknotes were treated with 0.05 M H_2SO_4, 1:25, for 10, 20, 30 minutes respectively at 80°C. The intrinsic viscosity was determined before treatment as well as after 10-, 20- and 30-minutes treatment, respectively. The results can be found in the table below as well as under section 4.1.3.

Table 3. Results of intrinsic viscosity measurement for Banknotes treated with 0.05 M sulfuric acid for 0, 10, 20 and 30 minutes, respectively.

Treatment Duration	Ø Intrinsic Viscosity [ml/g]	σ [ml/g]
0 minutes	576.5	6.8
10 minutes	434.1	1.1
20 minutes	409.7	0.9
30 minutes	382.1	0.8

3.6 Ionic Liquid

Ionic Liquid (1,5-diazabicyclo (4.3.0) non-5-enium acetate [DBNH][OAc]) was synthesized in a customized 6-liter reactor at Aalto University (Sixta et al., 2015). Equimolar amounts of acetic acid (glacial, 100%, Merck, Germany) were slowly added to 1,5-diazabicyclo (4.3.0) non-5-ene (DBN, CAS: 3001-72-7, 99%, Fluorochem, UK) by using a peristaltic pump. To ensure a complete conversion the solution was stirred at a constant rate for up to 2 hours. Throughout the process, the temperature was kept constant at 70°C using a cooling jacket to avoid overheating due to the exothermic nature of the reaction.

Die approbierte gedruckte Originalversion dieser Diplomarbeit ist an der TU Wien Bibliothek verfügbar
The approved original version of this thesis is available in print at TU Wien Bibliothek.

3.7 Dissolution Studies

The solubility of the differently pretreated banknotes (after acetone treatment, after bleaching, after LiCl/DMAc dissolution, respectively) in [DBNH][OAc] at different temperatures was investigated. A (ZEISS Axio Scope A1, Zeiss AG, Germany) microscope with a heating stage and magnification of 5x and 10x was used. A small amount of banknote sample was placed on the microscope glass plate. Next a small amount of ionic liquid was dropped on it and to establish a homogeneous temperature distribution the measurement chamber was closed via a plate. The heating plate was set to the desired temperatures (80, 85 and 90°C, respectively) and the dissolution process was observed for 30 minutes. Pictures of the process were taken every 10 minutes for documentation. The temperatures showing the best results were consequently used for dope preparation.

3.8 Dope Preparation

The so-called dopes, cellulosic material dissolved in ionic liquid (IL), were prepared in a vertical kneader equipped with vacuum pump and a heating jacket (Sixta et al., 2015). The pretreated banknotes were ground, dried at 105°C in an oven over night and the dry matter content (DMC) was determined, prior to the dissolution. Dopes were prepared from bleached BNs and BNs cleaned by LiCl/DMAc dissolution and precipitation to produce green and white fibers, respectively. A consistency of 13 wt.% BNs, based on dry weight, was used. The IL [DBNH][OAc] was melted at 80°C in a water bath, and then mixed with the Banknotes in the vertical agitator for 180 mins under reduced pressure (below 40 mbar) and constant stirring (30 rpm). Parameters for the dope preparations are summarized in Table 7.

The dissolution behavior of the IL is affected by water (moisture content should be observed) (Troshenkowa et al., 2010). To ensure proper dissolution, the chamber of the kneader should be as dry as possible. Therefore, before adding IL, the chamber was thoroughly cleaned and dried.

Once the BNs were sufficiently dissolved, the dope was filtered by a filter press equipped with a stainless-steel mesh (mesh size 5µm) at 80°C, to remove bigger, undissolved particles. Due to the high proportion of contaminations present in the Banknotes, many undissolved particles have been separated.

Die approbierte gedruckte Originalversion dieser Diplomarbeit ist an der TU Wien Bibliothek verfügbar
The approved original version of this thesis is available in print at TU Wien Bibliothek.
TU Bibliothek Your knowledge hub WIEN

Consequently, the cellulose consistence of the dopes must be considered as <13wt%. The effect of the filtration was monitored by microscopic inspection by taking samples before and after the filtration process. Not all the undissolved particles could be removed by filtration, so some remained in the dope.

The resulting dopes from bleached BNs showed a different appearance compared to standard dopes (Sixta et al. 2015). The dopes were greyish rather than slightly orange. The rheological properties of the prepared dopes have been compared to standard dopes, as shown in section 4.3. The viscoelastic properties of the dope originated from the LiCl/DMAc cleaned BNs were similar to the properties of a standard dope.

3.9 Rheology

For the determination of the rheological properties of the dope an Anton Paar MCR 300 rheometer was used (Asaadi et al., 2018). A rotating plate of 25 mm was used and positioned 1 mm above the heated ground plate. A dynamic frequency sweep within the angular velocity range of 0.1 – 100 s^{-1} at different temperatures in the range of 55 – 85°C was performed. The zero-shear viscosity η_0* and the crossover point of G′ and G″ were determined under the assumption of the validity of the Cox-Merz rule (Sixta et al., 2015).

3.10 Fiber Spinning

Fibers were spun using two different dry-jet wet spinning systems (Sixta et al., 2015), a smaller system (KS15 Fourné, Maschinenbau GmbH, Germany) for smaller dopes and a big spinning unit (KS80 Fourné, Maschinenbau GmbH, Germany) used for one big spinning trial. Each spinning unit is equipped with a spinneret (KS15: monofilament, capillary diameter 100 µm, capillary length 200 µm and KS80: multifilament, 400 holes, capillary diameter 100 µm, capillary length 200 µm), a coagulation bath filled with deionized water (temperature set to 5°C (KS15) and < 11°C (KS80)) and a velocity adjustable godet couple. The dopes were transferred into a cylinder where the temperature was set according to the rheological data to reach the desired viscoelastic properties.

Die approbierte gedruckte Originalversion dieser Diplomarbeit ist an der TU Wien Bibliothek verfügbar
The approved original version of this thesis is available in print at TU Wien Bibliothek.

The dopes were extruded through the spinneret with a constant extrusion throughput of 0.01 $cm^3\ min^{-1}$ and 8.5 $cm^3\ min^{-1}$ for KS 15 and KS 80 respectively (constant extrusion velocity V_e), stretched into an airgap and immersed into the temperature controlled, chilled coagulation bath. The formed filaments were collected at the godet couple, where the take-up velocity (V_{tu}) is adjusted to attain the targeted draw ratios ($DR = V_{tu}/V_e$). The exact spinning conditions for all spinning trials are summarized under Table 9.

The fibers were removed from the godets with a razor blade, washed thoroughly with hot water (approximately 80°C), air dried and subsequently stored under controlled conditions for tensile measurements.

Die approbierte gedruckte Originalversion dieser Diplomarbeit ist an der TU Wien Bibliothek verfügbar
The approved original version of this thesis is available in print at TU Wien Bibliothek.

3.11 Characterization of Fibers

Mechanical as well as chemical and optical properties of the fibers were determined. The methodology of the used analysis procedures is described in the following sections.

3.11.1. Mechanical Properties

Using a Favigraph (Textechno Herbert Stein, Germany) with a load cell of 20cN, the linear density and tenacity measurements of all fibers were performed under dry and wet conditions (Asaadi et al., 2018). Prior to the dry measurements, the fibers were conditioned for at least 24 hours (65 ± 2 % RH, 20 ± 2 ºC). For the wet tensile testing, fibers were first submerged in a water container for 10 seconds then tested under water. Fibers are tested individually, while the linear density is measured according to the vibroscopic method. The tenacity is measured by the principle of constant rate extension under dry as well as wet conditions. For both, dry and wet tensile testing, the gauge length was 20 mm, with a test speed of 20 mm/min and a pretension weight of 100 mg. The pretension for dry and wet tests was 0.6 cN/tex and 0.25 cN/tex, respectively. From each bundle of fibers collected at distinct draw ratios, 20 single fibers were tested, and the results recorded. The results of the tensile testing measurements can be found under section 4.4.2.

3.11.2. Birefringence

By determining the birefringence Δn (Asaadi et al., 2018), the optical property of a fiber to polarize light (refractive index), an estimate of the orientation factor of the fiber can be made (de Vries, 1959). For the measurement three fibers with similar linear densities were aligned and fixed on a microscope glass slide using double-sided tape. By means of a Zeiss Axio Scope A1 polarizing microscope with a B 5λ-Berek kipp-compensator three spots were analyzed. From each spot, the optical retardation Γ is determined. Assuming the cellulose density value is 1.5 g/cm^3 (Männer et al., 2001), the diameter of the filament (d_s) can be calculated from the linear density. Finally, the birefringence Δn is defined as the quotient of the optical retardation Γ and the diameter (d_s) (see Equation (2)).

Die approbierte gedruckte Originalversion dieser Diplomarbeit ist an der TU Wien Bibliothek verfügbar
The approved original version of this thesis is available in print at TU Wien Bibliothek.

$$\Delta n = \frac{\Gamma}{d_s} \quad (2)$$

The total orientation factor (f_t) can be calculated as the ratio of the birefringence and the maximum birefringence of cellulose 0.062 (Adusumalli et al., 2009). The results of the birefringence measurements can be found under section 4.4.3.

3.11.3. Scanning Electron Microscopy

The surface and cross-section morphology of the fibers were investigated using a Zeiss Sigma VP SEM operating at 2 kV and 3 kV, respectively. To properly analyze the cross-section a clean cut must be guaranteed (Ma et al., 2015). Therefore, a bundle of fibers is tensioned in an aluminum tray and covered with water. The water is frozen by the use of liquid nitrogen. The ice is broken and simultaneously the fibers as well. The fibers are air dried overnight and placed on the sample holder. Via a Quorum Q150R S plus sputter unit the fibers were coated. Thereby, an even, electrically conductive thin layer of Gold/Palladium (80 Au/20 Pd) is applied (deposition rate of approximately 11.8 nm/min in Argon atmosphere at 0.3 bar). 90 seconds of sputtering is applied to the samples resulting in a layer thickness of approximately 17.7 nm. Green and white fibers were analyzed and are depicted under section 4.4.4.

3.11.4. Gel Permeation Chromatography

Gel permeation chromatography (GPC), sometimes also referred to as size exclusion chromatography (SEC) is a powerful tool to determine the molar mass distribution of pulps and fibers (Pitkänen & Sixta, 2020). For this purpose, the cellulosic samples are dissolved in 90 g/L LiCl - N,N-dimethylacetamide (DMAc) solution at room temperature under constant stirring. Prior to that, the samples are activated in deionized water, acetone, and DMAc for several hours, respectively. Finally, the dissolved samples are diluted with pure DMAc resulting in a sample concentration of 1 g/L and a LiCl concentration of 9 g/L. Next, the samples are transferred into syringes and filtered through 0.2 µm syringe filters and analyzed using a Dionex Ultimate 3000 module (Thermo Fisher Scientific Inc., Waltham, US) equipped with a Shodex DRI (RI-101) (Showa Denko, Ogimachi, Japan), and Viscotek/Malvern SEC/MALS 20 multi-angle light-scattering (MALS) detector (Malvern Panalytical Ltd., Malvern, UK).

Die approbierte gedruckte Originalversion dieser Diplomarbeit ist an der TU Wien Bibliothek verfügbar
The approved original version of this thesis is available in print at TU Wien Bibliothek.

3.11.5. X-Ray Diffraction Measurements

X-ray diffraction (XRD) is a very useful and widely used non-destructive measurement method for characterizing the crystalline structure of matter (Moriam et al., 2021). An incident X-ray beam is focused on the sample surface and diffracted in many specific directions caused by the crystalline structure, more specifically by the interaction of the beam with the electron shell of periodically arranged atoms. The intensity of these diffracted beams varies. By measuring the angles and the intensities of the diffracted beams, one can determine the lattice spacing between the crystalline phases. Fundamental for the XRD measurements is the Bragg equation (3). It puts the wavelength of the incident X-rays λ [m], the distance between the planes of the crystal lattice d [m] and the diffraction angle θ [°] in relation. When incident X-rays are diffracted in phase, constructive interference only occurs when the difference in the travelled distance (2*d*sin(θ)) is a multiple of the wavelength λ.

$$n * \lambda = 2 * d * \sin(\theta) \quad (3)$$

By solving the Bragg equation, using a given wavelength λ, it is possible to calculate the diffraction angle positions of XRD diffractions of particular lattice planes (hkl). Not only the intensity ratio of the peaks, but also their presence (or absence) correlates with the material investigated.

XRD measurements were performed for white and green fibers using a SmartLab RIGAKU CuKα X-ray instrument at an 2θ range from 5° to 60°. Crystallinity and crystal dimensions were determined according to (Frost et al., 2009). Crystal dimensions (D [Å]) are calculated as defined by the Scherrer equation (4), with the dimensionless shape factor K = 0.9, the X-ray wavelength λ = 0,15419 nm, the β the full width at half the maximum intensity (FWHM) of the diffraction peak (Monshi et al., 2012) in radians and θ the diffraction angle of the peak.

$$D_{(hkl)} = \frac{K\,\lambda}{\beta \cos\theta} \quad (4)$$

Crystallinity index is defined as the ratio between the crystalline peak and the total crystalline area.

Die approbierte gedruckte Originalversion dieser Diplomarbeit ist an der TU Wien Bibliothek verfügbar
The approved original version of this thesis is available in print at TU Wien Bibliothek.

$$\text{CI}\,[\%] = \frac{area\ of\ the\ crystalline\ peak}{total\ crystalline\ are} \quad (5)$$

Results of the XRD analysis can be found under 4.4.6.

3.12 Inductively Coupled Plasma - Optical Emission Spectroscopy

To get a better understanding of the chemical composition of the contaminations within the banknotes, as well as to determine the effect of certain pre-treatment methods on the concentration of contaminations, ICP-OES analysis (Inductively Coupled Plasma - Optical Emission Spectroscopy) was conducted. For this purpose, an Agilent 5900 SVDV ICP-OES (Agilent Technologies, US) was used. Prior to the analysis, samples needed to be brought into solution. The digestions were carried out according to the standards (ISO 14869-3:2017) and (SFS-EN 16170:2016:en). The first digestion was executed using HNO_3, H_2O_2, HCl and HF followed by the second digestion with H_2O and H_3BO_3. Both digestions were performed in a Milestone Ethos Closed Vessel Microwave Digestion System (Milestone Inc., Italy). For the measurement itself, suitable standards were used. 20 different elements were investigated, namely Aluminum (Al), Boron (B), Barium (Ba), Calcium (Ca), Copper (Cu), Iron (Fe), Magnesium (Mg), Manganese (Mn), Nickel (Ni), Lead (Pb), Strontium (Sr), Titanium (Ti), Zinc (Zn), Bismuth (Bi), Indium (In), Gallium (Ga), Silver (Ag), Cadmium (Cd), Cobalt (Co) and Chromium (Cr). Elements that could be detected (concentrations higher than the limit of quantification for each element) are summarized in Table 4 and Table 5. Further comments and interpretations of the results can be found in section 4.1.4.

Table 4. Results of ICP measurements for each pre-treatment step. Elements with initial concentrations > 500ppm.

ELEMENT / SAMPLE	Al [ppm]	B [ppm]	Ba [ppm]	Ca [ppm]	Cu [ppm]	Fe [ppm]	Zn [ppm]	Bi [ppm]
Milled BNs	4206	2768	5412	3868	1074	1755	4386	4239
Sieved BNs	5310	3659	6924	4056	819	1539	5466	5299
Magnetic tr. BNs	4469	3162	5528	2859	779	1112	4220	4062
Acetone tr. BNs	4155	2819	4855	2695	735	971	3712	3577
Bleached BNs	380	73	39	360	390	990	140	0
LiCl cleaned BNs	280	9	0	13	20	17	0	0

Die approbierte gedruckte Originalversion dieser Diplomarbeit ist an der TU Wien Bibliothek verfügbar
The approved original version of this thesis is available in print at TU Wien Bibliothek.
TU Bibliothek Your knowledge hub WIEN

Table 5. Results of ICP measurements for each pre-treatment step. Elements with initial concentrations < 500ppm.

ELEMENT / SAMPLE	In [ppm]	Mg [ppm]	Mn [ppm]	Ni [ppm]	Ti [ppm]	Pb [ppm]	Sr [ppm]
Milled BNs	135.3	460.7	137.5	80.1	169.8	7.4	13.0
Sieved BNs	140.8	486.6	236.8	71.0	177.5	9.4	8.7
Magnetic tr. BNs	131.6	298.3	124.6	62.9	171.3	0.0	5.5
Acetone tr. BNs	127.5	270.0	122.0	58.9	165.1	11.8	0.0
Bleached BNs	7.5	180.0	15.0	52.0	62.0	45.0	24.0
LiCl cleaned BNs	0.0	7.2	0.0	0.0	4.2	0.0	0.0

3.13 Fourier-Transform Infrared Spectroscopy

The chemical structure of all samples was measured by attenuated total reflectance-Fourier transform infrared (ATR-FTIR) spectroscopy (Hospodarova et al., 2018) (Carrillo et al., 2004). For this purpose, a PerkinElmer FT-IR Spectrometer was used at an interval from 600 – 4000 cm^{-1} at a resolution of 2 cm^{-1} and 32 scans per sample. In this versatile and non-destructive measurement technique infrared light is sent through an IR light transmitting crystal. On top of that crystal the samples are placed and are marginally penetrated by the IR light, which is reflected several times. The absorbance of distinct frequencies/wavenumbers can be detected. Responsible for this are molecular vibrations such as symmetric and asymmetric stretching, wagging, scissoring, rocking, or twisting. These vibrations are caused by the strength of the bond, the masses of the atoms and by electronegativity. Depending on the position, intensity and shape of the obtained peaks, conclusions about the chemical bonds are made.

FTIR analysis was performed for samples of each pre-treatment step and for all spun fibers. Selected spectra are depicted in chapter 4.6.

Die approbierte gedruckte Originalversion dieser Diplomarbeit ist an der TU Wien Bibliothek verfügbar
The approved original version of this thesis is available in print at TU Wien Bibliothek.

3.14 Differential Scanning Calorimetry (DSC) & Thermogravimetric Analysis (TGA)

Differential scanning calorimetry (DSC) is one of the most widely used thermal analysis techniques and one of the most useful analytical tools for studying the thermal properties and phase changes of materials, here regenerated fibers (Suñol et al., 2003). For example, it is possible to obtain information about phase transitions, reaction enthalpies, or specific heat capacity. The heat flux into and out of a sample and a reference is measured as a function of temperature while the sample is heated, cooled, or kept isothermal at a constant temperature. The measured signal is the energy consumed or produced during a chemical or physical reaction. Information about exothermic reactions, which decrease the enthalpy such as oxidation or crystallization, and reactions which lead to an increase of the enthalpy, so called endothermic reactions, such as melting or evaporating, can be obtained by DSC-measurements. Additionally, to the enthalpy, the sample mass change is also measured by thermogravimetric analysis (TGA). The weight loss or gain due to reactions (e.g., evaporation or oxidation) can thereby also be taken into account. The combination of DSC and TGA measurements is often referred to as Simultaneous Thermal Analysis (STA).

In the framework of this thesis, samples of each pre-treatment step as well as green and white fibers have been analyzed with a Netzsch STA 449 F3 Jupiter under helium inert gas. First the samples were heated from 40°C to 650°C with a constant heating rate of 10 K/min followed by an isothermal phase at 650°C for 10 minutes and finally a cooldown phase to room temperature with a maximum rate of 40 K/min. Results of the STA can be found under section 4.7.

Die approbierte gedruckte Originalversion dieser Diplomarbeit ist an der TU Wien Bibliothek verfügbar
The approved original version of this thesis is available in print at TU Wien Bibliothek.

3.15 Elemental Analysis

Elemental analysis was performed using a FlashSmart EA CHNS/O with MV (Thermo Scientific, United States) (Ma et al., 2021). For this work, the carbon, hydrogen, nitrogen and sulphur contents were analyzed. To do this, the samples are first combusted. The gases are guided to a catalyst and a copper reduction reactor using helium as the carrier gas. The gases are then separated by a gas chromatography column. Finally, the gases are detected with a thermal conductivity detector. Samples after each pre-treatment step as well as the produced fibers have been analyzed. The results of the elemental analysis can be found under section 4.5.

3.16 Carbohydrate Analysis

The carbohydrates and lignin of several samples were determined according to (Sluiter et al., 2008). First, glass crucibles (30 ml, porosity 4) were dried at 105°C for at least one hour and weighed. The samples were ground, air dried for several hours and the dry matter content was determined. 300 ± 15 mg sample was transferred into a test tube and 3 ml 72% H_2SO_4 was added and mixed thoroughly with the help of a glass rod. This was followed by 60 minutes of incubation at 30 ± 3 °C in a water bath while being mixed every 5 minutes. The mixture was transferred into a DURAN bottle using 84 ml distilled water resulting in an acid concentration of the solution of 4%. A sugar recovery standard (SRS) from the mono sugars D-(+)glucose, D-(+)xylose, D-(+)galactose, L(+)arabinose, and D-(+)mannose was prepared by mixing the sugars with 84 ml water and adding 3 ml 72% H_2SO_4. The SRS should resemble the carbohydrate concentration of the pulp hydrolysate and is also measured by HPAEC. During the acid hydrolysis sugars may be destructed, the SRS is later used to correct these losses. All samples as well as the SRS were autoclaved at 121 °C for one hour. The hydrolysate was filtered through the dried and weighed crucibles. The remaining solids were washed with 150 ml distilled water, dried overnight at 105°C and weighed to determine the concentration of the acid insoluble (lignin, contaminations) components. The filtrate was diluted 100x. A part was transferred into HPAEC vials with a syringe equipped with a 0.2 µm filter and subsequently measured by Thermo Scientific Dionex ICS-3000.

Another part was measured by a Shimadzu UV2550 UV-VIS spectrometer for the determination of the acid soluble lignin content.

Die approbierte gedruckte Originalversion dieser Diplomarbeit ist an der TU Wien Bibliothek verfügbar
The approved original version of this thesis is available in print at TU Wien Bibliothek.
TU Bibliothek Your knowledge hub WIEN

The result from the chromatographic measurement gives information about the monosaccharide content of the hydrolyzed pulp. To conclude from the mono sugars to the actual polysaccharide composition of the pulp, the calculation by Janson is applied (Janson, 1970).

Due to the significant contamination of the BNs, it was not possible to distinguish between lignin content and other non-polysaccharide components. Consequently, the insoluble lignin (Klason lignin) and other insoluble components are summarized and given as "insoluble fraction". Similarly, the acid-soluble lignin as well as other acid-soluble components are summarized and given as "soluble fraction". Both fractions are summarized as "non-polysaccharides".

The insoluble fraction was determined simply by measuring the difference of the crucibles weight before and after the filtration and is given as a percentage to the initial sample weight used for the measurement. The soluble fraction was estimated by the usage of a UV-VIS spectrophotometer at a wavelength of 205 nm with an absorption coefficient of 110 $Lg^{-1}cm^{-1}$, calculated with the help of Lambert – Beer law.

$$A = \varepsilon * l * c \qquad (6)$$

With A the absorbance [-], ε the molar attenuation coefficient [m^2 mol^{-1}], l the optical path lengths [m] and c the concentration [mol m^{-3}].

Carbohydrate analysis was conducted for milled BNs, bleached BNs and LiCl cleaned BNs, respectively. The results can be found in the table below as well as under section 4.1.5.

Table 6. Results of carbohydrate analysis for milled, bleached and LiCl cleaned BNs respectively. The results for cellulose, hemicellulose and non-polysaccharides is given in [%].

SAMPLE	Cellulose [%]	Hemicellulose [%]	Non-Polysaccharides [%]
Milled Banknotes	86.1	1.0	13.1
Bleached Banknotes	88.5	1.0	10.7
LiCl cleaned Banknotes	94.5	0.8	4.7

Die approbierte gedruckte Originalversion dieser Diplomarbeit ist an der TU Wien Bibliothek verfügbar
The approved original version of this thesis is available in print at TU Wien Bibliothek.

4. Results and Discussion

4.1 Impact of the Pre-treatment Process

The effects of the pre-treatment steps on the banknotes were investigated using different analytical methods. Relatively simple methods such as ash content determination and FTIR analysis were used as quality/effect controls. These methods were helpful in selecting suitable treatment methods by indicating a possible purification. More complex methods e.g., GPC or carbohydrate analysis have been conducted after the pre-treatment sequence has been developed. In the following section, the results of the measurements regarding the pre-treatment sequence are depicted and interpreted.

4.1.1. Particle Size Distribution

In Figure 12 (a) the particle size distribution (PSD) of the milled banknotes is depicted. In total two fractions, particles < 200 µm and particles > 200 µm can be found. By sieving the banknotes with a sieve (mesh size 200 µm) it was possible to remove almost all of the smaller particles as seen in Figure 12 (b). The direct comparison of the milled and the sieved BNs as seen in Figure 12 (c) makes this obvious. Figure 12 (d) directly compares the banknotes after bleaching with the sieved banknotes. Almost no difference can be observed between those two PSD analyses. This means, that neither the bleaching nor the other treatment steps before had a significant impact on the particle size distribution of the banknotes.

The smaller particle fraction (< 200 µm), has an average particle diameter of d(0.5) ~ 80 µm and the larger fraction (> 200 µm) a diameter of d(0.5) ~ 560 µm. The final bleached banknotes show an almost identical average diameter of d(0.5) ~ 559 µm.

In conclusion, the only mentionable influence on the particles size distribution had the sieving process, where particles smaller than 200 µm were separated. All following treatment steps had little to basically no influence on the PSD and did not decrease the average particle diameter.

Die approbierte gedruckte Originalversion dieser Diplomarbeit ist an der TU Wien Bibliothek verfügbar
The approved original version of this thesis is available in print at TU Wien Bibliothek.

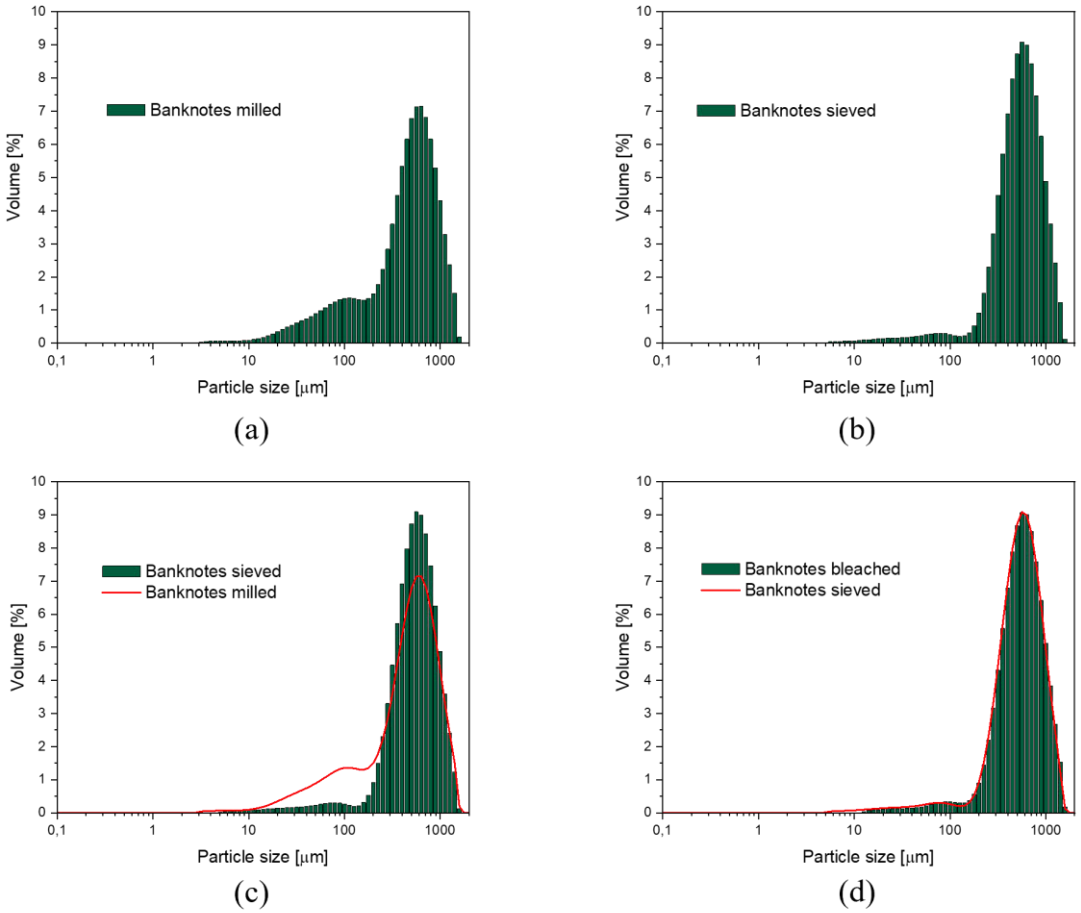

Figure 12. Particle size distribution volume [%] as a function of particle size [µm] of the banknotes after milling (a) and after sieving (b) as well as a direct comparison of both (c) and a comparison of the bleached banknotes and the sieved banknotes (d).

Die approbierte gedruckte Originalversion dieser Diplomarbeit ist an der TU Wien Bibliothek verfügbar
The approved original version of this thesis is available in print at TU Wien Bibliothek.

4.1.2. Ash content

Figure 13 illustrates the gradual decline of the ash content and consequently the reduction of the amount of inorganic impurities for each pre-treatment step. The initial banknotes show a very high ash content of >7% indicating a big amount of inorganic materials present. It can be observed that each treatment step had a positive effect in reducing the ash content more or less drastically, except for the acetone treatment. This can be explained by the removal of mainly organic compounds during this treatment step. When solely organic compounds are removed from the Banknotes, the relative amount of inorganic compounds is consequently increased. Consequently, more residues are detected after the incineration. In other words, if only organic matter is removed from the Banknotes, the ash- content is increased.

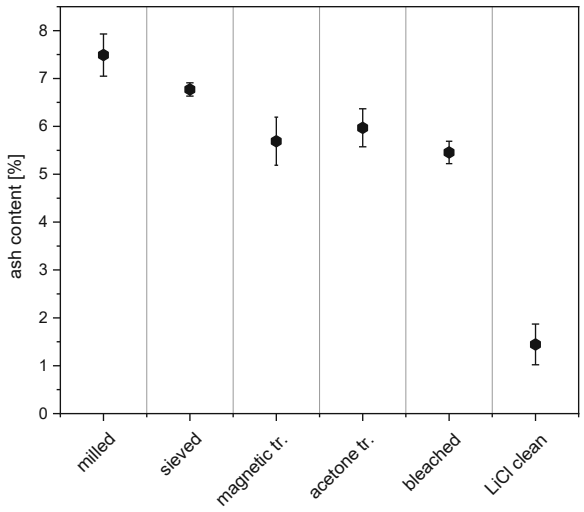

Figure 13 Ash content [%] of samples for each pre-treatment step.

By far the biggest impact on the ash-content had the dissolution in LiCl/DMAc. In this step, a significant number of pigments was removed, which were, supposedly, mainly inorganic compounds. This explains the big reduction during this step. Compared to commercial pulps, which usually have an ash content well below 1% (McCall & Jurgens, 1951) the ash-content at the end of the treatment sequence was still elevated (>1%). The increased ash-content might be explained by an unsuccessful removal of the LiCl in the final step. This assumption could not be verified by any of the applied methods.

Die approbierte gedruckte Originalversion dieser Diplomarbeit ist an der TU Wien Bibliothek verfügbar
The approved original version of this thesis is available in print at TU Wien Bibliothek.

4.1.3. Intrinsic Viscosity

The intrinsic viscosity of a pulp affects the spinnability of the dope tremendously. (Asaadi et al., 2016). Preferably it should be in a range of 450 ± 50 ml g^{-1} to achieve the best spinnability.

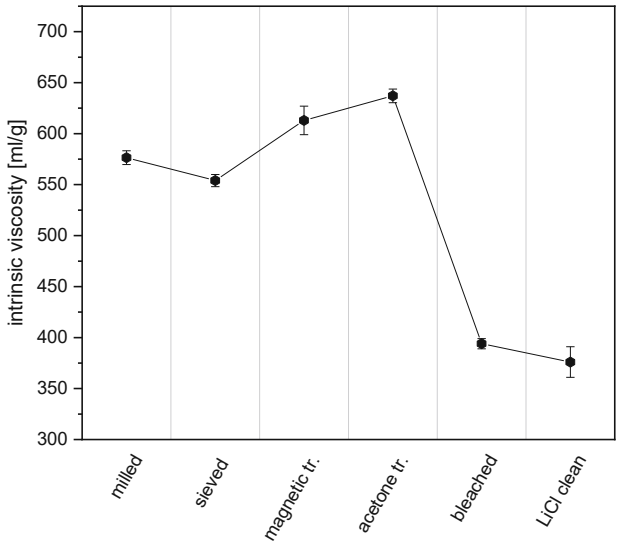

Figure 14 Illustration of the intrinsic viscosity [ml/g] along the pre-treatment sequence

Figure 14 demonstrates the progression of the intrinsic viscosity. Due to the high contamination of the cellulose, a significant number of particles could not be dissolved in the CED during the intrinsic viscosity measurements despite thoroughly shaking the vials and even increasing the dissolution time. This led to disturbances of the measurements, higher deviations of the results and less conclusive results. With this in mind, the results of the measurements should be considered with caution and only the trend should be taken into account.

The changes of the intrinsic viscosity in the first few steps were, supposedly, due to the reduction of the inorganic and non-cellulosic organic compounds. This resulted in an increase of cellulose and thus led to a more viscous solution.

Sodium hypochlorite bleaching is a harsh method, which not only effects the impurities, but also the cellulose itself. Consequently, a drastic drop can be observed after the bleaching treatment. In acidic as well as basic conditions first the amorphous regions of the cellulose are affected and depending on the conditions and the treatment time also a shortening of the crystalline polymer chains can be observed (Benavides, 2011). Thus, the average degree of polymerization is gradually decreased and consequently, the intrinsic viscosity reduced.

Die approbierte gedruckte Originalversion dieser Diplomarbeit ist an der TU Wien Bibliothek verfügbar
The approved original version of this thesis is available in print at TU Wien Bibliothek.
TU Bibliothek Your knowledge hub WIEN

After the bleaching process, an intrinsic viscosity of slightly below 400 ml g^{-1} was measured. This served as a benchmark for all the trials, as it has proven successful.

The dissolution of cellulose in a LiCl / DMAc solution has almost no effect on the degree of polymerization and the molar mass distribution (Dupont, 2003). As the values are very similar and are in line with the standard deviation, it can be assumed that there is no significant difference before and after the dissolution.

Generally, there are several different methods that are used to reduce and adjust the intrinsic viscosity of cellulose-based pulps for the spinning process e.g.: radiation treatment (E-beam), mechanical milling, acid or base treatment and enzymatic hydrolysis (Kumar et al., 2009). As the intrinsic viscosity was already in a suitable range after the bleaching treatment, no further adjustments had to be made.

Though, it could be contemplated to change the bleaching process to a more environmentally friendly option, for instance, to a treatment with H_2SO_4, which was investigated in addition as prove of concept. The intrinsic viscosity was successfully reduced to a suitable range by treating banknotes with 0.05 M H_2SO_4, 1:25, for 10, 20, 30 minutes respectively at 80°C (Asaadi et al., 2016). In Figure 15 the changes of the intrinsic viscosity are illustrated. A severe degradation takes place in the first 10 minutes.

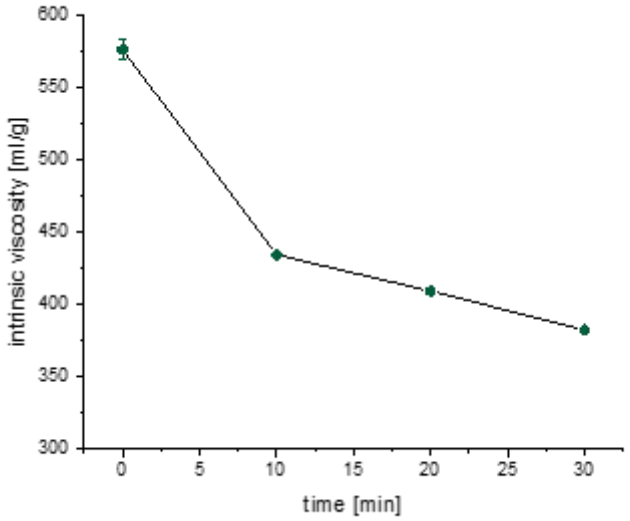

Figure 15. Decrease of intrinsic viscosity by H_2SO_4 treatment.

Die approbierte gedruckte Originalversion dieser Diplomarbeit ist an der TU Wien Bibliothek verfügbar
The approved original version of this thesis is available in print at TU Wien Bibliothek.

First the amorphous regions of the cellulose are destroyed, followed by a degradation of the crystalline regions. These two degradation steps show different kinetics and consequently the degradation is faster at the beginning and slows down in the very end. The intrinsic viscosity could be easily adjusted. However, the decolorization was less effective compared to the bleaching process which means that a higher level of contamination in the product must be expected. Furthermore, using this substrate a dope was produced. The viscoelastic properties were similar compared to the other dopes produced during this work. Fibers were produced as prove of concept.

4.1.4. ICP-OES

Milled, sieved, magnetic treated, acetone treated, bleached and samples dissolved in a LiCl / DMAc solution and subsequently precipitated have been analyzed by ICP-OES, respectively. Numerous elements and their concentrations in the samples have been determined. The results of the ICP-OES analyses for each treatment step are depicted in Figure 16. Additional to the elements listed below in the graphs, bismuth, cadmium, cobalt, chromium, gallium, lead, silver and strontium were measured. However, the results for these elements were all below the respective limit of quantification. The exact values of the measurements can be found in Table 4 and Table 5.

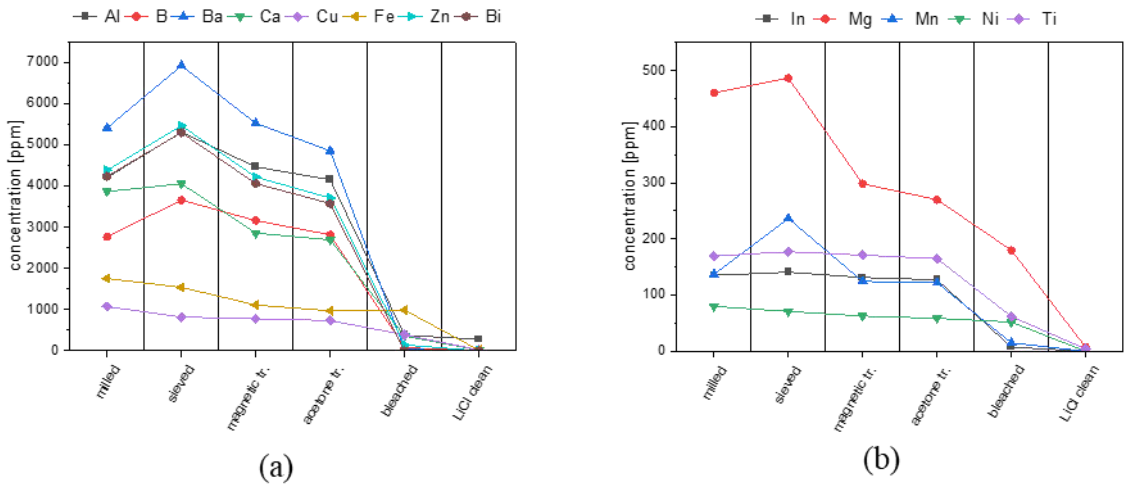

Figure 16. Results of ICP-OES analyses. Concentrations [ppm] of certain elements for each pre-treatment step. Elements with higher initial concentrations (>500 ppm) are depicted in (a) and elements with lower initial concentrations (<500ppm) are depicted in (b).

Die approbierte gedruckte Originalversion dieser Diplomarbeit ist an der TU Wien Bibliothek verfügbar
The approved original version of this thesis is available in print at TU Wien Bibliothek.

The concentrations of the elements investigated are affected by the individual treatment steps. For example, the sieving process leads to a relative increase in the concentration of some elements (e.g., barium, zinc, or bismuth), but to a decrease in the concentration of other elements (e.g., iron, copper, or nickel). Treatment of the banknotes with a magnet or with acetone, on the other hand, led to a slight but nevertheless definite decrease in the concentrations of all the elements examined. However, the bleaching process undoubtedly had the greatest influence on these elements.

By bleaching the banknotes with sodium hypochlorite, almost all the elements investigated could either be completely removed from the samples (concentration below the limit of quantification) or the concentration could be greatly reduced. Merely the iron and copper were quite unimpressed by this harsh treatment. By dissolving the banknotes in LiCl / DMAc solution, thereby separating the leftover green pigments from the dissolved cellulose, and finally precipitating the white cellulose, the concentration of all elements investigated could be reduced to very low, insignificant values.

Traces of metals in textiles are not uncommon. However, the values are usually much lower than those detected here. Although some metals have been completely removed, such as Pb, the limit is >1 ppm, some other metals are still detectable in too high concentrations. Aluminum in particular stands out. With 280 ppm Al is clearly above the usual values of comparable fibers (cotton 2.27 - 7.23 mg/kg, viscose 2.06 - 9.65). But also copper with 20 ppm has a comparably increased value (cotton 1.96 - 4.40 mg/kg, viscose 2.03 - 2.26 mg/kg) (Sungur & Gülmez, 2015).

Many of the elements that could be observed and measured by ICP are metals. Metals play a major role in the dye industry and are often components of dyes and pigments (Stallmann, 1960). The intaglio inks used in banknote production also contain metallic components. These usually consist of two fractions: metallic pigments and an organic fraction that acts as an ink vehicle (Kyrychok et al., 2014). Aluminum is found, for example, in the pigment ultramarine, a sulfur-containing sodium aluminum silicate, which covers a broad color spectrum in various chemical compositions (from ultramarine violet to ultramarine blue to ultramarine red) (Hofmann et al., 1964).

Die approbierte gedruckte Originalversion dieser Diplomarbeit ist an der TU Wien Bibliothek verfügbar
The approved original version of this thesis is available in print at TU Wien Bibliothek.

Phthalocyanines and their derivatives are a group of pigments that are used in many areas of textile and paper dyeing and account for about 25% of the artificial organic pigments. Phthalocyanines consist of four isoindoles, each of which is linked by a nitrogen atom and thus it forms a ring. These pigments are well-known for their extremely high thermal stability and resistance against all kinds of solvents. The non-substituted macromolecule phthalocyanine is a dark blue / black pigment. The different derivatives, each with a metal in the centre of the phthalocyanine ring, have different colors. The complex compound with Fe, iron (II)phthalocyanine ($C_{32}H_{16}FeN_8$) is a dark purple pigment. Zinc phthalocyanine ($C_{32}H_{16}N_8Zn$) is a violet pigment, nickel (II) phthalocyanine ($C_{32}H_{16}N_8Ni$) is dark blue and aluminum phthalocyanine chloride ($C_{32}H_{16}N_8AlCl$) is a yellow pigment. Halogenated and sulfonated derivatives of phthalocyanines are also widely used pigments. For example, the blue copper phthalocyanine complex is transformed into a green complex by chlorination (Löbbert, 2000).

The nature and chemical composition of the very stable green pigments of the BNs became interesting soon during the investigations for this thesis. It was not possible to destroy nor dissolve the pigments, neither by very harsh conditions and the use of aggressive chemicals nor through the otherwise very effective bleaching process. The findings of the ICP-OES measurements led to the assumption that the green pigments most likely are some forms of either iron- or copper-complexes. More about the investigations regarding the green pigments can be found in section 4.8.

Die approbierte gedruckte Originalversion dieser Diplomarbeit ist an der TU Wien Bibliothek verfügbar
The approved original version of this thesis is available in print at TU Wien Bibliothek.

4.1.5. Carbohydrate Analysis

Carbohydrate analysis was conducted for the initial ground BNs as well as for the treated substrates used for dope production and fiber production (bleached banknotes and LiCl / DMAc cleaned BNs). In Figure 17 the results of the measurements can be observed. As already mentioned in section 3.16, it is not possible do distinguish between lignin content and other non-polysaccharide components due to the nature of the measurement. That is why the content of soluble lignin, insoluble lignin, other soluble components, and other insoluble components of the BNs are summarized and given here as non-polysaccharides.

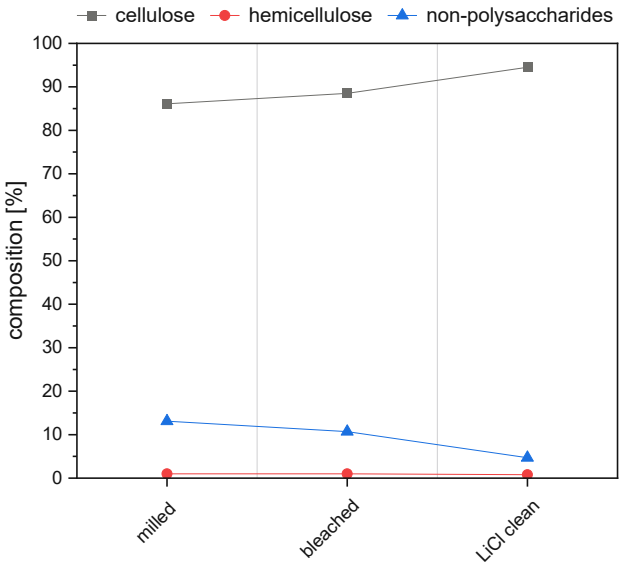

Figure 17. cellulose, hemicellulose, and non-polysaccharide composition [%] of the initial milled BNs, bleached BNs and LiCl cleaned BNs, respectively.

The core of the banknotes is cotton, so it was expected that the hemicellulose content is very low (<1%) (de Morais Teixeira et al., 2010), which was confirmed by the results above. It can be seen, that due to the treatment process the non-polysaccharide content is gradually decreased, from 13.1% to 10.7% and finally 4.7% for the milled, bleached and LiCl cleaned banknotes, respectively. The remaining 4.7% of non-polysaccharides are either lignin or other impurities present in the banknotes. The total lignin content for white cotton is <1% (de Morais Teixeira et al., 2010). Consequently, the relative cellulose content is quite high. The pre-treatment steps caused an increase of the cellulose content from 86.1% (initial banknotes) to almost 95% (cleaned BNs used to produce white fibers). The final cellulose content of almost 95% proves that the main component of the banknotes must be high quality cotton (de Morais Teixeira et al., 2010).

Die approbierte gedruckte Originalversion dieser Diplomarbeit ist an der TU Wien Bibliothek verfügbar
The approved original version of this thesis is available in print at TU Wien Bibliothek.
TU Bibliothek Your knowledge hub WIEN

4.2 Dissolution Results

The dissolution behavior of the different materials used for dope production was investigated as described in section 3.7. By observing the dissolution behavior under microscope at different temperatures, the optimum temperature for the dope preparation was chosen. The best dissolution was observed at 85°C for all materials, which was consequently used for the dope production (Asaadi et al., 2016). The parameters used for the dope production are summarized in Table 7.

Table 7. Kneading parameters for all dopes. (*) dopes prepared by Inge Schlapp – Hackl (Aalto University).

Sample	Intrinsic Viscosity [ml/g]	Pulp Consistency [%]	Temp. [°C]	Kneading Speed [rpm]	Time [mins]	Dope Prep. Unit
BN 1 – green	434 ± 1	13	85	30	180	Small Kneading Unit
BN 2 – green	419 ± 2	13	85	30	180	
BN 3 – green	394 ± 5	13	85	30	180	
BN – white *	376 ± 7	13	85 & 90	30	120 (85°C) & 60 (90°C)	
BN – green *	385 ± 1	14	85	30	180	Big Kneading Unit

It took 180 minutes to fully dissolve the cellulosic fraction of the BNs (bleached BN) used to produce green fibers in the small as well as the big kneading unit both heated to 85°C. The LiCl / DMAc cleaned banknotes, which served as starting material for the white fibers, did show a poor dissolution behavior at 85°C in the small kneading unit. After 120 minutes at 85°C the temperature was increased to 90°C and the cellulose dissolved within 60 minutes. Compared to standard dopes from Enocell–4 pulp or other cellulosic materials e.g., birch wood an increased dissolution time was observed. Usually, the cellulose is dissolved in the ionic liquid within approximately 90 minutes (Asaadi et al., 2016).

Die approbierte gedruckte Originalversion dieser Diplomarbeit ist an der TU Wien Bibliothek verfügbar
The approved original version of this thesis is available in print at TU Wien Bibliothek.

Each dope was filtered after the dissolution in the ionic liquid at elevated temperatures. While the purified white banknotes showed an almost full dissolution and only neglectable amounts of undissolved particles, the green dopes showed a different picture. Undissolved non-cellulosic particles could be observed at the filter after filtration. In the case of the big dope, it was even necessary to filter the dope three times. Each time with a new filter and each time, undissolved residues were found on the filter.

4.3 Dope Rheology

The viscoelastic properties of a dope play an essential role for the spinning process. According to (Sixta et al., 2015) the ideal complex viscosity which is needed for spinning is in a range of 20.000 – 30.000 Pa s. (Haslinger, Wang, et al., 2019) outlined higher values for textile waste recycling (between 32.700 – 78.000 Pa s). The viscoelastic properties of the dopes measured as stated in section 3.9 by an Anton Paar rheometer are summarized in Table 8.

Table 8. Complex viscosity (η*), omega (Ω), storage modulus and loss modulus at 60ºC of all the dopes prepared for fiber production measured with rheometer. (*) produced and measured by Helena Sederholm (Aalto University), (**) dope produced and measured by Inge Schlapp – Hackl (Aalto University).

Sample	Intrinsic Viscosity [ml/g]	Pulp Consistency [%]	η* [Pa s]	Ω [s-1]	G′= G′′ [Pa]
Enocell – 4*	n/a	13	60063	0.4452	5054
BN 1 – green	434 ± 1	13	166120	0.0488	1983
BN 2 – green	419 ± 2	13	134510	0.0335	1273
BN 3 – green	394 ± 5	13	56274	0.2813	2718
BN – white**	376 ± 7	13	22555	0.6614	2359
BN – green**	385 ± 1	14	128880	No CoP	No CoP

Die approbierte gedruckte Originalversion dieser Diplomarbeit ist an der TU Wien Bibliothek verfügbar
The approved original version of this thesis is available in print at TU Wien Bibliothek.

The dopes used to spin green Ioncell® fibers from banknotes have partly significant higher complex viscosity values ranging from 56 274 – 166 120 Pa s at 60°C. The dope to spin white Ioncell® fibers from banknotes on the other hand, shows a complex viscosity of 22 555 Pa s at 60°C, which is exactly in the range as stated by (Sixta et al., 2015).

As seen in Figure 18 (a), the complex viscosity values for both the green and the white dopes over the angular frequency are shifted to lower values compared to the standard dope produced from Enocell – 4 pulp. However, the shape of the curves is very similar. Especially in the area of higher angular frequencies an almost parallel course can be observed.

The dynamic moduli are represented by the storage modulus G' and the loss modulus G''. While G' reflects the reversible, elastic deformations, G'' illustrates the irreversible deformations. Both values are influenced by the proportion of long and short polymer chains in the cellulose. As can be seen in Figure 18 (b) both G' and G'' increase with rising angular frequency. Same observations were also made by (Haslinger, Wang, et al., 2019).

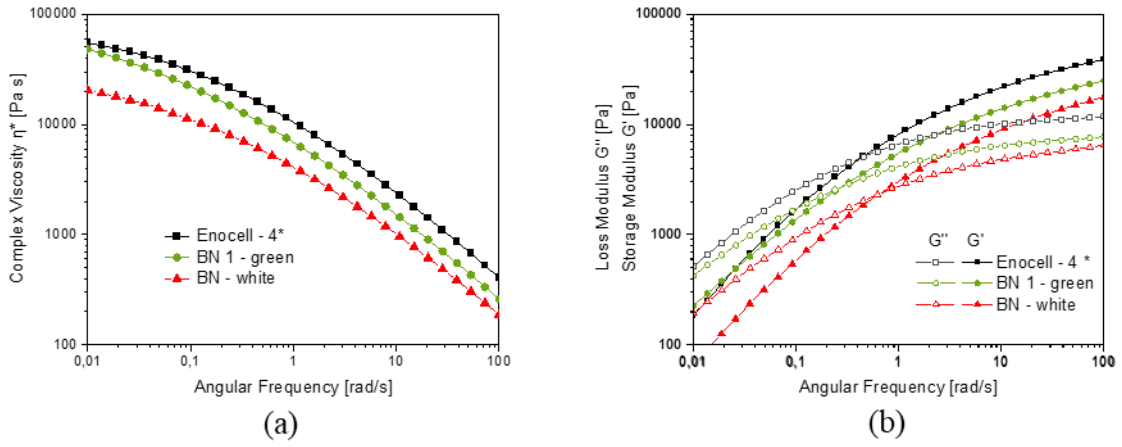

Figure 18. Complex viscosity (η*) against angular frequency (a) and storage modulus (G`) & loss modulus (G``) against angular frequency (b) for dopes used to produce green and white fibers, respectively at 60 °C. (*) Enocell - 4 dope produced and measured by Helena Sederholm (Aalto University).

Die approbierte gedruckte Originalversion dieser Diplomarbeit ist an der TU Wien Bibliothek verfügbar
The approved original version of this thesis is available in print at TU Wien Bibliothek.

4.4 Fibers – Spinning & Properties

The following section is dedicated to the fibers which were produced in the course of this thesis. Here the details of the fiber production, the mechanical, chemical, and structural properties of the fibers are summarized.

4.4.1. Fiber Spinning

The dopes spinnability is reflected by the draw ratio reached during the spinning process. Therefore, the spinning quality can be categorized according to the draw ratio and defined as non- (DR<2), poor- (DR = 2-8), good- (DR = 8-14) and excellent spinnability (DR>14) (Asaadi et al., 2016). The spinnability is affected by many physical as well as chemical factors including temperature, supramolecular structure, rate of crystallization, cross linking, phase behavior and diffusion (Gupta & Kothari, 1997).

As seen in Table 9, fibers spun from banknotes show a poor to good spinnability.

Table 9. Summary of the spinning conditions. (*) fibers spun by Inge Schlapp-Hackl (Aalto University)

Sample	Pulp Consistency [%]	Spinning Temp. [°C]	Bath Temp. [°C]	Extrusion Velocity [m min^{-1}]	Max DR	Spinning Unit
BN 1 – green	13	60	5	1.3	11	KS 15 Spinning Unit (Monofilament)
BN 2 – green	13	60	5	1.3	9	
BN 3 – green	13	60	5	1.3	7	
BN – viscosity adjusted	13	60	5	1.3	7	
BN – white*	13	66	5	1.3	8	
BN – green*	14	71	10.1	2.7	8	KS 80 (Multi-filament 400 holes)

Die approbierte gedruckte Originalversion dieser Diplomarbeit ist an der TU Wien Bibliothek verfügbar
The approved original version of this thesis is available in print at TU Wien Bibliothek.

(Haslinger, et al., 2019) reached a maximum DR of 8.8 for fibers spun from cotton polyester blended textile waste. Although Ioncell® fibers from banknotes reached values in the range of 7 to 11, maximum DRs of 12 and 17.4 for fibers from dyed textile waste and cotton waste, respectively were reached by (Haslinger, Wang, et al., 2019) and (Asaadi et al., 2016). A reason for the poorer performance could be the increased amount of contaminations.

Moreover, it was possible to produce a small piece of fabric from the green fibers spun with the big spinning unit. Therefore, 12.5 g of the green Ioncell® fibers from BNs (BN – green) with DR < 8 were spin - finished using an Afilan CVS liq (used as lubricant) and Leomin PN pa (used as antistatic agent) in proportion 80:20. Subsequently, the spin finished Ioncell® fibers were opened by a Trash Analyzer, 281C (Mesdan, Italy) and mixed with 12.5 g of Tencel fibers (1.3 dtex, 38 mm). The 50 / 50 blend was then homogenized using a Carding Machine 337A (MESDAN-LAB, Italy). Via a drafting machine (Stiro Roving Lab 3371, Mesdan, Italy) the mixture was formed into a roving. Yarn was finally spun using a ring spinning device (Ring Lab 82BA, Mesdan, Italy). Ultimately, a piece of fabric was knitted using a knitting machine (CMS ADF 32W E7.3 multi-gauge, Stoll, Germany). The opened fiber mix (green Ioncell® fibers from BNs and Tencel fibers), as well as the spun yarn and the final piece of fabric are depicted in Figure 19.

Figure 19. (a) mix of opened fibers (50% green, spin finished Ioncell® fibers from BNs and 50% Tencel fibers), (b) spun yarn next to the homogenized blend and (c) final knitted piece of fabric. Fibers spun by Inge Schlapp-Hackl (Aalto University), fibers treated from here on until the finished fabric (a-c) by Marja Rissanen (Aalto University)

Die approbierte gedruckte Originalversion dieser Diplomarbeit ist an der TU Wien Bibliothek verfügbar
The approved original version of this thesis is available in print at TU Wien Bibliothek.

4.4.2. Mechanical Properties

The obtained green Ioncell fibers from Banknotes spun with the monofilament unit KS15 exhibit quite uniform results in the dry tensile tests. There is only a small deviation in the maximum elongation (7.2 – 8.1 %) and tenacity (35.2 – 37.2 cN/tex) at rupture not only for the different filaments (BN1, BN2, BN3, respectively) but also for DR = 7 and 11 of BN1 (Figure 20).

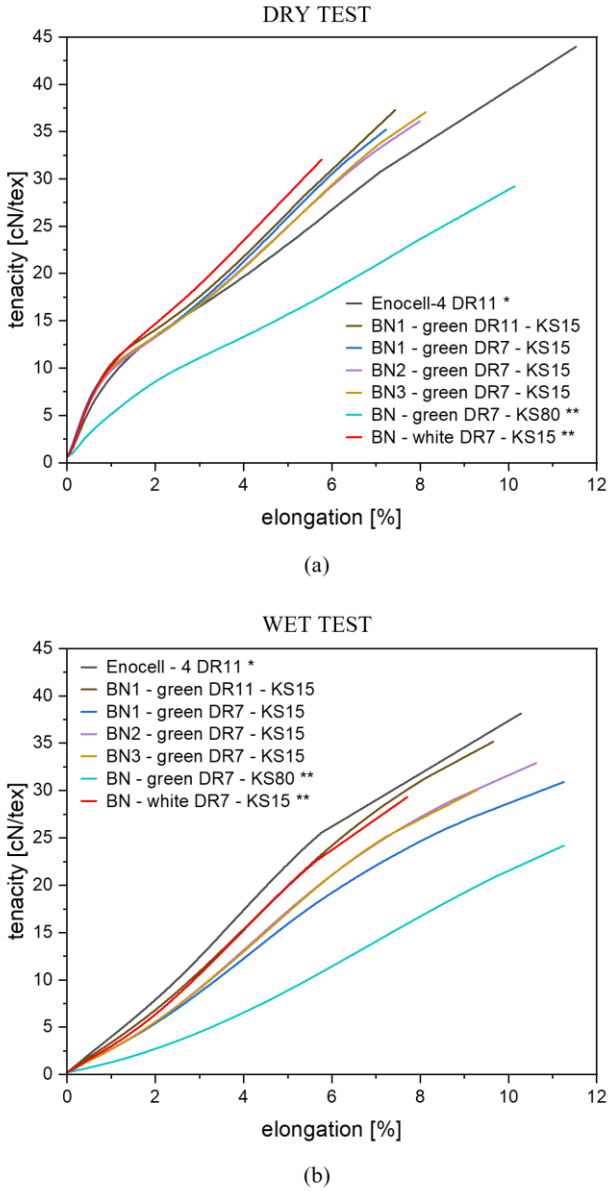

Figure 20. Tenacities [cN/tex] of all the spun fibers and Enocell – 4 fibers as a function of elongation [%] under dry (a) and wet (b) conditions. (*) Fibers spun and measured by Helena Sederholm (Aalto University), (**) Fibers spun by Inge Schlapp-Hackl (Aalto University) and measured by Marja Rissanen (Aalto University).

Die approbierte gedruckte Originalversion dieser Diplomarbeit ist an der TU Wien Bibliothek verfügbar
The approved original version of this thesis is available in print at TU Wien Bibliothek.

The results of the wet tensile tests for the same fibers, however, show a greater deviation, despite the same method of production of the dopes for all green fibers and the very similar spinning conditions. Here we can see a clear difference between the single fibers with a maximum elongation of 9.3 – 11.2 % and tenacity of 30.0 – 35.2 cN/tex.

In Table 10 the values of the tensile tests are summarized. The BN1-green DR11 – KS 15 Ioncell fibers show a higher tenacity at the point of rupture in the tensile test, though a shorter elongation compared to the fibers produced from the same dope at lower draw ratio (DR = 7). The white banknote fibers show a similar behaviour during the tensile strength test. However, the final properties achieved are significantly lower compared to the green fibers. The values for tenacity and elongation in both the dry (5.8 % and 32.0 cN/tex) and wet (7.7 % and 29.3 cN/tex) tensile tests compared to the green banknote fibers also spun with the smaller spinning unit are reduced. By far the largest deviation is shown by the green fibers spun with the help of the large spinning unit (multifilament, KS80). These fibers show a much lower maximum tenacity at rupture than all other green fibers produced, in both the dry (10.1 % and 29.2 cN/tex) and wet (11.4 % and 24.2 cN/tex) tensile tests. However, the elongation of these fibers is greater than the values achieved for the green and white fibers spun with the small unit. Compared to the Ioncell® fibers made of Enocell-4 pulp used as a reference, all produced fibers from BNs exhibit a reduced performance. Commercially used fibers such as lyocell or viscose fibers achieve similar results as the Ioncell® fibers from banknotes. Lyocell staple fibers, for example, reach an elongation of around 13% with an average tenacity of approximately 36 cN/tex (Adusumalli et al., 2009) and viscose fibers achieve an average elongation of 15 – 20 % and an average tenacity of 25 cN/tex (Adusumalli et al., 2019). From this point of view, the Ioncell® fibers produced from banknotes reached reasonable and respectable values.

Die approbierte gedruckte Originalversion dieser Diplomarbeit ist an der TU Wien Bibliothek verfügbar
The approved original version of this thesis is available in print at TU Wien Bibliothek.

Table 10. Summary of fiber testing results at point of rupture for all produced fibers. (*) Fibers spun and measured by Helena Sederholm (Aalto University), (**) Fibers spun by Inge Schlapp-Hackl (Aalto University) and measured by Marja Rissanen (Aalto University).

FIBER	DRY		WET	
	Elongation [%]	Tenacity [cN/tex]	Elongation [%]	Tenacity [cN/tex]
Enocell – 4 DR11*	11.5 ± 2.6	43.9 ± 6.8	10.2 ± 2.0	38.1 ± 6.2
BN – green DR11 – KS15	7.4 ± 0.9	37.3 ± 3.9	9.7 ± 1.1	35.1 ± 2.9
BN – green DR7 – KS15	7.8 ± 0.5	36.1 ± 1.0	10.4 ± 1.0	31.3 ± 1.4
BN – green DR7 – KS80**	10.1 ± 1.2	29.2 ± 3.6	11.3 ± 0.9	24.1 ± 2.6
BN – white DR7 – KS15**	5.8 ± 0.9	32.0 ± 3.2	7.7 ± 1.1	29.3 ± 3.3

4.4.3. Birefringence

Table 11 shows the results of the birefringence measurements for green and white Ioncell® fibers from banknotes as well as for Ioncell® fibers from Enocell-4 pulp (Haslinger et al., 2020). The overall orientation of the green fibers produced differs depending on both the spinning unit which was used and the draw ratios. Green fibers spun with the monofilament spinning unit tend to show a relatively high overall orientation, though exhibit a lower total orientation compared to standard Ioncell® fibers from Enocell-4 pulp. However, the results show an increased standard deviation. Green fibers spun with the larger multifilament spinning unit also show a relatively high overall orientation but appear to be more uniform and homogeneous and show a reduced standard deviation. Compared to the other fibers listed in the table below, the white fibers have the greatest overall orientation of all.

The birefringence of perfectly oriented fibers is 0.057 according to literature (Sixta et al., 2015). Though the results of the Ioncell® fibers spun from recycled BNs show significant lower values than perfectly oriented fibers. The values for Lyocell fibers spun at different draw ratios and consistencies are usually between 0.025 – 0.050 (Kim et al., 2002). Compared to the birefringence of the fibers mentioned above, Ioncell® fibers spun from recycled BNs achieve respectable values.

Die approbierte gedruckte Originalversion dieser Diplomarbeit ist an der TU Wien Bibliothek verfügbar
The approved original version of this thesis is available in print at TU Wien Bibliothek.

Die approbierte gedruckte Originalversion dieser Diplomarbeit ist an der TU Wien Bibliothek verfügbar
The approved original version of this thesis is available in print at TU Wien Bibliothek.

Table 11. Summary of birefringence measurements of Enocell-4 fibers as well as of the produced green and white fibers. (*) values taken from (Haslinger et al., 2020), (**) fibers spun by Inge Schlapp-Hackl (Aalto University) and measured by Marja Rissanen (Aalto University).

Sample	DR	Δn	Total Orientation	Absolute Errors		Spinning Unit
				int. var. ±	meas. ±	
ENOCELL – 4*	11	0.040 ± 0.005	0.65 ± 0.09	n/A	n/A	KS 15 Dry – Jet Wet Spinning Unit (Monofilament)
BN 1 – green fibers	7	0.0426 ± 0.0110	0.687 ± 0.177	0.0039	0.0071	
	11	0.0384 ± 0.0109	0.620 ± 0.176	0.0036	0.0073	
BN 2 – green fibers	7	0.0370 ± 0.0065	0.597± 0.105	0.0014	0.0051	
BN 3 – green fibers	7	0.0380 ± 0.0078	0.613 ± 0.126	0.0019	0.0059	
BN – white fibers**	7	0.0425 ± 0.0057	0.686 ± 0.092	0.0012	0.0046	
BN – green fibers**	7	0.0359 ± 0.0029	0.578 ± 0.047	0.0007	0.0022	KS 80 – DJW Spinning Unit (Multi-filament)

4.4.4. Scanning Electron Microscopy

The cross-section and the surface morphology of green as well as white Ioncell® fibers from banknotes can be seen in Figure 21 and Figure 22, respectively.

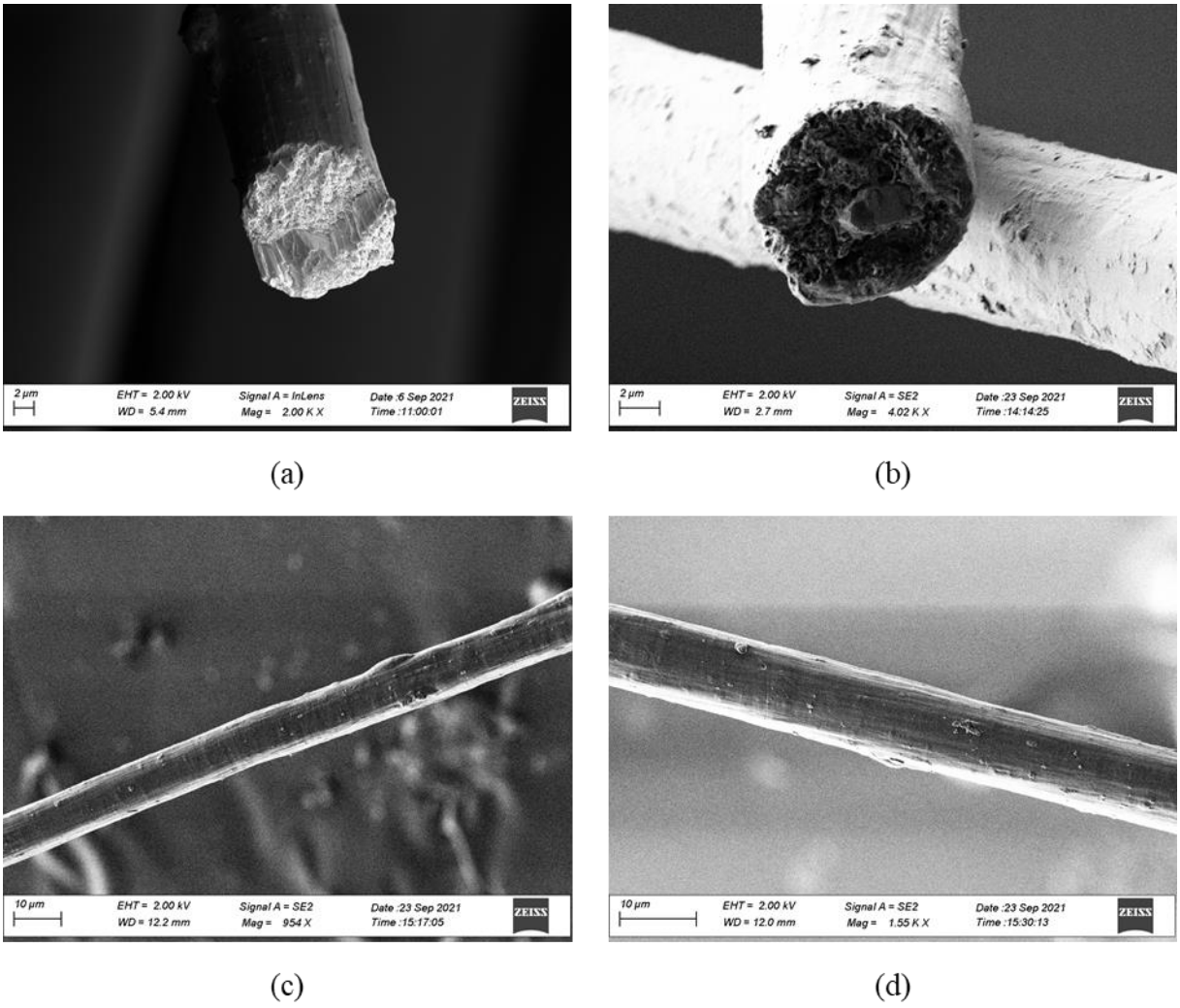

Figure 21. Cross-section (a) and (b) as well as surface morphology (c) and (d) of green fibers spun at DR 7 by monofilament spinning unit characterized by SEM operating at 2.00 kV.

In Figure 21 (a) the beautiful dense fibral structure of one green Ioncell® fiber made from banknotes is shown. Based on the optical microscope evaluation fibers were very uneven, and the grains which can be clearly seen in (b) and (c) are irregularities at the surface of the fiber.

Die approbierte gedruckte Originalversion dieser Diplomarbeit ist an der TU Wien Bibliothek verfügbar
The approved original version of this thesis is available in print at TU Wien Bibliothek.

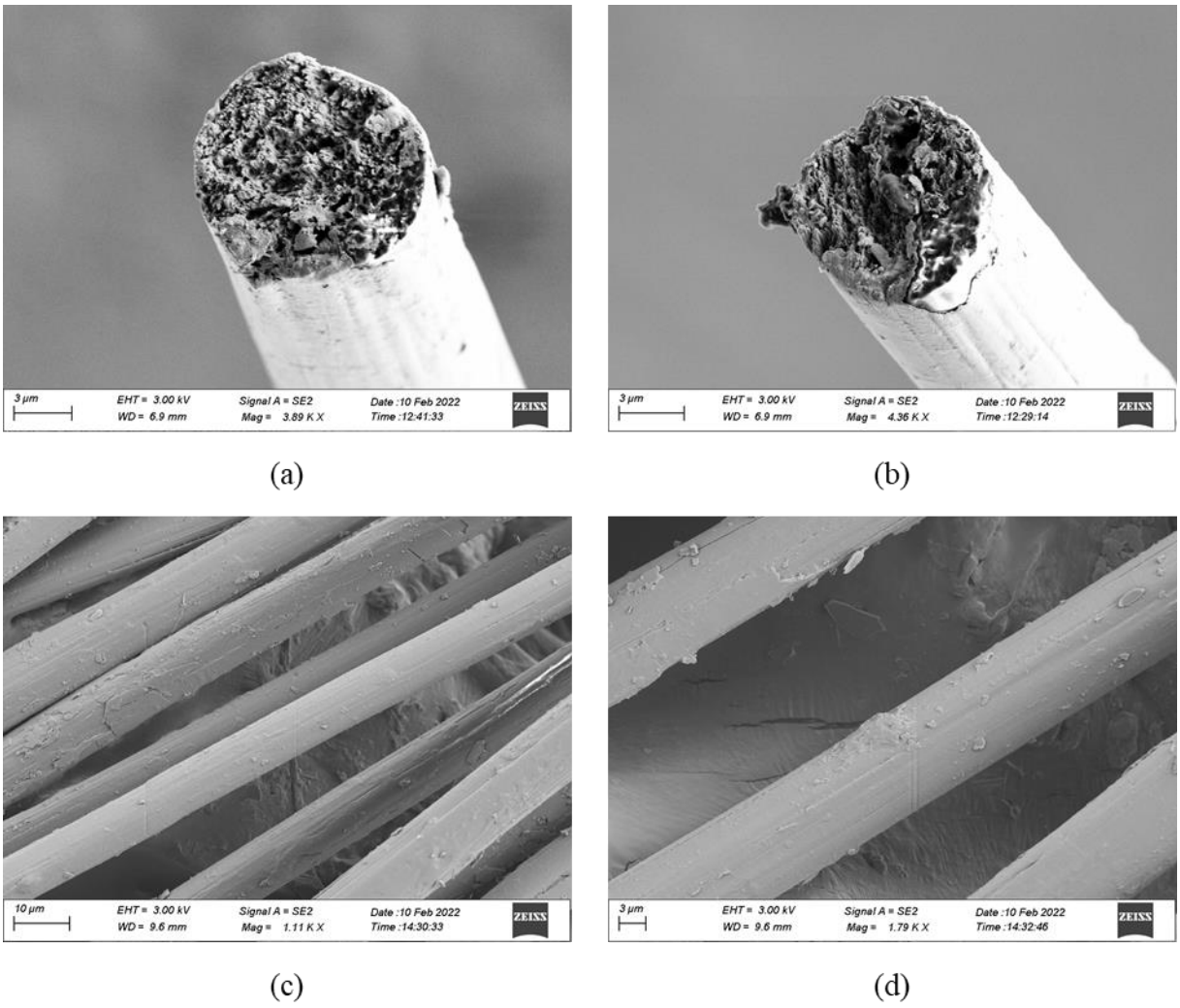

Figure 22. Cross-section (a) and (b) as well as surface morphology (c) and (d) of white fibers spun at DR 7 by monofilament spinning unit characterized by SEM operating at 3.00 kV. Fibers produced by Inge Schlapp-Hackl (Aalto University) and measured by Eva Gonzalez (Aalto University)

The fibril structure of a white Ioncell® fiber spun from banknotes is presented in Figure 22 (a) & (b). Compared to the green fibers, it seems, that the white fibers have a less smooth and seemingly more brittle surface (Figure 22 (c) & (d)).

The round shape and the dense fibril structure of the fibers observable in the SEM pictures above (Figure 21 and Figure 22) are very typical for Ioncell® fibers. To produce yarns for textile applications fibers should ideally exhibit a diameter of 1-2 dtex which is approximately 10 – 13µm. Both the white and green Ioncell® fiber spun from banknotes show diameters close to this desirable range. With the green fibers having marginally higher and the white fibers a bit lower values with diameters slightly below 10µm. However, for both fibers produced, it should be noted that the deviation is merely small and almost negligible.

Die approbierte gedruckte Originalversion dieser Diplomarbeit ist an der TU Wien Bibliothek verfügbar
The approved original version of this thesis is available in print at TU Wien Bibliothek.

4.4.5. Molecular Mass Distribution

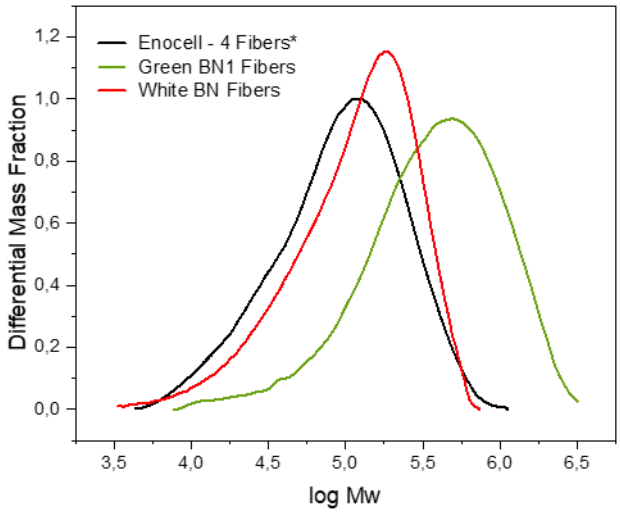

Figure 23. Results of gel permeation chromatography measurements. Molecular Mass Distribution of Ioncell® fibers from Enocell-4 pulp, and green and white Ioncell® fibers from banknotes.
(*) Fibers produced and measured by Helena Sederholm (Aalto University).

The molecular mass distribution of the green and white Ioncell® fibers spun from banknotes as well as the Ioncell® fibers from Enocell – 4 pulp are quite dissimilar, as shown in Figure 23. The green banknote fibers show a similar distribution compared to the Enocell-4 fibers, however, the curve is shifted to higher molecular weights by almost one decimal. The white banknote fibers exhibit a narrower molecular weight distribution. The white banknotes also show a shift to higher molecular weights, though the difference is not as prominent, with about a quarter of a decimal. The difference of the molar mass distribution between the green and the white BN fibers is unexpected. (Dupont, 2003) states that a dissolution of cellulose in a LiCl / DMAc solution has little to almost no influence on the molacular mass distribution. Consequently, the difference is caused by the initial intrinsic viscosity of the substrate (bleached material: 394 ml/g; LiCl/DMAc treated material: 376 ml/g) and the dope production temperature (bleached material: 85 °C; LiCl/DMAc treated material: 85 & 90 °C).

Die approbierte gedruckte Originalversion dieser Diplomarbeit ist an der TU Wien Bibliothek verfügbar
The approved original version of this thesis is available in print at TU Wien Bibliothek.

4.4.6. X-Ray Diffraction Measurements

XRD measurements have been conducted for white and green Ioncell® fibers spun from banknotes.

Table 12. Results of XRD measurements of green and white Ioncell® fibers spun from banknotes. Orientation [%], Anis-Ratio [%], Crystallinity [%] and Crystal size of L1-10, L110 and L020 [Å], respectively

SAMPLE	Orientation [%]	Anis - Ratio [%]	Crystallinity [%]	L1-10 [Å]	L110 [Å]	L020 [Å]
Green BN1 Fibers	67.7 ± 3.8	70.4 ± 2.9	24.0 ± 0.4	42.1	36.1	33.1
White BN Fibers	72.0 ± 1.9	88.5 ± 0.8	31.7 ± 0.1	42.0	45.7	37.4

Table 12 summarizes the orientation, anis-ratio, and crystallinity of the produced fibers. Furthermore, the respective crystal sizes of the hkl planes L1-10, L110 and L0202 are shown. The crystalline orientation of the green banknote fibers is relatively low and slightly higher for the white Ioncell® fibers. The anis-ratio, which is the ratio between isotropic versus anisotropic scattering is low for the green Ioncell® fibers. This indicates the presence of a metal contamination (green pigment). In general, another reason for the decreased anis-ratios are randomly oriented amorphous materials. However, due to the increased value for the white fibers, this is quite unlikely. The crystallinity for the white fibers almost reaches the crystallinity of standard fibers, where values of up to 36% are achieved. Whereas the crystallinity of the green fibers is very low (Sixta et al., 2015).

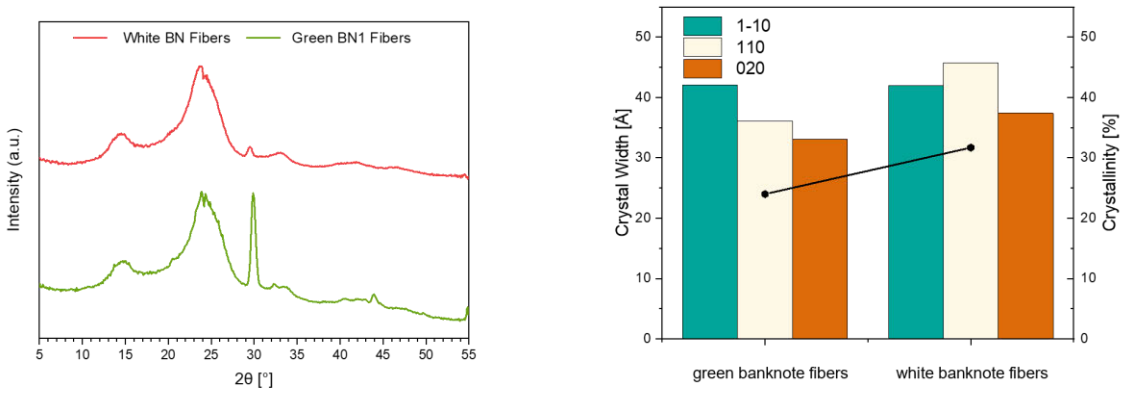

(a) (b)

Figure 24. Results of X-ray diffraction analysis for green and white banknote fibers, respectively. (a) intensity over 2θ [°] and (b) crystal width [Å] of reflection planes ([1-10], [110], [020], respectively) and crystallinity [%] of the fibers. Measured by Daisuke Sawada (Aalto University)

Die approbierte gedruckte Originalversion dieser Diplomarbeit ist an der TU Wien Bibliothek verfügbar
The approved original version of this thesis is available in print at TU Wien Bibliothek.

In Figure 24 (a) the spectra for both white and green Ioncell® fibers from banknotes is given as intensity over 2θ. In (b) the crystal size perpendicular to the reflection planes (h k l) are given as 1-10, 110 and 220 as well as the calculated crystallinities of the fibers are illustrated.

The spectra for both white and green Ioncell® fibers from banknotes in the range of 5-55° as seen above is a very typical representation of a cellulose II spectrum. Thereby, cellulose II is illustrated by the reflections at 15, 25 and 30°, formed by the lattice planes.(Fink et al., 1995).

The spectrum of the green Ioncell® fibers shows a very prominent reflection at 29.8°, which is only very weakly pronounced in the spectrum of the white Ioncell® fibers. In addition, a smaller reflection can be seen at 43.9°, which has completely disappeared in the white Ioncell® fibers spectrum. If these two distinct reflections could be assigned to a spectrum of a certain compound, the mystery of the green color would be solved. More details can be found under section 4.8.

4.5 Elemental Analysis

The respective chemical compositions of the treated banknotes and of the green and white Ioncell® fibers from banknotes are listed in Table 13. In addition, the elemental composition of the green pigments, which were separated by centrifugation from the cellulose dissolved in LiCl/DMAc solution, and the acetone-soluble red colors were examined, which are also shown in Table 13.

In the first two mechanical pre-treatment steps (sieving and magnetic separation) no major chemical changes in the composition of the banknotes compared to the initial milled BNs were recognized. The marginal reduction of nitrogen and hydrogen by the subsequent acetone treatment and bleaching is rather negligible. Though, surprisingly, the white cellulose sample cleaned and purified by LiCl/DMAc dissolution has a very low carbon content (17.43%) and a relatively high nitrogen content. This might be caused by an incomplete removal of the LiCl/DMAc solution. The green and white Ioncell® fibers from banknotes are in the range of comparable cotton fibers with a slightly lower carbon content (de Morais Teixeira et al., 2010).

Die approbierte gedruckte Originalversion dieser Diplomarbeit ist an der TU Wien Bibliothek verfügbar
The approved original version of this thesis is available in print at TU Wien Bibliothek.

Besides, the green fibers exhibit a noticeably higher nitrogen content, caused by the presence of the green pigment.

Table 13. Elemental composition (C, N, H, S) [%] with respective standard deviations of each pre-treatment step as well as for green and white banknote fibers and separated red color and green pigments. Measured by Eva Gonzalez (Aalto University)

Sample Name	Ø C [%]	σ	Ø N [%]	σ	Ø H [%]	σ	Ø S [%]	σ
Milled Banknotes	42.20	0.08	0.43	0.01	5.99	0.02	0.00	0.00
Sieved Banknotes	42.32	0.10	0.42	0.02	6.01	0.04	0.00	0.00
Magnetic treated Banknotes	42.42	0.19	0.37	0.02	5.96	0.02	0.00	0.00
Acetone treated Banknotes	41.88	0.21	0.36	0.01	5.91	0.05	0.00	0.00
Bleached Banknotes	41.95	0.29	0.20	0.01	5.88	0.03	0.00	0.00
LiCl cleaned Banknotes	17.43	0.29	1.23	0.06	5.60	0.19	0.00	0.00
Green BN1 Fibers	40.25	0.05	0.64	0.02	5.65	0.04	0.00	0.00
White BN Fibers	40.50	0.40	0.10	0.01	6.08	0.08	0.00	0.00
Acetone solubles (red colour)	63.71	0.30	1.12	0.03	9.21	0.02	0.28	0.04
Green Pigments	32.57	0.32	8.46	0.31	8.31	0.21	0.00	0.00

The red color and the green pigments show a completely different composition. The red color consists of predominantly carbon (63%) and hydrogen (9%). This indicates that mainly organic materials could be separated by the treatment with acetone. Although the ink was dried in an oven at 105°C for several hours, residual acetone contamination might be present. In addition, small amounts of sulphur were detected. An explanation for the sudden appearance would be the accumulation and concentration of sulphur components by separation Whereas the sulphur content of the other banknote samples is below the limit of quantification (< 100 ppm) and consequently not detectable.

The green pigments show an increased nitrogen content. Residuals of the DMAc solvent cannot be excluded, however, the elevated nitrogen content might be caused by the green pigment. The determination of the green pigment is discussed in more detail under section 4.8.

Die approbierte gedruckte Originalversion dieser Diplomarbeit ist an der TU Wien Bibliothek verfügbar
The approved original version of this thesis is available in print at TU Wien Bibliothek.

4.6 FTIR – Analysis

The spectra of the FTIR studies of selected banknote samples are illustrated in Figure 25.

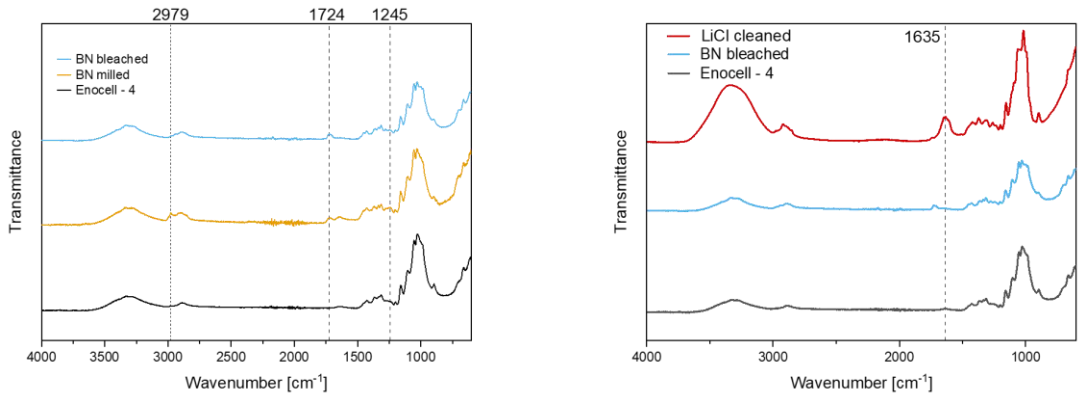

Figure 25. FTIR spectra of Enocell – 4, milled BNs, bleached BNs as well as LiCl cleaned BNs for comparison.

IR spectroscopy is used to determine the chemical structure of molecules. Excitation with IR radiation causes certain molecules to vibrate and thus absorb the radiation. The prerequisite for this is on the one hand the fulfilment of the resonance condition and on the other hand the change of the dipole moment. The resulting oscillations can be divided into valence and deformation oscillations. During valence oscillations, bond distances change symmetrically or asymmetrically. The deformation vibrations occur in various forms, such as bending, rocking, twisting, wagging or all their possible combinations. The resulting spectrum can generally be divided into two areas, from which different information about the chemical composition of the sample is extracted. In the higher wavenumber area, about 2000 cm^{-1} and above, single functional groups are detected with very high accuracy. For example, the OH unit is easily identified by a broad peak at about 3600-3200cm^{-1}. The second area, the so-called fingerprint area, is located at lower wavenumbers, about 2000 cm^{-1} and below. Here it is difficult to make precise statements about specific functional groups, however, this range is unique for each molecule (Griffiths & de Haseth, 2007).

The spectra listed above (Figure 25) show broad peaks in the range of about 3500 - 3100 cm^{-1}. These peaks illustrate the oxygen - hydrogen bond of water. The cellulose polymer chains are connected by water molecules, and these are detected in this area. Furthermore, residual moisture is also represented by this peak.

Die approbierte gedruckte Originalversion dieser Diplomarbeit ist an der TU Wien Bibliothek verfügbar
The approved original version of this thesis is available in print at TU Wien Bibliothek.
TU Bibliothek Your knowledge hub WIEN

In general, it can be observed that the spectra are very similar. Only the spectrum of the LiCl cleaned banknotes shows an additional pronounced peak at 1635 cm^{-1}. This peak might present C=O stretching vibrations of remaining DMAc molecules. Individual small peaks that disappear during treatment indicate successful purification steps, for example, the disappearance of the peak at 2979 cm^{-1} of the milled BN in Figure 25 (a), presumably caused by a C-H compound.

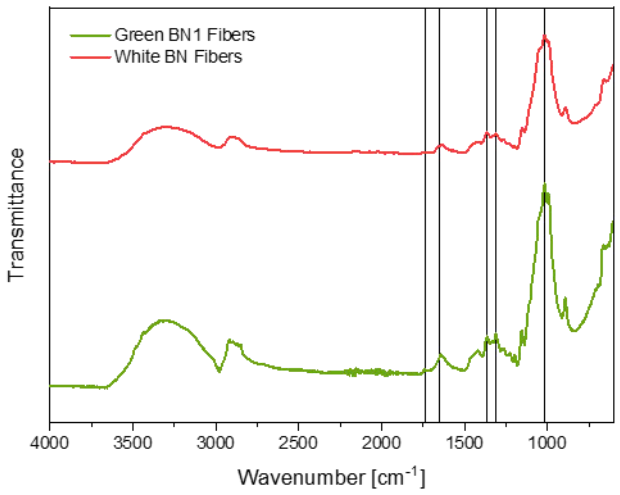

Figure 26. Comparison of FTIR spectra from green Ioncell® fibers produced from bleached banknotes and white Ioncell® fibers produced from LiCl cleaned banknotes.

A direct comparison of the green and white Ioncell® fibers from banknotes shows that there is virtually no difference between the spectra, see Figure 26. The inserted auxiliary lines show that all the dominant peaks can be found in both spectra. The only difference is the intensity of the transmittance. Compared to related fibers, such as lyocell and viscose-type fibers, similar spectra have been obtained (Hospodarova et al., 2018) (Carrillo et al., 2004).

Die approbierte gedruckte Originalversion dieser Diplomarbeit ist an der TU Wien Bibliothek verfügbar
The approved original version of this thesis is available in print at TU Wien Bibliothek.

4.7 Simultaneous Thermal Analysis (STA)

All samples, including samples of each pre-treatment step, the separated red dyes, the separated green pigments as well as the green and white fibers, have been measured by STA. The most important results are presented in Figure 27.

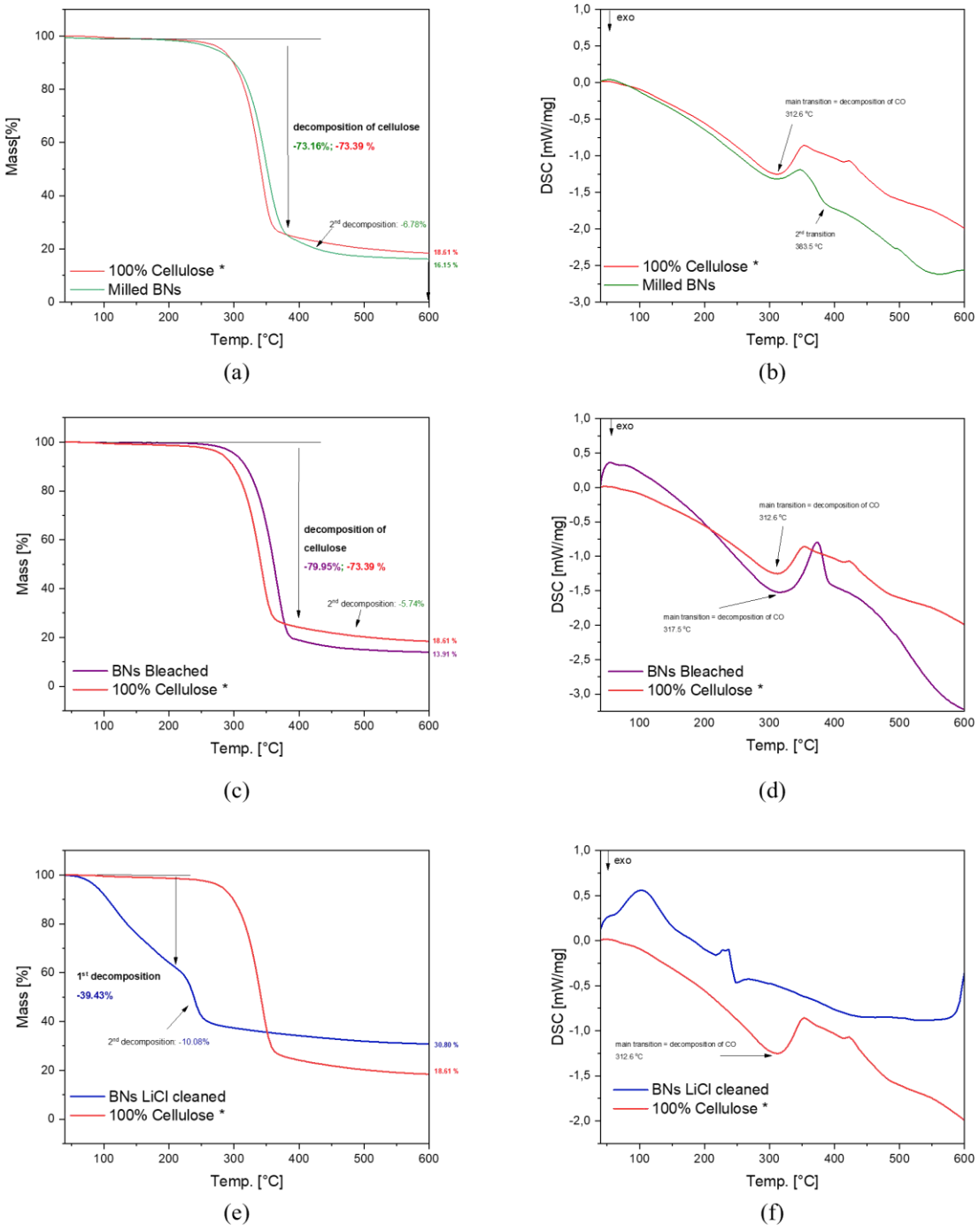

Figure 27. Results of STA measurements of milled BNs (a) & (b), bleached BNs (c) & (d) and LiCl cleaned BNs (e) & (f), respectively. TGA graphs on the left and DSC graphs on the right. (*) 100% cellulose sample was measured by Inge Schlapp – Hackl (Aalto University)

Die approbierte gedruckte Originalversion dieser Diplomarbeit ist an der TU Wien Bibliothek verfügbar
The approved original version of this thesis is available in print at TU Wien Bibliothek.

In Figure 27 (a) & (b) a sample of 100% cellulose is compared with a sample of chemically untreated milled banknotes. It can be observed that the two TGA graphs (a) are very alike. The decomposition of the cellulose around 300°C, as indicated, is almost identical. The reduction of the mass is -73.16% and -73.39% for milled banknotes and 100% cellulose, respectively. Hardly surprising, considering that the banknotes are made up of 90% cotton. A second transition at 383.5°C can be noticed for the milled BNs where an additional mass reduction of 6.78% happens. The difference after the main transition is very clearly depicted in the DSC graph (see (b)). Finally, 16.15% remains as residue. The clear discrepancy between the 16.15% and the 7.49% in the ash content measurement can be explained by the fact that the STA measurement was carried out under inert gas and therefore no conventional combustion took place.

Although one would assume that the graphs of the more purified banknotes would become more alike to those of 100% cellulose, the results for bleached BNs show a different picture (Figure 27 (c) & (d)). The main transition has shifted by almost 5°C from 312.6°C for milled Banknotes to 317.5°C for the bleached BNs. The second transition of the bleached BNs can be described as more exothermal compared to milled BNs. The residue was slightly reduced to 13.91%.

The results for the LiCl cleaned banknotes have almost nothing in common with the results for 100% cellulose (see Figure 27 (e) & (f)). An endothermal reaction including a significant mass reduction can be seen at around 100°C. This could be caused by residue water and indicates an insufficient drying. The following transitions at ~150°C and at ~225°C are also substantially different from all other samples. Ultimately, a residue of 30.80% remains after the measurement at 600°C, which is not in line with the result of 1.45% from the ash-content measurement (see Table 1). A contamination of the sample with LiCl and/or DMAc as well as a faulty measurement cannot be excluded.

Along the pre-treatment process two different types of dyes were separated from the banknotes, as described in section 3.2. By acetone treatment red dyes were dissolved. These dyes were then purified by evaporation of the acetone. Furthermore, green pigments were separated from the BNs by LiCl/DMAc treatment and sedimentation. In Figure 28 the results of the STA measurements for these dyes are depicted.

Die approbierte gedruckte Originalversion dieser Diplomarbeit ist an der TU Wien Bibliothek verfügbar
The approved original version of this thesis is available in print at TU Wien Bibliothek.

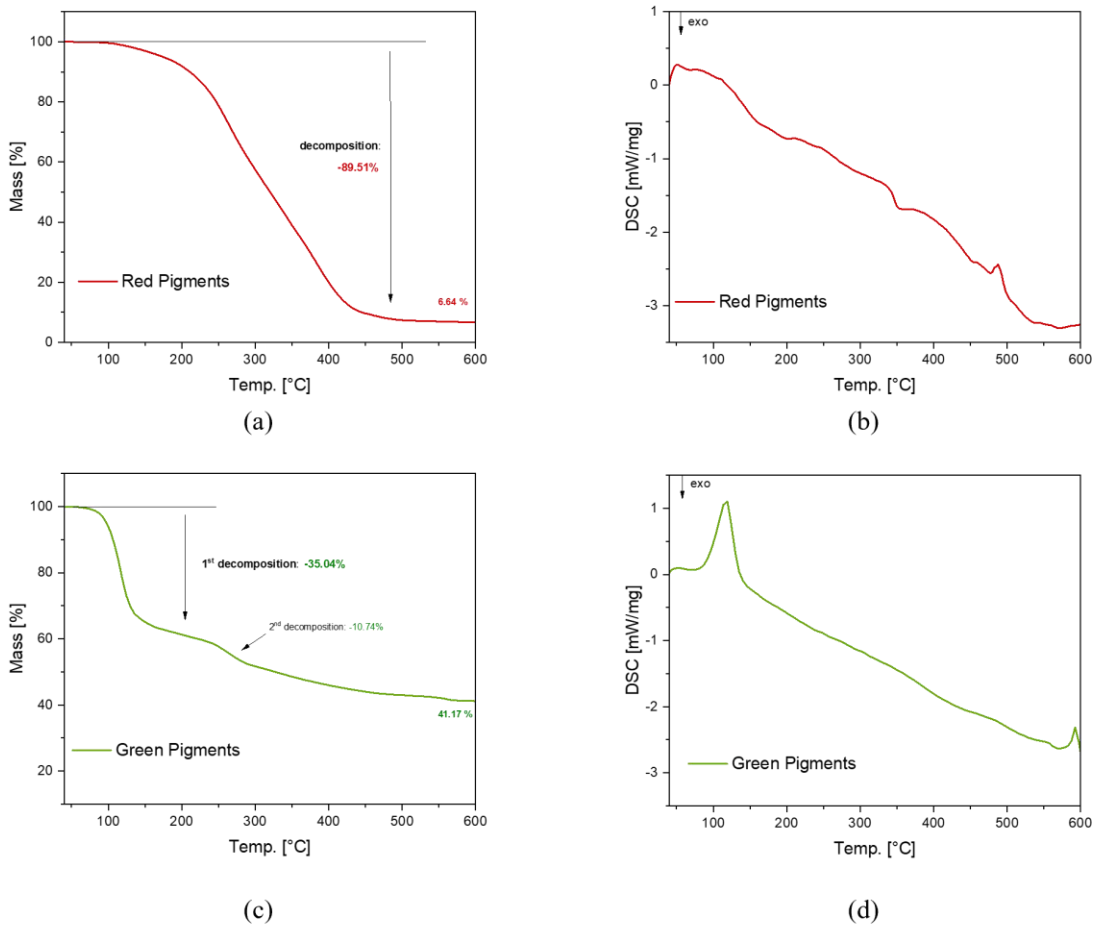

Figure 28. Results of STA measurements of red dyes, separated by acetone and green pigments, separated by LiCl/DMAc treatment and sedimentation. TGA graphs on the left and DSC graphs on the right.

Figure 28 (a) shows an almost complete decomposition of the red component between 130°C and 450°C. The final residue is roughly 6.64%. A sequence of several transitions can be recognized considering the results of the DSC (see (b)). This suggests that the sample may not be a single substance. A variety of substances may have been dissolved in acetone. Contamination by acetone can be ruled out, as the boiling point of acetone is 56°C. It is hardly possible to determine the exact nature of the sample by STA measurement.

The green pigments were possibly contaminated by LiCl/DMAc solution and dissolved cellulose, due to inaccuracies during decantation. The STA results of the pigments are presented in Figure 28 (c) & (d). A decomposition and endothermal reaction at around 85°C with an accompanying mass reduction of 35.04% is observed. Evaporation of DMAc as well as the decomposition of cellulose can be ruled out. The boiling point for DMAc is 165°C and the decomposition for cellulose is usually at around 300°C (see Figure 27). A second transition inducing a mass reduction of 10.74% between 200 and 300°C is observable.

Die approbierte gedruckte Originalversion dieser Diplomarbeit ist an der TU Wien Bibliothek verfügbar
The approved original version of this thesis is available in print at TU Wien Bibliothek.
TU Bibliothek Your knowledge hub WIEN

Lastly, a significant endothermal reaction above 580°C with additional mass reduction is seen. The final residue at 600°C accounts to 41.17%, indicating a quite stable component which could be the green pigment or remains of it.

In Figure 29 the results of the STA measurements of the green as well as the white Ioncell® fibers from banknotes are depicted. Although an almost identical main transition temperature of around 315°C can be observed, the decomposition itself is vastly different. For the green fibers the cellulose decomposition resulted in a mass loss of 70.43% while the mass loss for the white fibers is 97.30%. Additionally, the laws of physics do not quite comply with the residue of -5.93% for the white fibers. The ash residue of 20.82% for the green fibers is unexpectedly high, considering that the ash residue for bleached BNs, which was used as initial material for the production of the green fibers, was 13.91%.

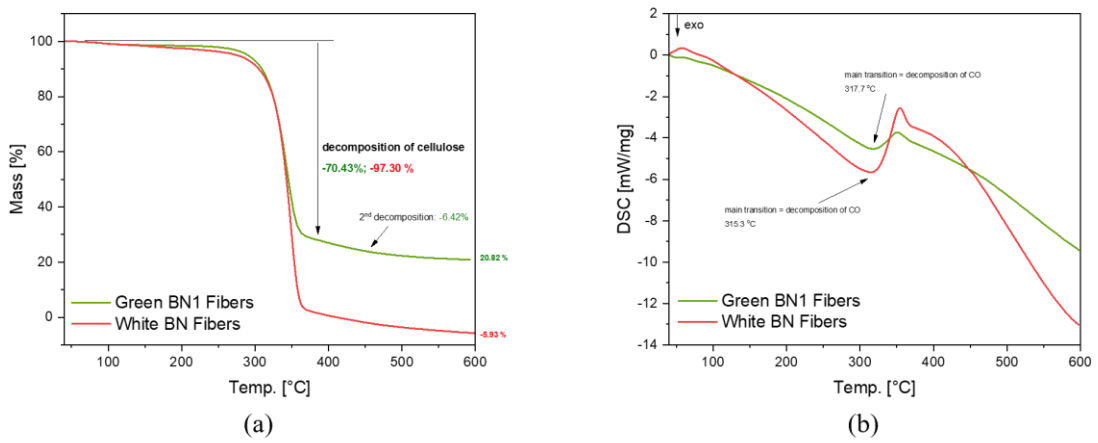

Figure 29. Results of STA measurements for green and white Ioncell® fibers from banknotes. (a) TGA graph and (b) DSC graph.

Die approbierte gedruckte Originalversion dieser Diplomarbeit ist an der TU Wien Bibliothek verfügbar
The approved original version of this thesis is available in print at TU Wien Bibliothek.

4.8 Green Pigments

The extraordinary stability of the green color became apparent very quickly. Partially very aggressive treatment methods, such as hypochlorite or ozone bleaching, acidic treatment at elevated temperatures, dissolution trials in LiCl / DMAc solution or IL, could neither dissolve nor destroy the green color.

The successful separation of the pigments from the cellulose by dissolving the cellulose and separating the pigment by centrifugation was a major step towards identifying the nature of the pigment. However, due to the insolubility of the pigment, many methods (e.g., liquid NMR) can`t be used for the determination of the structure.

Based on the ICP analysis, some green metallic complexes could already be excluded. After the bleaching process, after all colors disappeared except for the green one, only Fe and Cu were detected in higher concentrations (see Figure 16). Consequently, it can be assumed that it must be a metallic complex with one of these metals.

There are many copper-based pigments that give green color, such as copper (II) acetate, malachite, copper resinate or phthalocyanine green. However, many of these pigments can be excluded directly, either because of their chemical composition, which is not in line with the ICP measurement, or because of their applications. In addition, the pigment illustrated a high chemical stability and so pigments that are soluble in water for instance, are also directly ruled out. One pigment that quickly attracted the attention during the research was phthalocyanine green. This pigment is used in a wide variety of applications, such as in inks, in oil paint or many plastics (Gregory, 2000). This chlorinated copper complex (chemical structure, see Figure 30) exhibits an extremely high solvent-, acid- and alkali- resistance. For some solvents, such as trifluoroacetic acid (TFA) or tetrahydrofuran (THF), it has only very limited solubility, while in others, such as benzene and toluene, it has almost no solubility at all. (Ghani et al., 2012). In addition, the metal complex is stable up to several hundred degrees Celsius, with a melting point of slightly below 800°C and shows high stability to radiation (Saadati Ardestani et al., 2020).

Die approbierte gedruckte Originalversion dieser Diplomarbeit ist an der TU Wien Bibliothek verfügbar
The approved original version of this thesis is available in print at TU Wien Bibliothek.

The elemental analysis of the green pigments shows elevated nitrogen levels of 8.46%. Even more notable is, that the nitrogen content of the green Ioncell® fibers from banknotes is more than six times higher than the nitrogen content of their white counterpart (see Table 13). Furthermore, a high thermal stability of the green pigments until 600°C was shown in the STA, see Figure 28 (c) & (d). In addition, the XRD spectroscopy result also points to this pigment. Phthalocyanine green shows a single very prominent peak at 27° (Saadati Ardestani et al., 2020). Compared with the spectrum of the green fibers (see Figure 24), it appears to be very similar.

All these findings, the high stability against very aggressive treatment methods, the suitable application area, the increased nitrogen content, the thermal stability up to 600°C and the appearance of a very prominent and fitting peak in the XRD measurement, suggest that the green pigment is very likely phthalocyanine green.

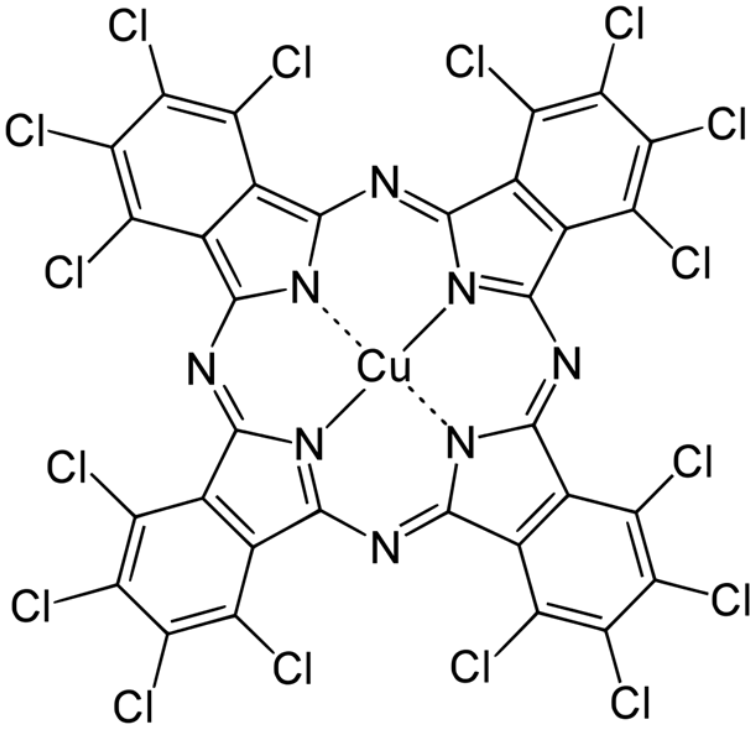

Figure 30. Chemical structure of phthalocyanine green.

Die approbierte gedruckte Originalversion dieser Diplomarbeit ist an der TU Wien Bibliothek verfügbar
The approved original version of this thesis is available in print at TU Wien Bibliothek.

5. Conclusion

A sequence of treatment steps was successfully developed during this thesis to separate non-cellulosic components from the pure cotton in Euro banknotes, resulting in a final recovery rate of above 70%. Through the first five successive treatment steps, milling, sieving, magnetic treatment, acetone treatment and bleaching with sodium hypochlorite, contaminations of the banknotes could already be reduced to acceptable values while the relative cellulose content was increased by almost 2.5%. Subsequently, green Ioncell® fibers were produced from these pretreated bills. Several spinning trials with a small dry-jet wet spinning unit were conducted. Furthermore, one spinning trial with a bigger dry-jet wet spinning unit was performed and a greater number of fibers was produced. These green fibers were used to produce a small piece of fabric. Due to the small amount of fibers a 50/50 blend of green Ioncell® fibers from banknotes and Tencel fibers was prepared and further processed into yarn and next into a garment. By dissolving the cotton of already bleached banknotes in a supersaturated LiCl / DMAc solution at room temperature and then separating the green pigments by centrifugation, followed by precipitation of the dissolved cellulose in water, the amount of contaminations was reduced to an absolute minimum. Simultaneously the relative cellulose content could be increased to 94.5%. From this purified material white fibers have been produced. Further investigations would be necessary to improve the final cellulose content even more. Optimizations of the pre-treatment sequence could also be considered with respect to the yield. Especially during the sieving phase, a considerable number of losses occurs, consisting of not only non-cellulosic, but also cellulosic components. Besides the recycling of the “lost” fractions (removed metals or colors) could be pursued. Moreover, the used chemicals acetone and sodium hypochlorite could be replaced by more environmentally friendly alternatives.

Although the properties of the produced fibers do not reach the values of comparable Ioncell® fibers, the values are still within a reasonable range compared to commercially used fibers. There was a significant discrepancy in the achieved mechanical properties between the green Ioncell® fibers produced with the big and the small dry-jet wet spinning unit. While the fibers produced from the smaller unit achieved the best results, the fibers from the big spinning unit had the poorest performance. The white Ioncell® fibers from banknotes had significantly lower values in both mechanical properties as well as in the birefringence measurement compared to the green Ioncell® fibers from banknotes as summarized in section 4.4.2.

Die approbierte gedruckte Originalversion dieser Diplomarbeit ist an der TU Wien Bibliothek verfügbar
The approved original version of this thesis is available in print at TU Wien Bibliothek.

However, the white fibers showed a notably higher crystallinity than the green Ioncell® fibers. The structure of cellulose II could be verified in both green and white Ioncell® fibers from banknotes by XRD. Via a significant difference in the spectra of the XRD measurements the nature of the green pigments (phthalocyanine green) was most likely confirmed. The spectra from the FTIR measurements are very similar for both the green and the white fibers and are alike compared to the spectra of other man-made cellulosic fibers.

All things considered; the initial objectives of this thesis have been achieved. A sequence of treatment steps has been effectively developed which has finally made it possible to recycle old banknotes. Green and white Ioncell® fibers from banknotes were successfully produced.

Die approbierte gedruckte Originalversion dieser Diplomarbeit ist an der TU Wien Bibliothek verfügbar
The approved original version of this thesis is available in print at TU Wien Bibliothek.

6. References

Adusumalli, R. B., Keckes, J., Martinschitz, K. J., Boesecke, P., Weber, H., Roeder, T., Sixta, H., & Gindl, W. (2009). Comparison of molecular orientation and mechanical properties of lyocell fibre tow and staple fibres. *Cellulose*, *16*(5), 765–772. https://doi.org/10.1007/s10570-009-9292-2

Adusumalli, R. B., Venkateshan, K. C., Kunchi, C., & Vadlamani, S. R. (2019). Tensile testing of single fibres. *Procedia Structural Integrity*, *14*, 150–157. https://doi.org/10.1016/j.prostr.2019.05.020

ANDRÉ M. STRIEGEL. (2002). ADVANCES IN THE UNDERSTANDING OF THE DISSOLUTION MECHANISM OF CELLULOSE IN DMAc/LiC. *Journal of the Chilean Chemical Society*.

Aristovnik, A., & Čeč, T. (2009). *Compositional Analysis of Foreign Currency Reserves in the 1999-2007 Period : The Euro vs. The Dollar as Leading Reserve Currency*. https://mpra.ub.uni-muenchen.de/14350/

Asaadi, S., Hummel, M., Ahvenainen, P., Gubitosi, M., Olsson, U., & Sixta, H. (2018). Structural analysis of Ioncell-F fibres from birch wood. *Carbohydrate Polymers*, *181*, 893–901. https://doi.org/10.1016/j.carbpol.2017.11.062

Asaadi, S., Hummel, M., Hellsten, S., Härkäsalmi, T., Ma, Y., Michud, A., & Sixta, H. (2016). Renewable High-Performance Fibers from the Chemical Recycling of Cotton Waste Utilizing an Ionic Liquid. *ChemSusChem*, *9*(22), 3250–3258. https://doi.org/10.1002/cssc.201600680

Bajpai, P. (2017). Structure and Properties of Cellulose and Nanocellulose. In *Pulp and Paper Industry* (pp. 27–40). Elsevier. https://doi.org/10.1016/b978-0-12-811101-7.00003-4

Beattie, A. (2015). history money. *Investopedia LLC.* http://www.investopedia.com/articles/07/roots_of_money.asp?view=print

Berger, M., Campos, J., Carolli, M., Dantas, I., Forin, S., Kosatica, E., Kramer, A., Mikosch, N., Nouri, H., Schlattmann, A., Schmidt, F., Schomberg, A., & Semmling, E. (2021). Advancing the Water Footprint into an Instrument to Support Achieving the SDGs – Recommendations from the "Water as a Global Resources" Research Initiative (GRoW). *Water Resources Management*, *35*(4), 1291–1298. https://doi.org/10.1007/s11269-021-02784-9

Cai, J., & Zhang, L. (2005). Rapid dissolution of cellulose in LiOH/urea and NaOH/urea aqueous solutions. *Macromolecular Bioscience*, *5*(6), 539–548. https://doi.org/10.1002/mabi.200400222

Cai, J., Zhang, L., Zhou, J., Li, H., Chen, H., & Jin, H. (2004). Novel fibers prepared from cellulose in NaOH/urea aqueous solution. *Macromolecular Rapid Communications*, *25*(17), 1558–1562. https://doi.org/10.1002/marc.200400172

Carrillo, F., Colom, X., Suñol, J. J., & Saurina, J. (2004). Structural FTIR analysis and thermal characterisation of lyocell and viscose-type fibres. *European Polymer Journal*, *40*(9), 2229–2234. https://doi.org/10.1016/j.eurpolymj.2004.05.003

Change, N. C. (2018). The price of fast fashion. In *Nature Climate Change* (Vol. 8, Issue 1, p. 1). Nature Publishing Group. https://doi.org/10.1038/s41558-017-0058-9

Chrapava, S., Touraud, D., Rosenau, T., Potthast, A., & Kunz, W. (2003). The investigation of the influence of water and temperature on the LiCl/DMAc/cellulose system. *Physical Chemistry Chemical Physics*, *5*(9), 1842–1847. https://doi.org/10.1039/b212665f

de Morais Teixeira, E., Corrêa, A. C., Manzoli, A., de Lima Leite, F., de Ribeiro Oliveira, C., & Mattoso, L. H. C. (2010). Cellulose nanofibers from white and naturally colored cotton fibers. *Cellulose*, *17*(3), 595–606. https://doi.org/10.1007/s10570-010-9403-0

Die approbierte gedruckte Originalversion dieser Diplomarbeit ist an der TU Wien Bibliothek verfügbar
The approved original version of this thesis is available in print at TU Wien Bibliothek.

de Vries, H. (1959). The Relation between Birefringence and Draw Ratio of Man-Made Fibers. In *JOURNAL OF POLYMER SCIENCE: Vol. XXXIV*. NOTTINGHAM SYMPOSIUM.

Dupont, A. L. (2003). Cellulose in lithium chloride/N,N-dimethylacetamide, optimisation of a dissolution method using paper substrates and stability of the solutions. *Polymer*, *44*(15), 4117–4126. https://doi.org/10.1016/S0032-3861(03)00398-7

ecb.europa.at. (2022). *https://www.ecb.europa.eu/euro/20_years_of_euro/html/index.en.html*.

ecb.europa.eu. (2022). *https://www.ecb.europa.eu/euro/banknotes/images/html/index.en.html*.

Eichinger, D., & Eibl M. (1996). Lenzing Lyocell-An interesting cellulose fiber for the textile industry. *Chemical Fibers International 46.1*, 26–29.

Elsayed, S., Hellsten, S., Guizani, C., Witos, J., Rissanen, M., Rantamäki, A. H., Varis, P., Wiedmer, S. K., & Sixta, H. (2020). Recycling of Superbase-Based Ionic Liquid Solvents for the Production of Textile-Grade Regenerated Cellulose Fibers in the Lyocell Process. *ACS Sustainable Chemistry and Engineering*, *8*(37), 14217–14227. https://doi.org/10.1021/acssuschemeng.0c05330

Elsayed, S., Hummel, M., Sawada, D., Guizani, C., Rissanen, M., & Sixta, H. (2021). Superbase-based protic ionic liquids for cellulose filament spinning. *Cellulose*, *28*(1), 533–547. https://doi.org/10.1007/s10570-020-03505-y

Farr, J. P., Smith, W. L., & Steichen, D. S. (2003). Bleaching Agents. In *Kirk-Othmer Encyclopedia of Chemical Technology* (pp. 48–53). John Wiley & Sons, Inc. https://doi.org/10.1002/0471238961.1921182206011818.a01.pub2

Fink, H.-P., Hofmann, D., & Philipp, B. (1995). Some aspects of lateral chain order in cellulosics from X-ray scattering. In *CELLULOSE* (Vol. 2).

Frost, K., Kaminski, D., Kirwan, G., Lascaris, E., & Shanks, R. (2009). Crystallinity and structure of starch using wide angle X-ray scattering. *Carbohydrate Polymers*, *78*(3), 543–548. https://doi.org/10.1016/j.carbpol.2009.05.018

Gardivert, K. H., & Blackwell, J. (1975). The Structure of Native Cellulose*. In *BIOPOLYMERS* (Vol. 13).

Ghani, F., Kristen, J., & Riegler, H. (2012). Solubility properties of unsubstituted metal phthalocyanines in different types of solvents. *Journal of Chemical and Engineering Data*, *57*(2), 439–449. https://doi.org/10.1021/je2010215

Gregory, P. (2000). *Industrial applications of phthalocyanines*. https://doi.org/https://doi.org/10.1002/(SICI)1099-1409(200006/07)4:4<432::AID-JPP254>3.0.CO;2-N

Griffiths, P. R., & de Haseth, J. A. (2007). *Fourier Transform Infrared Spectrometry, Chemical Analysis: A Series of Monographs on Analytical Chemistry and Its Applications*.

Gross, A. S., & Chu, J. W. (2010). On the molecular origins of biomass recalcitrance: The interaction network and solvation structures of cellulose microfibrils. *Journal of Physical Chemistry B*, *114*(42), 13333–13341. https://doi.org/10.1021/jp106452m

Gupta, V. B., & Kothari, V. K. (1997). *Manufactured fibre technology*. Chapman & Hall.

Haslinger, S., Hummel, M., Anghelescu-Hakala, A., Määttänen, M., & Sixta, H. (2019). Upcycling of cotton polyester blended textile waste to new man-made cellulose fibers. *Waste Management*, *97*, 88–96. https://doi.org/10.1016/j.wasman.2019.07.040

Haslinger, S., Wang, Y., Rissanen, M., Lossa, M. B., Tanttu, M., Ilen, E., Määttänen, M., Harlin, A., Hummel, M., & Sixta, H. (2019). Recycling of vat and reactive dyed textile waste to new colored man-made cellulose fibers. *Green Chemistry*, *21*(20), 5598–5610. https://doi.org/10.1039/c9gc02776a

Die approbierte gedruckte Originalversion dieser Diplomarbeit ist an der TU Wien Bibliothek verfügbar
The approved original version of this thesis is available in print at TU Wien Bibliothek.

Haslinger, S., Ye, Y., Rissanen, M., Hummel, M., & Sixta, H. (2020). Cellulose Fibers for High-Performance Textiles Functionalized with Incorporated Gold and Silver Nanoparticles. *ACS Sustainable Chemistry and Engineering*, *8*(1), 649–658. https://doi.org/10.1021/acssuschemeng.9b06385

Hauru, L. K. J. (2017). *Lignocellulose solutions in ionic liquids*.

Hauru, L. K. J., Hummel, M., Michud, A., & Sixta, H. (2014). Dry jet-wet spinning of strong cellulose filaments from ionic liquid solution. *Cellulose*, *21*(6), 4471–4481. https://doi.org/10.1007/s10570-014-0414-0

Hofmann, U., Herzenstiel, E., Schonemann, E., & Schwarz, K.-H. (1964). *Ultramarin*.

Hospodarova, V., Singovszka, E., & Stevulova, N. (2018). Characterization of Cellulosic Fibers by FTIR Spectroscopy for Their Further Implementation to Building Materials. *American Journal of Analytical Chemistry*, *09*(06), 303–310. https://doi.org/10.4236/ajac.2018.96023

ioncell.fi/research/. (2022). *https://ioncell.fi/research/*.

IPCC. (2006). *Intergovernmental Panel on Climate Change (IPCC), 2006. IPCC Guidelines for National Greenhouse Gas Inventories, Volume 5, Waste. IPCCINCINERATION AND OPEN BURNING OF WASTE*. https://www.ipcc-nggip.iges.or.jp/public/2006gl/vol5.html

ISO 14869-3:2017. (n.d.). *Soil quality — Dissolution for the determination of total element content — Part 3: Dissolution with hydrofluoric, hydrochloric and nitric acids using pressurised microwave technique*. Https://Www.Iso.Org/Standard/60536.Html.

Janson, J. (1970). Calculation of the polysaccharide composition of wood and pulp, Pap. . *Puu*, 323–329.

Jia, F., Yin, S., Chen, L., & Chen, X. (2020). The circular economy in the textile and apparel industry: A systematic literature review. In *Journal of Cleaner Production* (Vol. 259). Elsevier Ltd. https://doi.org/10.1016/j.jclepro.2020.120728

Kim, D. B., Lee, W. S., Jo, S. M., Lee, Y. M., & Kim, B. C. (2002). Physical properties of lyocell fibers spun from different solution-dope phases. *Journal of Applied Polymer Science*, *83*(5), 981–989. https://doi.org/10.1002/app.2278

Klemm, D., Heublein, B., Fink, H. P., & Bohn, A. (2005). Cellulose: Fascinating biopolymer and sustainable raw material. In *Angewandte Chemie - International Edition* (Vol. 44, Issue 22, pp. 3358–3393). https://doi.org/10.1002/anie.200460587

Kumar, P., Barrett, D. M., Delwiche, M. J., & Stroeve, P. (2009). Methods for Pretreatment of Lignocellulosic Biomass for Efficient Hydrolysis and Biofuel Production. *Industrial & Engineering Chemistry Research*, *48*(8), 3713–3729. https://doi.org/10.1021/ie801542g

Kyrychok, T., Kyrychok, P., Havenko, S., Kibirkštis, E., & Miliunas, V. (2014). The influence of pressure during intaglio printing on banknotes durability. *Mechanika*, *20*(3), 327–331. https://doi.org/10.5755/j01.mech.20.3.7393

Leykin, A., & Ioelovich, M. (2004). NANO-CELLULOSE AND ITS APPLICATIONS. In *Journal* (Vol. 6). https://www.researchgate.net/publication/262672538

Löbbert, G. (2000). Phthalocyanines. In *Ullmann's Encyclopedia of Industrial Chemistry*. Wiley-VCH Verlag GmbH & Co. KGaA. https://doi.org/10.1002/14356007.a20_213

Luján-Ornelas, C., Mancebo del C. Sternenfels, U., & Güereca, L. P. (2018). Life cycle assessment of Mexican polymer and high-durability cotton paper banknotes. *Science of the Total Environment*, *630*, 409–421. https://doi.org/10.1016/j.scitotenv.2018.02.177

Ma, Y. (2018). *Fibre spinning from various low refined, recycled lignocelluloses using ionic liquid*.

Die approbierte gedruckte Originalversion dieser Diplomarbeit ist an der TU Wien Bibliothek verfügbar
The approved original version of this thesis is available in print at TU Wien Bibliothek.
TU Bibliothek Your knowledge hub WIEN

Ma, Y., Asaadi, S., Johansson, L. S., Ahvenainen, P., Reza, M., Alekhina, M., Rautkari, L., Michud, A., Hauru, L., Hummel, M., & Sixta, H. (2015). High-Strength Composite Fibers from Cellulose-Lignin Blends Regenerated from Ionic Liquid Solution. *ChemSusChem*, *8*(23), 4030–4039. https://doi.org/10.1002/cssc.201501094

Ma, Y., Hummel, M., Kontro, I., & Sixta, H. (2018). High performance man-made cellulosic fibres from recycled newsprint. *Green Chemistry*, *20*(1), 160–169. https://doi.org/10.1039/c7gc02896b

Ma, Y., Hummel, M., Määttänen, M., Särkilahti, A., Harlin, A., & Sixta, H. (2016). Upcycling of waste paper and cardboard to textiles. *Green Chemistry*, *18*(3), 858–866. https://doi.org/10.1039/c5gc01679g

Ma, Y., Rissanen, M., You, X., Moriam, K., Hummel, M., & Sixta, H. (2021). New method for determining the degree of fibrillation of regenerated cellulose fibres. *Cellulose*, *28*(1), 31–44. https://doi.org/10.1007/s10570-020-03513-y

MacFarlane, Douglas R., Kar, M., Pringle, & Jennifer M. (2017). *Fundamentals of Ionic Liquids: From Chemistry to Applications*. 1–25. https://doi.org/https://doi.org/10.1002/9783527340033.ch1

Mändar, K., Sõber, T., Kõljalg, S., Rööp, T., Mändar, R., & Sepp, E. (2016). Microbiological contamination of the euro currency in Estonia. *Infectious Diseases*, *48*(10), 772–774. https://doi.org/10.1080/23744235.2016.1201725

Männer, J., Ivanoff, D., Morley, R. J., & Jary, S. (2001). Tencel ® -New Cellulose Fibers for Carpets. . *Lenzinger Berichte 89*, 60–71.

Maurer, R. J., Sax, A. F., & Ribitsch, V. (2013). Moleular simulation of surface reorganization and wetting in crystalline cellulose I and II. *Cellulose*, *20*(1), 25–42. https://doi.org/10.1007/s10570-012-9835-9

McCall, E. R., & Jurgens, J. F. (1951). Chemical Composition of Cotton. *Textile Research Journal*, *21*(1), 19–21. https://doi.org/10.1177/004051755102100105

Michud, A. (2016). Development of a novel process for the production of man-made cellulosic fibers from ionic liquid solution. *Aalto University, School of Chemical Engineering, Department of Biorefineries*, 18.

Monshi, A., Foroughi, M. R., & Monshi, M. R. (2012). Modified Scherrer Equation to Estimate More Accurately Nano-Crystallite Size Using XRD. *World Journal of Nano Science and Engineering*, *02*(03), 154–160. https://doi.org/10.4236/wjnse.2012.23020

Moriam, K., Sawada, D., Nieminen, K., Hummel, M., Ma, Y., Rissanen, M., & Sixta, H. (2021). Towards regenerated cellulose fibers with high toughness. *Cellulose*, *28*(15), 9547–9566. https://doi.org/10.1007/s10570-021-04134-9

Nishiyama, Y., Langan, P., & Chanzy, H. (2002). Crystal structure and hydrogen-bonding system in cellulose Iβ from synchrotron X-ray and neutron fiber diffraction. *Journal of the American Chemical Society*, *124*(31), 9074–9082. https://doi.org/10.1021/ja0257319

O'sullivan, A. C. (1996). *Cellulose: the structure slowly unravels*. https://doi.org/10.1023/A:1018431705579

Parviainen, A., King, A. W. T., Mutikainen, I., Hummel, M., Selg, C., Hauru, L. K. J., Sixta, H., & Kilpeläinen, I. (2013). Predicting cellulose solvating capabilities of acid-base conjugate ionic liquids. *ChemSusChem*, *6*(11), 2161–2169. https://doi.org/10.1002/cssc.201300143

Pinkert, A., Marsh, K. N., Pang, S., & Staiger, M. P. (2009). Ionic liquids and their interaction with cellulose. *Chemical Reviews*, *109*(12), 6712–6728. https://doi.org/10.1021/cr9001947

Die approbierte gedruckte Originalversion dieser Diplomarbeit ist an der TU Wien Bibliothek verfügbar
The approved original version of this thesis is available in print at TU Wien Bibliothek.

Pitkänen, L., & Sixta, H. (2020). Size-exclusion chromatography of cellulose: observations on the low-molar-mass fraction. *Cellulose*, *27*(16), 9217–9225. https://doi.org/10.1007/s10570-020-03419-9

Potthast, A., Rosenau, T., Sixta, H., & Kosma, P. (2002). Degradation of cellulosic materials by heating in DMAc/LiCl. In *TETRAHEDRON LETTERS* (Vol. 43).

Rapsikevičienė, J., Gurauskienė, I., & Jučienė, A. (2019). Model of industrial textile waste management. *Environmental Research, Engineering and Management*, *75*(1), 43–55. https://doi.org/10.5755/j01.erem.75.1.21703

Rosenau, T., Potthast, A., Sixta, H., & Kosma, P. (2001). *The chemistry of side reactions and byproduct formation in the system NMMO/cellulose (Lyocell process)*. www.elsevier.com/locate/ppolysci*Correspondingauthor.Fax:143-1-36006-6059.

S. Kalia, B. S. Keith, & I. Kaur (eds.). (2011). *Cellulose Fibers: Bio-and Nano-Polymer Composites*.

Saadati Ardestani, N., Sodeifian, G., & Sajadian, S. A. (2020). Preparation of phthalocyanine green nano pigment using supercritical CO2 gas antisolvent (GAS): experimental and modeling. *Heliyon*, *6*(9). https://doi.org/10.1016/j.heliyon.2020.e04947

Schautzer, A., & Stix, H. (2019). *Approaching 20 years of euro cash in Austria: What has changed, and what's next?* https://www.oenb.at/dam/jcr:6050bfa9-7335-4376-bbb2-21bf117f5e98/09_schautzer_stix_mop_Q1_Q2_19.pdf

SFS-EN 16170:2016:en. (n.d.). Sludge, treated biowaste and soil. Determination of elements using inductively coupled plasma optical emission spectrometry (ICP-OES). *Https://Sales.Sfs.Fi/Fi/Index/Tuotteet/SFS/CEN/ID2/1/439037.Html.Stx*.

Singh, N. P. (2008). Polymer Banknotes-A Viable Alternative to Paper Banknotes. *Asia-Pacific Business Review*, *IV*(2).

Sixta, H., Michud, A., Hauru, L., Asaadi, S., Ma, Y., King, A. W. T., Kilpeläinen, I., & Hummel, M. (2015). Ioncell-F: A High-strength regenerated cellulose fibre. *Nordic Pulp & Paper Research Journal*, *30*(1), 43–57. https://doi.org/doi:10.3183/npprj-2015-30-01-p043-057

Sluiter, A., Hames, B., Ruiz, R., Scarlata, C., Sluiter, J., Templeton, D., & Crocker, D. (2008). *Determination of Structural Carbohydrates and Lignin in Biomass Laboratory Analytical Procedure (LAP) Issue Date: 7/17/2005*. www.nrel.gov

Stallmann, O. (1960). *Use of Metal Complexes in Organic Dyes and Pigments*. https://pubs.acs.org/sharingguidelines

statista.com. (2021, July 8). *https://www.statista.com/statistics/1112656/cash-use-in-europe-by-country/*. Statista.Com.

statista.com. (2022). *https://de.statista.com/statistik/daten/studie/6331/umfrage/weltweite-produktionsmenge-von-textilfasern-seit-1975/*.

Sun, N., Rahman, M., Qin, Y., Maxim, M. L., Rodríguez, H., & Rogers, R. D. (2009). Complete dissolution and partial delignification of wood in the ionic liquid 1-ethyl-3-methylimidazolium acetate. *Green Chemistry*, *11*(5), 646–665. https://doi.org/10.1039/b822702k

Sungur, Ş., & Gülmez, F. (2015). Determination of metal contents of various fibers used in textile industry by MP-AES. *Journal of Spectroscopy*, *2015*. https://doi.org/10.1155/2015/640271

Suñol, J. J., Saurina, J., Carrillo, F., & Colom, X. (2003). COMPARISON OF THE THERMAL BEHAVIOR OF THREE CELLULOSE FIBERS MERCERIZED OR SUBMITTED TO SOLAR DEGRADATION. In *Journal of Thermal Analysis and Calorimetry* (Vol. 72).

Die approbierte gedruckte Originalversion dieser Diplomarbeit ist an der TU Wien Bibliothek verfügbar
The approved original version of this thesis is available in print at TU Wien Bibliothek.

Swatloski, R. P., Spear, S. K., Holbrey, J. D., & Rogers, R. D. (2002). Dissolution of cellose with ionic liquids. *Journal of the American Chemical Society*, *124*(18), 4974–4975. https://doi.org/10.1021/ja025790m

Tripathi, S. K., Bhardwaj, N. K., & Roy Ghatak, H. (2019). Optimization of ozone bleaching conditions for improving wheat straw pulp quality using response surface methodology. *Ozone: Science and Engineering*, *41*(2), 137–145. https://doi.org/10.1080/01919512.2018.1508331

Troiano, G., Mercurio, I., Golfera, M., Nante, N., Melai, P., Lancia, M., & Bacci, M. (2017). Cocaine contamination of banknotes: a review. *European Journal of Public Health*, *27*(6), 1097–1101. https://doi.org/10.1093/eurpub/ckx100

Troshenkowa, Svetlana, & Dariusz Wawro. (2010). "Dissolved state of cellulose in ionic liquids—the impact of water." *Fibres Text East Eur 18*, 80.

Ureña Benavides, E. E. (2011). *CELLULOSE NANOCRYSTALS PROPERTIES AND APPLICATIONS IN RENEWABLE NANOCOMPOSITES*.

Wada, M., Heux, L., & Sugiyama, J. (2004). Polymorphism of cellulose I family: Reinvestigation of cellulose IVl. *Biomacromolecules*, *5*(4), 1385–1391. https://doi.org/10.1021/bm0345357

Wakefield, M., Delaney, L., & Finlay, R. (2019). *A Cost-benefit Analysis of Polymer Banknotes*.

Wang, H., Gurau, G., & Rogers, R. D. (2012). Ionic liquid processing of cellulose. *Chemical Society Reviews*, *41*(4), 1519–1537. https://doi.org/10.1039/c2cs15311d

Woodings, C. (2001). Regenerated cellulose fibres. *Elsevier*.

Worrell, E. (2014). Recycling in Waste Management Policy. In *Handbook of Recycling: State-of-the-art for Practitioners, Analysts, and Scientists* (pp. 497–501). Elsevier Inc. https://doi.org/10.1016/B978-0-12-396459-5.00033-7

Yousef, S., Kuliešienė, N., Sakalauskaitė, S., Nenartavičius, T., & Daugelavičius, R. (2021). Sustainable green strategy for recovery of glucose from end-of-life euro banknotes. *Waste Management*, *123*, 23–32. https://doi.org/10.1016/j.wasman.2021.01.007

Zhang, C., Liu, R., Xiang, J., Kang, H., Liu, Z., & Huang, Y. (2014). Dissolution mechanism of cellulose in N,N-dimethylacetamide/lithium chloride: Revisiting through molecular interactions. *Journal of Physical Chemistry B*, *118*(31), 9507–9514. https://doi.org/10.1021/jp506013c

Zimmels, Y., Tuval, Y., & Lin, I. (1977). Principles of high-gradient magnetogravimetric separation. *IEEE Transactions on Magnetics*, *13*(4), 1045–1052. https://doi.org/10.1109/TMAG.1977.1059516

Die approbierte gedruckte Originalversion dieser Diplomarbeit ist an der TU Wien Bibliothek verfügbar
The approved original version of this thesis is available in print at TU Wien Bibliothek.

7. Appendix

List of Figures

Page

Figure 1. The path of Ioncell® production (ioncell.fi/research, 2022). 3

Figure 2. Illustration of a 5€ Banknote-Specimen and its features (ecb.europa.eu, 2022). 6

Figure 3. Molecular structure of cellulose. D - glucose monomer units linked by β (1-4) D - glycosidic bonds with n as the degree of polymerization (Klemm et al, 2005). 7

Figure 4. Interconversions of the polymorphs of cellulose (O´Sullivan, 1996) 8

Figure 5. Dissolution process of cellulose in LiCl / DMAc solution (Zhang et al., 2014). 10

Figure 6. Three different ionic liquids currently used in the Ioncell® process. 11

Figure 7. Cellulose-dissolution model in protic ILs with competitive hydrogen-bond donation from cellulose and the protic cation with the basic anion. (Parviainen et al., 2013). 11

Figure 8. Simplified illustration of a Dry- Jet Wet Spinning Unit (Michud., 2016). 12

Figure 9. Structure formation steps: a) cellulose, b) dissolution, c) solution, d) inlet cone, e) capillary, f) die swell, g) draw, h) desolvation, i) washing, j) drying (Hauru, 2017). 13

Figure 10. Banknotes provided by Federico Frascà (a) and by the Bank of Finland (b). 14

Figure 11. Developed pre-treatment sequence to remove non-cellulosic compounds from euro banknotes. 15

Figure 12. Particle size distribution volume [%] as a function of particle size [µm] of the banknotes after milling (a) and after sieving (b) as well as a direct comparison of both (c) and a comparison of the bleached banknotes and the sieved banknotes (d). 38

Figure 13 Ash content [%] of samples for each pre-treatment step. 39

Figure 14 Illustration of the intrinsic viscosity [ml/g] along the pre-treatment sequence 40

Figure 15. Decrease of intrinsic viscosity by H_2SO_4 treatment. 41

Figure 16. Results of ICP-OES analyses. Concentrations [ppm] of certain elements for each pre-treatment step. Elements with higher initial concentrations (>500 ppm) are depicted in (a) and elements with lower initial concentrations (<500ppm) are depicted in (b). 42

Figure 17. cellulose, hemicellulose, and non-polysaccharide composition [%] of the initial milled BNs, bleached BNs and LiCl cleaned BNs, respectively. 45

Figure 18. Complex viscosity (η*) against angular frequency (a) and storage modulus (G`) & loss modulus (G``) against angular frequency (b) for dopes used to produce green and white fibers, respectively at 60 °C. (*) Enocell - 4 dope produced and measured by Helena Sederholm (Aalto University). 48

Die approbierte gedruckte Originalversion dieser Diplomarbeit ist an der TU Wien Bibliothek verfügbar
The approved original version of this thesis is available in print at TU Wien Bibliothek.
TU Bibliothek Your knowledge hub WIEN

Figure 19. (a) mix of opened fibers (50% green, spin finished Ioncell® fibers from BNs and 50% Tencel fibers), (b) spun yarn next to the homogenized blend and (c) final knitted piece of fabric. Fibers spun by Inge Schlapp-Hackl (Aalto University), fibers treated from here on until the finished fabric (a-c) by Marja Rissanen (Aalto University) 50

Figure 20. Tenacities [cN/tex] of all the spun fibers and Enocell – 4 fibers as a function of elongation [%] under dry (a) and wet (b) conditions. (*) Fibers spun and measured by Helena Sederholm (Aalto University), (**) Fibers spun by Inge Schlapp-Hackl (Aalto University) and measured by Marja Rissanen (Aalto University). 51

Figure 21. Cross-section (a) and (b) as well as surface morphology (c) and (d) of green fibers spun at DR 7 by monofilament spinning unit characterized by SEM operating at 2.00 kV. 55

Figure 22. Cross-section (a) and (b) as well as surface morphology (c) and (d) of white fibers spun at DR 7 by monofilament spinning unit characterized by SEM operating at 3.00 kV. Fibers produced by Inge Schlapp-Hackl (Aalto University) and measured by Eva Gonzalez (Aalto University) 56

Figure 23. Results of gel permeation chromatography measurements. Molecular Mass Distribution of Ioncell® fibers from Enocell-4 pulp, and green and white Ioncell® fibers from banknotes. (*) Fibers produced and measured by Helena Sederholm (Aalto University)..... 57

Figure 24. Results of X-ray diffraction analysis for green and white banknote fibers, respectively. (a) intensity over 2θ [°] and (b) crystal width [Å] of reflection planes ([1-10], [110], [020], respectively) and crystallinity [%] of the fibers. Measured by Daisuke Sawada (Aalto University) 58

Figure 25. FTIR spectra of Enocell – 4, milled BNs, bleached BNs as well as LiCl cleaned BNs for comparison. 61

Figure 26. Comparison of FTIR spectra from green Ioncell® fibers produced from bleached banknotes and white Ioncell® fibers produced from LiCl cleaned banknotes. 62

Figure 27. Results of STA measurements of milled BNs (a) & (b), bleached BNs (c) & (d) and LiCl cleaned BNs (e) & (f), respectively. TGA graphs on the left and DSC graphs on the right. (*) 100% cellulose sample was measured by Inge Schlapp – Hackl (Aalto University) 63

Figure 28. Results of STA measurements of red dyes, separated by acetone and green pigments, separated by LiCl/DMAc treatment and sedimentation. TGA graphs on the left and DSC graphs on the right. 65

Figure 29. Results of STA measurements for green and white Ioncell® fibers from banknotes. (a) TGA graph and (b) DSC graph..... 66

Figure 30. Chemical structure of phthalocyanine green. 68

Die approbierte gedruckte Originalversion dieser Diplomarbeit ist an der TU Wien Bibliothek verfügbar
The approved original version of this thesis is available in print at TU Wien Bibliothek.

List of Tables

Page

Table 1. Mean values [%] and standard deviations σ [%] of ash-content measurements. 23

Table 2. Results of the intrinsic viscosity measurement of each pre-treatment step..... 25

Table 3. Results of intrinsic viscosity measurement for Banknotes treated with 0.05M sulfuric acid for 0, 10, 20 and 30 minutes, respectively. 25

Table 4. Result of ICP measurement for each pre-treatment step. Elements with initial concentrations > 500ppm. 32

Table 5. Results of ICP measurement for each pre-treatment step. Elements with initial concentrations < 500ppm. 33

Table 6. Results of carbohydrate analysis for milled, bleached and LiCl cleaned BNs respectively. The results for cellulose, hemicellulose and non-polysaccharides is given in [%]. 36

Table 7. Kneading parameters for all dopes prepared. (*) dopes prepared by Inge Schlapp – Hackl (Aalto University). 46

Table 8. Complex viscosity (η*), omega (Ω), storage modulus and loss modulus at 60ºC of all the dopes prepared for fiber production measured with rheometer. (*) produced and measured by Helena Sederholm (Aalto University), (**) dope produced and measured by Inge Schlapp – Hackl (Aalto University). 47

Table 9. Summary of the spinning conditions (*) fibers spun by Inge Schlapp-Hackl (Aalto University) 49

Table 10. Summary of fiber testing results at point of rupture for all produced fibers. (*) Fibers spun and measured by Helena Sederholm (Aalto University), (**) Fibers spun by Inge Schlapp-Hackl (Aalto University) and measured by Marja Rissanen (Aalto University). 53

Table 11. Summary of birefringence measurement of Enocell-4 fibers as well as of the produced green and white fibers. (*) fibers produced and measured by Helena Sederholm (Aalto University), (**) fibers spun by Inge Schlapp-Hackl (Aalto University) and measured by Marja Rissanen (Aalto University). 54

Table 12. Results of XRD measurements of green and white Ioncell® fibers from banknotes. Orientation [%], Anis-Ratio [%], Crystallinity [%] and Crystal size of hkl planes L1-10, L110 and L020 [Å], respectively 58

Table 13. Elemental composition (C, N, H, S) concentrations [%] with respective standard deviations of each pre-treatment step as well as for green and white banknote fibers and separated red color and green pigments. Measured by Eva Gonzalez (Aalto University) 60

Die approbierte gedruckte Originalversion dieser Diplomarbeit ist an der TU Wien Bibliothek verfügbar
The approved original version of this thesis is available in print at TU Wien Bibliothek.